Masteroppgave

NTNU
Norges teknisk-naturvitenskapelige universitet
Fakultet for informasjonsteknologi og elektroteknikk
Institutt for elkrafftteknikk

Robert Grindborg Karlsen

Evaluation of available capacity in distribution grids

Masteroppgave i Energy and Environmental Engineering
Veileder: Olav Bjarte Fosso
Medveileder: Iver Bakken Sperstad & Susanne Sandell
Juni 2022

NTNU
Norwegian University of
Science and Technology

Robert Grindborg Karlsen

Evaluation of available capacity in distribution grids

Masteroppgave i Energy and Environmental Engineering
Veileder: Olav Bjarte Fosso
Medveileder: Iver Bakken Sperstad & Susanne Sandell
Juni 2022

Norges teknisk-naturvitenskapelige universitet
Fakultet for informasjonsteknologi og elektroteknikk
Institutt for elkraftteknikk

NTNU
Norwegian University of
Science and Technology

Abstract

The electricity grid, which enables the electricity transport of renewable energy from producers to consumers, has a central role in the green shift. However, an aging grid combined with the accelerating rate of electrification of the energy system is challenging the Norwegian distribution system operators (DSOs), and the increase in load demand is driving the need for grid upgrades and development. In addition to faster grid development, higher utilization of existing components and infrastructure will be crucial to meet the increased demand and the transition towards a green energy system.

The installation of Advanced metering system (AMS) infrastructure for all Norwegian electricity consumers has given the grid operators large amounts of new available data. This can potentially be used to improve the utilization of the existing grid, in order to reduce the costs of developing the grid, both for the DSOs and the electricity customers. Hence, the main objective of this master project has been to investigate how the smart meter load data can be used to provide better insight into the available capacity and the potential for load increase in distribution grids.

A methodological approach for evaluation of the available capacity in distribution grids is proposed. The methodological approach can be used to provide better insight into the room for connection of new end users and increased load demand. The main focus of the approach is the remaining capacity of the grid components, such as power lines and transformers, during normal operation and during outage situations.

The methodological approach is utilized on a part of the distribution grid of the industrial park Øra in Fredrikstad. The available capacity of the industrial distribution grid is evaluated for normal operation and for outage situations. The analysis is based on network data and historical load measurements for two radials, referred to as Radial A and Radial B, of the industrial distribution grid. The radials are connected through a reserve branch, that can be used to supply the isolated end user in case of outages in certain branches of the high-voltage part of the distribution grid. The results show that, based on the load demand from the last three years, the ratings of the grid components, in general, are sufficient to cover today's load demand, both under normal operation and in case of outages.

In the coming years, electrification of industrial processes and connection of new power-intensive industries will possibly put pressure on the existing grid and challenge the DSO. In order to investigate a system with improved utilization of the capacity of the existing grid components, the historical aggregated load demand supplied by each distribution transformer in the grid is scaled such that the peak demand is equal to the nameplate rating of the transformer. Further, the available capacity in the grid is evaluated both under normal operation and for the most critical outage scenarios. The results show that, under normal operation, the ratings of the power lines in the two radials are still sufficient to cover the new demand after the load modifications. However, during outage of the main branch of Radial A or the main branch Radial B, the line rating of the remaining main branch is exceeded. An outage of the main branch of Radial B is most critical in terms of the size and number of overload events in this future scenario.

Sammendrag

Strømnettet legger til rette for transport av elektrisk energi mellom produsenter og forbrukere, og har derfor en sentral rolle i det grønne skiftet. Kombinasjonen av et aldrende nett og den pågående elektrifiseringen av energisystemet utfordrer de norske nettselskapene. Det stadig økende forbruket fører med seg et stort behov for oppgradering og utvikling av strømnettet. I tillegg til raskere nettutvikling, vil det være avgjørende å utnytte eksisterende komponenter og infrastruktur på en bedre måte for å klare å håndtere overgangen til et grønnere energisystem.

Utrullingen av smarte strømmålere, eller avanserte måle- og styringssystemer (AMS), til alle nettkunder i Norge har gitt nettselskapene tilgang til store mengder ny informasjon. Den nye informasjonen kan potensielt bli brukt til å forbedre utnyttelsen av det eksisterende strømnettet, og på denne måten redusere kostnadene knyttet til nettutvikling, både for nettselskapene og kundene. På bakgrunn av dette, har hovedmålet for denne masteroppgaven vært å undersøke hvordan tilgangen på lastdata kan benyttes for bedre innsikt i ledig kapasitet og potensiale for økt forbruk i distribusjonsnett.

En metode for vurdering av ledig kapasitet i distribusjonsnettet er beskrevet. Metoden kan benyttes for å få en bedre innsikt i muligheten for tilkobling av nye kunder og økt forbruk. Metoden fokuserer hovedsakelig på ledig kapasitet i nettkomponenter, som kraftlinjer og transformatorer, under normaldrift og i utfallssituasjoner.

Videre er metoden benyttet på en del av distribusjonsnettet ved Øra Industripark i Fredrikstad. Den ledige kapasiteten i nettet er vurdert under normaldrift og i forskjellige utfallssituasjoner. Analysen er basert på nettverksdata og historiske lastmålinger for to radialer i det industrielle distribusjonsnettet, referert til som Radial A og Radial B. De to radialene er koblet sammen via en reserveforbindelse som kan benyttes til å forsyne isolerte kunder i tilfelle utfall i enkelte deler av det høyspente distribusjonsnettet på industriområdet. Basert på lastdata fra de tre siste årene viser resultatene at kapasiteten til nettkomponentene i all hovedsak er god nok til å dekke dagens forbruk, både under normaldrift og i utfallssituasjoner.

I de kommende årene vil sannsynligvis elektrifisering av industrielle prosesser og etablering av ny kraftkrevende industri som legger press på det eksisterende strømnettet være en stor utfordring for nettselskapene. For å kunne undersøke et distribusjonsnett hvor eksisterende kapasitet er utnyttet i større grad er den historiske lasten som forsynes av hver distribusjonstransformator skalert slik at topplasten for treårsperioden ble lik den installerte effekten til transformatoren. Deretter er ledig kapasitet i nettet vurdert både under normaldrift og i de mest kritiske utfallssituasjonene. Resultatene viser at kapasiteten i nettet var tilstrekkelig for å dekke det nye forbruket under normaldrift. Imidlertid fører utfall av hovedlinjen i Radial A eller hovedlinjen i Radial B, som knytter sekundærstasjonen sammen med resten av nettet i radialene, til overskredet kapasitet i den gjenværende hovedlinjen. Videre viser resultatene at utfall på hovedlinjen i Radial B vil være mest kritisk med tanke på størrelsen på og antall timer med overlast i dette fremtidsscenarioet.

Preface

This master project was performed during the spring of 2022 at the Department of Electric Power Engineering at the Norwegian University of Science and Technology (NTNU), and concludes my five year Master of Science (M.Sc.) degree in Energy and Environmental Engineering. The work is done in cooperation with SINTEF Energy Research and Norgesnett, and is related to the Centre for Intelligent Electricity Distribution (CINELDI).

I would like to thank my main supervisor, Professor Olav Bjarte Fosso, and co-supervisors Iver Bakken Sperstad and Susanne Sandell from SINTEF Energy Research, for great guidance throughout the semester. Your inputs and availability have been highly appreciated. I would also like to thank Norgesnett for sharing the data set used in the project, and for additional inputs throughout the work.

Lastly, I would also like to thank my friends, family, girlfriend and classmates for valuable support and discussions throughout the work with this master project.

Table of Contents

List of Figures

List of Tables

1 Introduction

1.1 Motivation

Norway has set ambitious goals to reduce the annual greenhouse gas emissions from their 1990 levels by 50-55% within 2030 [1]. Simultaneously as the world is working to limit the global temperature rise to 1.5 °C, the demand for energy is increasing [2]. Electrification in combination with progressively cleaner electricity production emerges is a crucial tool for achieving the climate goals [3]. Hence, the electricity grid, which enables the electricity transport of renewable energy from producers to consumers, has a central role in the green shift.

An aging grid combined with the accelerating rate of electrification of the energy system is challenging the Norwegian distribution system operators (DSOs). For instance, electrification of industrial processes of existing industries and establishment of new, power-intensive industries are putting pressure on the existing distribution grid. By law the DSOs are obligated to offer connection and deliver electricity to all customers within their supply area [4]. Hence, the increase in load demand is driving the need for grid upgrades and development. The DSOs have expressed concern about keeping up with the demand, and in 2021, the Norwegian government established a committee, "The Electricity Grid Committee" (Norwegian: Strømnettutvalget), that will evaluate the regulatory barriers to faster grid development [5]. In addition to faster grid development, improved exploitation of existing components and infrastructure will be crucial to meet the increased demand and the transition towards a green energy system [6] [7].

Traditionally, the DSOs have had limited information about the underlying characteristics of the loads in distribution system beyond monthly or yearly consumption [6]. Therefore, the electric distribution grids are in general dimensioned to handle the "worst-case" scenario regarding expected peak load demand, and in a way that that minimizes the required operation intervention [6]. A problem with the traditional "fit and forget" approach is that it does not take into account the transformation of the energy system and may lead to over- or under dimensioning of the components in the network.

The installation of Advanced Metering System (AMS) infrastructure for all Norwegian electricity consumers has given the grid operators large amounts of new available data. AMS provides detailed information on consumption, load and voltages, and allows the DSOs to plan and operate the grid based on more accurate data [8]. This can potentially be used to improve the utilization of the existing grid, in terms of reducing the costs of developing the grid, both for the DSOs and the electricity customers.

The work of this project thesis is based on smart meter data from two radials in the industrial distribution grid of Øra, which is a port and industrial area outside the old town of Fredrikstad in the South-Eastern part of Norway. The industrial area has an assortment of different industries, including recycling industries, food industries and LNG storage and distribution. Today, the energy consumption of the Øra industries is partly covered by natural gas. In the coming years, parts of the existing industrial processes will be electrified and new, power-intensive industries will be established. Therefore, the electricity grid will need to handle an increased load demand. According to Norgesnett, the network capacity, and especially the line ratings of the cables, is considered as the limiting factor in the coming electrification process. Therefore, in order to achieve a good utilization of the existing and future grid capacity, it is important to obtain a better understanding of the load and supply situation in the industrial distribution grid.

1.2 Main objectives

The overall objective of this master project is to investigate how the smart meter load data can be used to provide better insight into the available capacity and potential for load increase in distribution grids.

In order to achieve this, three sub-objectives of the project are defined as following:

- Propose a methodology for evaluation of available capacity in distribution grids.
- Based on the proposed methodology, evaluate the available capacity in the two radials of the industrial grid of Øra under normal operation and in outage situations.
- Evaluate the potential for connection of new end-users and increased load demand in the two radials of the industrial grid of Øra.

1.3 Scope

The analysis of the industrial distribution grid of Øra is based on historical load data from the last three years. Since parts of the data set is considered as sensitive energy data, this is not attached to the thesis. The presented network data is anonymized and simplified.

The system is assumed to be lossless and with unity power factor, i.e., only real power is considered. Since the grid consists of relatively short power lines, this will probably not affect the overall results.

1.4 Relation to FME CINELDI

The work is related to FME CINELDI (Centre for Intelligent Electricity Distribution), led by SINTEF Energy Research. The main goal of CINELDI is to enable a cost-efficient realisation of the future flexible and robust electricity distribution grid.

In the pilot project *Probabilistic planning methodology*, CINELDI and the DSO Norgesnett are working on how AMS data can be utilized to improve distribution grid planning methodologies. This can lead to increased security of supply and up-time for customers, in addition to reduced costs for the grid companies [9].

The analysis of load data presented in this thesis is based on a Python code developed by SINTEF Energy Research. The code used as basis is open source and available through GitHub [10]. The software performs loading, anonymization, preprocessing, modification and analysis of mass load- and grid data. As a part of this master project, more functions regarding modification of the grid and analysis and presentation of the load data are implemented to the code.

1.5 Relation to the Specialization Project

This master thesis is partially a continuation of the specialization project "Load modelling and characteristics in an industrial distribution network", written during the autumn semester 2021 in the course *TET4520 - Electric Power Engineering and Energy Systems*. A brief summary of the project is provided in Appendix B. The analyzed part of the grid was the same as Radial A in this master project.

Certain parts of the theory, background and data set description are relevant for both project thesis. Therefore, some sections from the specialization are included in more or less modified versions. This applies to the following sections:

- Chapter 2.2.1 (Modified with reformulations and new figure (Figure 6)
- Chapter 2.2.2 (Slightly modified)
- Chapter 3.1.1 (Slightly modified)
- Chapter 4.1 (Modified with new paragraph)

1.6 Work process and thesis structure

The thesis is structured as following:

Chapter 1 - Introduction: Provides a brief description of the background, scope and contributors of the thesis.

Chapter 2 - Theory: Provides an overview of the essential theory and concepts of the Norwegian power system and reliability analysis of distribution systems.

Chapter 3 - Methodology: Presents methodological approach for evaluation of available capacity in distribution grids.

Chapter 4 - Data set: Presents relevant information about Øra industrial park, the distribution network and the load data set used in the analysis part.

Chapter 5 - Results and discussion: Presents and discusses the results obtained by applying the proposed methodological approaches for evaluation of available capacity in distribution grids on the industrial grid of Øra.

Chapter 6 - Conclusion and future work: Gives a summary of the project work, main results and remarks on the work conducted. Additionally, suggestions for future work are made.

2 Theory

2.1 The Norwegian power system

2.1.1 Power system structure

The electricity grid enables transport of power from producers to consumers, and consists of three grid levels; the transmission grid, the regional grid and the distribution grid [4]. The transmission grid, also known as the central grid, constitutes the "highways" of the power system, and is controlled by the designated transmission system operator (TSO) Statnett. This part of the grid connects the power producing areas to the consuming areas in a nationwide system [11].

According to EU legislation, both the regional level and the distribution level are considered as distribution grid [4]. This grid supplies the electricity consumers in the system and is operated and maintained by local distribution grid operators (DSOs). The fixed costs of grid development are high, and consequently it is not economically viable to build parallel grids in one area to create a competitive market for distributing electricity. Therefore, the electricity grid is a natural monopoly, and grid operations are not open to competition [12]. Today, the Norwegian distribution and regional grid is operated by about 100 different DSOs.

Figure 1 shows the three grid levels of the Norwegian power system, where the distribution level includes the grid with voltage levels up to 22 kV, the regional grid has voltage levels in the interval 33-132 kV and the transmission grid usually transmits power at 300 kV or 420 kV [4].

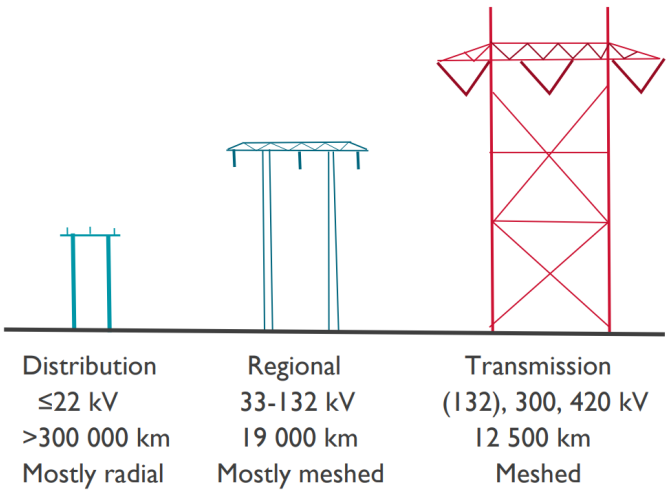

Figure 1: The three grid levels of the Norwegian power system [4].

The distribution level, which is the main focus of this thesis, can further be divided into two segments based on voltage level; the high voltage and low voltage distribution grid. The high voltage segment usually carries voltages of 11 to 22 kV, and links the regional grid to local distribution substations. Here, the voltage is lowered to the utilization level, that is used by lighting, household appliances and electronic devices. The final consumers are supplied through the low voltage segment, usually at 230 or 400 V [4][11].

Figure 1 indicates that the grid structure can be categorized as either meshed or radial. The distribution level consists often of radial grids, while the regional grid and the transmission grid are in most cases meshed. In a radial grid all network components are placed in series. Consequently, a consumer connected to any load point of a radial system requires all components between him- or herself and the supply point to be operating [13]. Figure 2 shows an example of a grid with radial structure. The grid has two main radials with five distribution substations in each radial,

represented by the squares.

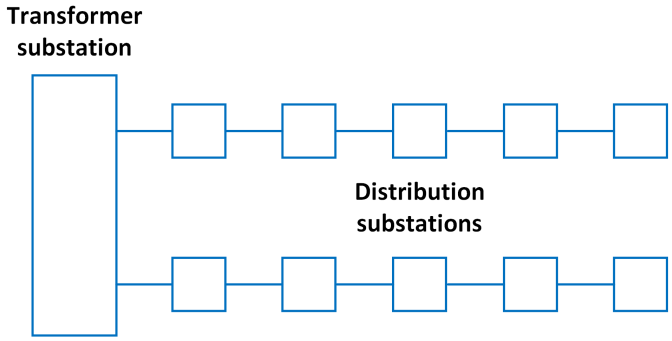

Figure 2: Radial distribution system.

According to a document published by Norgesnett on distribution system design, the high-voltage distribution system preferably should be designed as a meshed grid [14]. A meshed structure provides several supply options for each end-user, and Norgesnett suggests two alternative designs; the "ring grid" structure and the "traversing connection" structure.

Figure 3 and Figure 4 show examples of the ring distribution system and the traversing connection distribution system, respectively. For the ring distribution system all the consumers are supplied by the same transformer substation, while for the traversing connection grid it is possible to supply the consumers from different transformer substations. The radials are separated by breakers. Under normal conditions the breakers are open, i.e. no currents are flowing through the breakers, and hence the grids are operated as radial distribution grids. However, when a fault occurs in one of the radials and the fault location is detected, the downstream consumers can be supplied through one of the other radials. Accordingly, a meshed grid design provides improved flexibility and reduced duration of the interruptions compared to the radial grid design.

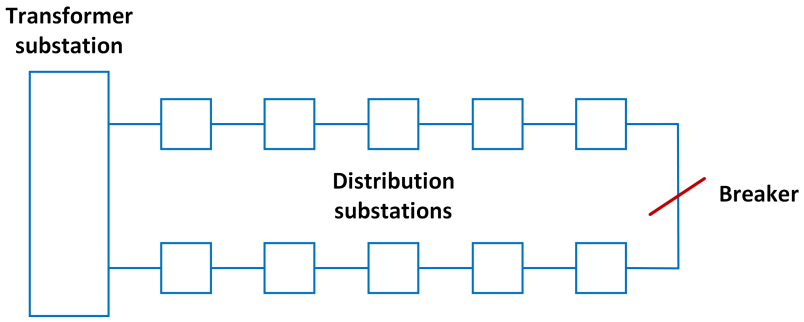

Figure 3: Ring distribution system, adapted from [14].

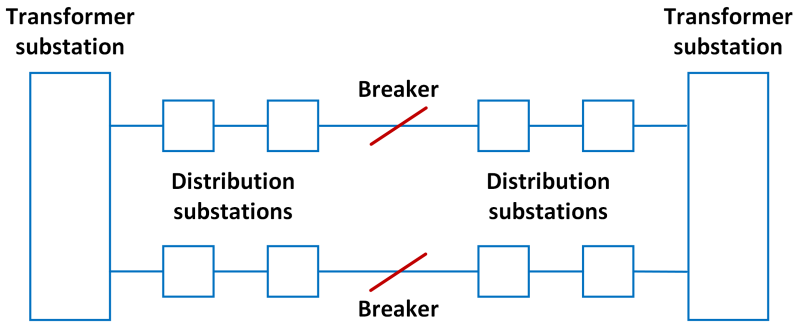

Figure 4: Traversing connection distribution system, adapted from [14].

2.1.2 Regulations

A restructuring of the energy industry started in England and Wales in 1989, and in 1990 the parliament of Norway followed with the Norwegian Energy Act (Norwegian: Energiloven) [15]. The Energy Act is based on the principle that electricity production and trading should be market-based, and the introduction has played an important role in the development of the Norwegian power system. As a result, the participant in the energy system needed to optimize their functions from a socio-economic point of view [16].

In order to ensure socially efficient operation, utilization and development of the grid, the TSO and DSOs in Norway are regulated by the Norwegian Energy Regulatory Authority (NVE-RME) [17]. For instance, the companies are regulated through an incentive-based revenue cap to ensure that they do not abuse their power as monopolists. The annual revenue caps are based partly on the grid companies actual costs and partly on a cost norm. The cost norm is decided based on the cost efficiency of the company. From 2023, the weight put on the cost norm used in calculation of revenue cap is increased from 60% to 70% [18]. This will provide an incentive for the grid companies to improve their efficiency.

The Energy Act states that the local grid companies are obligated to offer grid connection and deliver electric energy to all customers within their own geographical areas [19]. Before connection of a new customer or increased load from an existing costumer is allowed, the affected grid companies are evaluating whether the connection is *operationally sound* or not. The term operationally sound is not clearly defined in the laws, but, in general, it means that the quality and reliability of supply in other parts of the grid should be preserved. Given that the connection or load increase is considered as not operationally sound, measures to enable the connection are evaluated by the grid companies [20].

The grid companies are allowed to charge an investment contribution to cover the costs of connecting a new customer or for reinforcing the grid for an existing customer. The objective of the investment contribution arrangement is to visualize and make the customers responsible for the costs of the required grid upgrades. In this way, the costs are shared more equitably between the customers that trigger the investment and the other customers of the grid company [21].

In case of a failure in the system, Costs of Energy Not Supplied (CENS, Norwegian: KILE) is a measure of the value of the lost load for the customers. CENS was introduces in 2001 and takes into account both forced outages and planned disconnections. The arrangement provides an incentive for the grid companies to have a sufficient level of grid maintenance and investment in order to minimize the power outages [18]. The specific costs are depending on the categorisation of the affected customers and whether the interruption is notified or not. The CENS arrangement will over time lead to a decreased revenue cap for those grid companies with more frequent and severe interruptions than expected and an increased revenue cap for those with less frequent and severe interruptions [22].

2.2 Load modelling in the distribution grid

Forecasting of loads is an essential part of distribution grid planning. The individual, and aggregated, loads will vary for different parts of the year and different hours of the day, and the grid will have to handle all the different load demand combinations that occur during the year. Hence, in order to classify the worst-case operating conditions, it is in the interest of the DSO to find the peak loads of the system [6].

2.2.1 Load aggregation

Normally, when finding the peak load in a node with several underlying load points, it is not sufficient to just sum the maximum load of each individual consumer. A forecasting model used for prediction of future peak loads needs to take into consideration that not all customers reach peak load at the same time. Therefore, the total peak load of the system will be either equal to or less than the sum of all individual peak loads [23]. This is a result of load aggregation, and is important to account for in power system planning in order to prevent over-dimensioning.

The effect of load aggregation is illustrated in Figure 5, where P_1, P_2 and P_3 are the load profiles for three individual consumers over a time period T. The three loads are connected to the same node, and the curve $P_{\sum}$ illustrates the aggregated load at this node throughout the time period. $P_{\sum}$ reaches its peak at time t', but only one of the individual consumers, P_1, has its maximum load at this point [24].

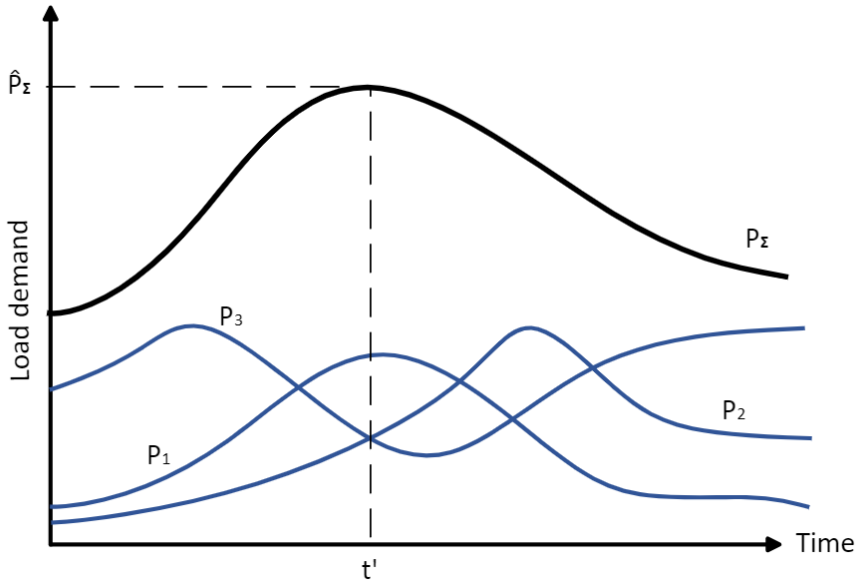

Figure 5: Effect of load aggregation for three individual loads, adapted from [24].

A factor that can be used to describe load aggregation in a system is the coincidence factor, c. The coincidence factor can be calculated from Equation 1. This factor describes the relationship between the coincident peak demand $\hat{P}_{\sum}$ of a group of customers within a specified period and the sum of their maximum demands $\sum_{i=1}^{n} \hat{P}_i$ within the same period [25]. In the calculation of coincidence factor, n is the number of load points connected to the node.

$$c = \frac{\hat{P}_{\sum}}{\sum_{i=1}^{n} \hat{P}_i} \tag{1}$$

where:

- c is the coincidence factor [-]
- $\hat{P}_{\sum}$ is the coincident peak demand of the n consumers [W]
- $\hat{P}_i$ is the individual peak demand of consumer i [W]

Since the sum of the individual peaks is always equal to or larger than the coincident peak, the coincidence factor will always be in the interval 0 to 1. A value of 1 means that all the individual loads connected to the node have their peak at the same time [24]. Therefore, the coincidence factor of a single load will always be equal to 1. In general, a lower coincidence factor is achieved by increasing the number of loads connected to the specific node [23]. The coincidence factor level will also be influenced by the nature of the customers, i.e., whether they form a heterogeneous group or a homogeneous group of customers [26].

The concept of lower coincidence factor for a higher number of loads is illustrated in Figure 6 for n normally distributed equal loads with the same individual peak demand of 10 MW. The parameter c_∞ is set to 0.2 and 0.4 for the two examples, and represents the coincidence factor for a completely aggregated system, i.e., the coincidence factor if all loads in the system have a demand equal to their average demand.

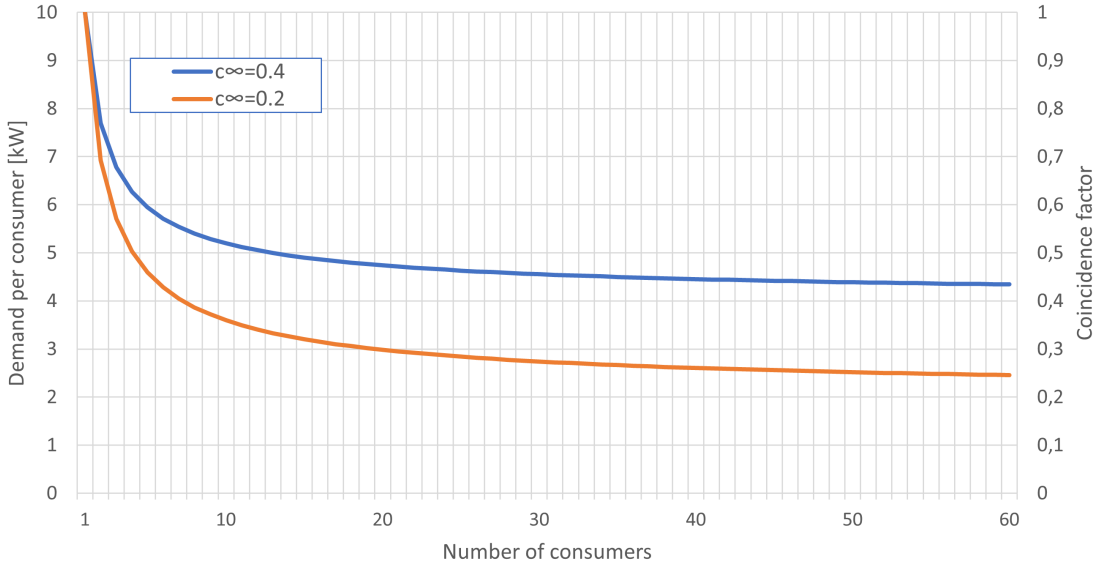

Figure 6: Peak load contribution per customer as a function of the number of customers, with the corresponding coincidence factors shown on the right axis. Adapted from [25].

2.2.2 Load duration curves and utilization time

Load duration curves are often used to illustrate the load demand during a time period. Figure 7 shows an example of a typical load duration curve during a year, where the hourly demand data is ordered in descending order of magnitude. The blue area represents the annual energy consumption, and equals the area under the load curve.

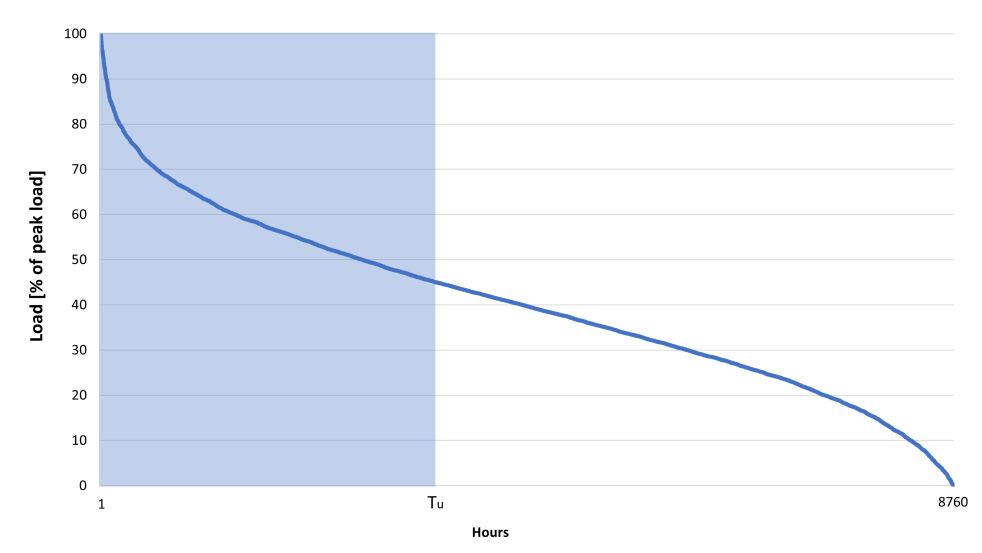

Figure 7: Example of load duration curve for one year.

The utilization time is marked in Figure 7 as T_u, and equals the width of the blue area. The utilization time can be defined as the time it would take at constant peak load to reach the consumer's total annual energy consumption, and can be calculated from the following formula:

$$T_u = \frac{W_{year}}{P_{peak}} \tag{2}$$

where:

- T_u is the utilization time [h]
- W_{year} is the annual energy consumption [kWh]
- P_{peak} is the annual peak load [kW]

In distribution grid planning, the peak load will often be unknown. Thus, a common method to estimate the annual peak load is to use standard values for utilization time for different consumer categories. The peak can then be found from the following equation, based on Equation 2 [6]:

$$P_{peak} = \frac{W_{year}}{T_u} \tag{3}$$

The actual value for utilization time is usually unknown. Therefore, the parameter has to be estimated for different consumer categories. An example of standard utilization times are shown in Table 1. These values are calculated for a region in the eastern part of Norway during a dimensioning (cold) year, and show that the utilization time will be higher for a group of consumers than for one single consumer. This is a result of load aggregation, and was discussed more extensively in the specialization project.

Table 1: Example of utilization times for different consumer categories located in the eastern part of Norway [24].

Consumer category	**Individual utilization time [h]**	**Aggregated utilization time [h]**
Households (detached houses)	3200	4200
Apartment building	2150	3900
Office buildings	3000	3700
School buildings	1600	2350
Retail stores	2900	3650
Health and social care	3000	3800
Hotels	3600	4300

2.3 Active distribution grid planning

Traditionally, the Norwegian distribution networks are designed to handle the worst-case scenario, and in a way that requires a minimum of operation intervention in the future [6]. The worst-case scenario is determined by the estimated peak loads, based on, for instance, the standard values for utilization time, described in 2.2.2.

The electric power system is currently undergoing substantial changes. As a result, a problem with the traditional "fit and forget" approach is that it does not take into account the transformation of the power system, and may lead to over dimensioning of components in the network and unnecessarily large costs related to grid reinforcement [6]. The power system is becoming more complex due to the proliferation of distributed generation (DG) from variable renewable energy (VRE) and more active end users. Further, electrification of transportation and industries is increasing the load demand [27][28]. The accelerating uncertainty in generation and load are challenging the DSOs [6].

At the same time, distribution grid planning is modernised due to more *active* operation and flexibility provided by and the producers (flexible DG), the consumers (flexible loads) and those that do both (prosumers) [29][28]. Development of advanced information and communication technologies (ICT) provides the opportunity to coordinate the new resources and make the grid more robust to operational disturbances. The introduction of smart meters offers huge amounts of new data, which can be utilized to improve the load- and generation models used in distribution grid planning [6]. Based on the new data, probabilistic methods for load and generation modelling can be used to capture the stochastic behaviour of power systems [30].

As the industrial distribution grid of Øra is a more traditional network with one-way power flow and passive loads, most of the elements from active distribution grid planning are out of the scope of this project. However, this is important aspects of the future power system and should be accounted for in decision processes in distribution grid planning. For instance, given that the approach for evaluation of available capacity of this master project shows that the rating of a grid component is exceeded for several hours during a year, active measures, such as battery energy storage systems (BESS) or flexible loads, could be an alternative to traditional ("passive") measures, such as grid reinforcement [28].

2.4 Basic Reliability Concepts

2.4.1 Definitions

A reliable electricity supply is vital for a modern society. However, the relevant power system reliability terminologies are defined in numerous different ways. The International Electrotechnical Commision (IEC) defines power system reliability as the probability that an electric power system can perform a required function under given conditions for a given time interval [31].

It is common to describe power system reliability by considering two functional aspects of the power system; system adequacy and system security [32]. The concept of system adequacy is in general related to the presence of sufficient facilities within a power system to satisfy the consumer demand [13]. These facilities include both those necessary to generate energy (generation adequacy) and the transmission and distribution networks necessary to transport the energy (network adequacy) [33]. Thus, the system adequacy is related to the static conditions of the power system. On the other hand, the system security means the ability of the system to withstand sudden disturbances such as short circuits or non-anticipated loss of system components. The classification is illustrated in Figure 8.

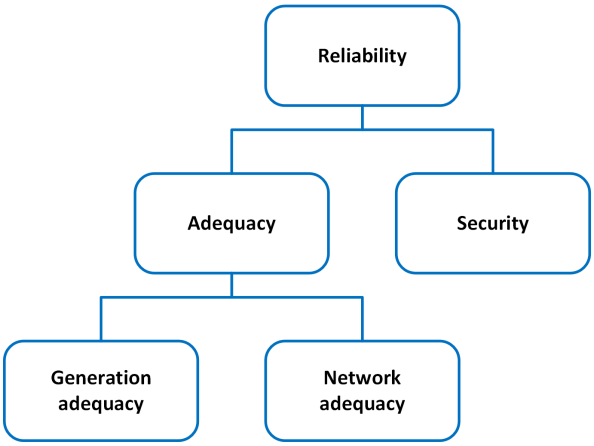

Figure 8: Classification of power system reliability aspects.

An overview of alternative definitions of reliability and related terms are presented in [34]. The article also presents a classification of threats to the power system reliability. Here, a *threat* is defined as "a potential cause of an accident, such as line outage, bus-bar break, or overload, which may lead to a power system failure and possibly a loss of electric power for users". The threats are divided into four categories; natural threats, accidental threats, malicious threats and emerging threats. An detailed description on each type of threat and their possible impact on the system is also provided.

2.4.2 Functional Zones and Hierarchical Levels

Reliability assessments of the power system can be categorized based on what segment of the system the assessment is addressing. The system is often divided into three main functional zones; generation, transmission and distribution. Further, the hierarchical levels of the power system can be formed as illustrated in Figure 9.

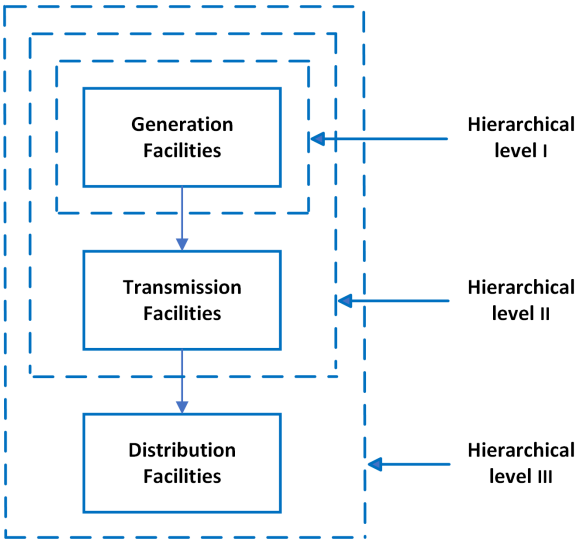

Figure 9: Functional zones and hierarchical levels of a power system, adapted from [13].

Hierarchical level I (HLI) is related to the generation facilities only, and hierarchical level II (HLII) consists of both the generation facilities and the transmission facilities. This level composes the so-called *bulk power system*, and reliability evaluation on this system is regularly performed. The third level, hierarchical level III (HLIII), refers to the complete power system, including generation transmission and distribution, and its ability to satisfy the energy demand of the consumers. Complete HLIII are not often performed due to the complexity of the problem. Instead reliability evaluation of the distribution system is generally conducted independently. Another reason for this, is that a failure in HLI or HLII would affect large parts of the power system, while a failure located in the traditional distribution grid will have mostly local effects [13].

For this master thesis, the distribution grid, and hence HLIII, is the main focus. In the evaluation of the industrial distribution grid of Øra in Chapter 5, the distribution network is investigated independently.

2.5 N-1 reliability criterion

Although the power system is stochastic by nature, most of the traditionally used planning, design and operational criteria are based on deterministic techniques.

A widely known principle for planning of network capacity is the *N-1 reliability criterion*. The intention of the criterion is to ensure an acceptable level of reliability and security margin in the system within a reasonable cost. There is no common definition of the N-1 criterion in literature. However, in general, when the criterion is fulfilled, the loss of any single element in the power system, such as a line or a transformer, should not prevent the supply of electric power [35]. The criterion can also be extended to an N-m criterion, taking into account m simultaneous, or close in time, system component outages [36].

In the evaluation of the industrial distribution grid of Øra in Chapter 5, the remaining capacity of the grid components determines the power transfer limits. Hence, given that the load supplied by a grid component, such as a power line or transformer, exceeds the rating of the component as a result of an outage of another grid component, the N-1 criterion is not fulfilled.

Since the criterion takes no account of the probability and economical consequences of outages, the traditional use of the N-1 criterion has been frequently questioned during the last years [37]. In the GARPUR project, a risk-based approach to reliability management of the transmission grid, which allows operation closer to the socio-economic optimum, was investigated [38]. [39] states that a probabilistic approach is more appropriate to reflect the actual likelihood and consequences of

failures and outages. In order to reduce the investments and improve the utilization of the current power transport capacity, Aabø Powerconsulting proposes to replace the N-1 criterion with a *N-0.9 criterion* [40] [41]. In other words, with this solution, the N-1 criterion is fulfilled only 90% of the time. This approach will increase the available capacity in the grid, and hence, facilitate to efficient utilization of the grid.

2.6 Contingency analysis

A contingency can be defined as a hypothetical outage of specified power system equipment [42]. Contingency analysis is an important tool in assessment of power system adequacy and security. The analysis is used for evaluation of "what if" scenarios in relation to topological changes and component failures, and been widely used in power system planning and security analysis for decades. In evaluation of complex power systems, there is an extensive number of possible system variations and outage scenarios. Therefore, a large number of contingencies must be considered and analyzed to ensure secure operation during power system planning and operation. The workload can be limited by carefully choose the contingency scenarios in order to cover a wider group of possibilities [43].

2.7 Rating of power lines and transformers

2.7.1 Power lines

For power lines, the line rating is usually given by the ampacity, the maximum operating current of the line. In general, there are three factors limiting the line rating; voltage, stability and thermal limits. Typically, the line rating of long power lines is determined by voltage and stability limits, while the rating of short lines are determined by the thermal limits [44].

Unlike the voltage and stability limits, that are defined mainly by reliability requirements, the thermal limits are also based on safety concerns. If the thermal limit of a power line is exceeded, the temperature in the line can be too high and lead to loss of tensile strength [45]. For overhead lines, this can cause reduction in the ground clearance, and is, in addition to annealing, the major concern of exceeding the thermal capacity. Thus, the thermal limits are often determined based on "worst-case" scenarios regarding, for instance, temperature, solar heating and wind conditions. This thermal rating, based on a conservative estimate of line capacity, is referred to as static line rating[44].

In the industrial grid of Øra, which will be analyzed in the case study in Chapter 5, most of the power transport is performed with underground cables. Obviously, underground cables is in more stable environment than overhead power lines, and hence, the factors determining the thermal limits will be different. For instance, the thermal properties of the surrounding ground has major impact . However, violation of the thermal limit of all types of power lines will over time lead to short term breakdown or decreased lifetime [46].

Today, most of the Norwegian DSOs use tabulated ampacity values provided by the manufacturer or the national standard NEN 62:75 composed in 1975 [47] [48]. Since there are large uncertainties in the actual capacity of the cables, the capacities are typically determined based on conservative estimates [48]. This could lead to overdimensioning of the distribution grids. To improve the utilization of actual line capacity, the dynamic thermal line rating can be calculated based on real-time operating conditions [44]. For instance, the Heimdall Neuron, developed by Heimdall power, is a sensor that can be installed on power lines and measure critical information, e.g., power, temperature and inclination of the line and the local weather conditions [49]. In [50], a framework for day-ahead thermal state forecasting for distribution network components, such as distribution transformers, underground cables and overhead lines, is proposed.

2.7.2 Power transformers

The power transformer enables transmission and distribution of electric power at different voltage levels, and is among the most important as well as one of the most expensive components in an electrical power system. Any malfunction of this component will affect the reliability of the entire system and possibly lead to large economical consequences for the DSO and the electricity customers [51].

In general, the power rating of a transformer is defined by the nameplate rating. The operating temperature inside a power transformer varies depending on the loading of the transformer, and the nameplate rating is normally, as the line rating of power lines, based on "worst-case" scenarios regarding weather and surrounding conditions. The nameplate rating is known as the *static transformer rating*, as there is no time limit to the rating [52]. Overloading of the transformer could lead to too high temperatures, and hence, unplanned outages or decreased lifetime [51]. In general, large power transformers are more vulnerable to to loading beyond the nameplate rating, and the consequences of a failure will be more severe for larger transformers [53].

Despite the fact that overloading normally will influence the efficiency and aging of power transformers, occasional and short-time overloading is in many cases accepted by the DSO. As the rating is defined by "worst-case" conditions, and therefore conservative estimates of the loading capability, it is possible, under the right circumstances, to overload the transformer with no consequences. [52] states that in cold regions like Norway, there is a great potential for increasing capacity usage of transformers. This could be a measure to improve the utilization of the existing grid distribution grid and reduce the costs from grid upgrades.

3 Methodology

In this chapter, a methodological approach for utilization of smart meter load data for improved insight into the available capacity of a distribution grid is presented. The approach can be used to provide more detailed information about the situation in the grid, and the consequences of new grid connections and increased load demand. Based on this, the need for passive measures, e.g., grid reinforcements, or active measures, e.g., flexibility measures, can be decided [28].

The methodology is customized for a distribution system with the thermal rating of the power lines as the limiting factor. As described in Chapter 2.7.1, this typically applies for systems with shorter lines, e.g., an industrial distribution grid. However, the main aspects of the approach can easily be transferred to grids with other limitations, such as voltage or stability limits. In this case, the power transfer limits must be decided based on the new main limiting factors.

It should be pointed out that there is no universal, one-size-fits-all solution in distribution grid planning [6]. For instance, the grids varies in terms of grid components, weather conditions, load characteristics and use of distributed generation (DG). Therefore, every distribution grid should be assessed individually.

The proposed methodological approach is presented in Figure 10. Later, the steps are presented in more detail.

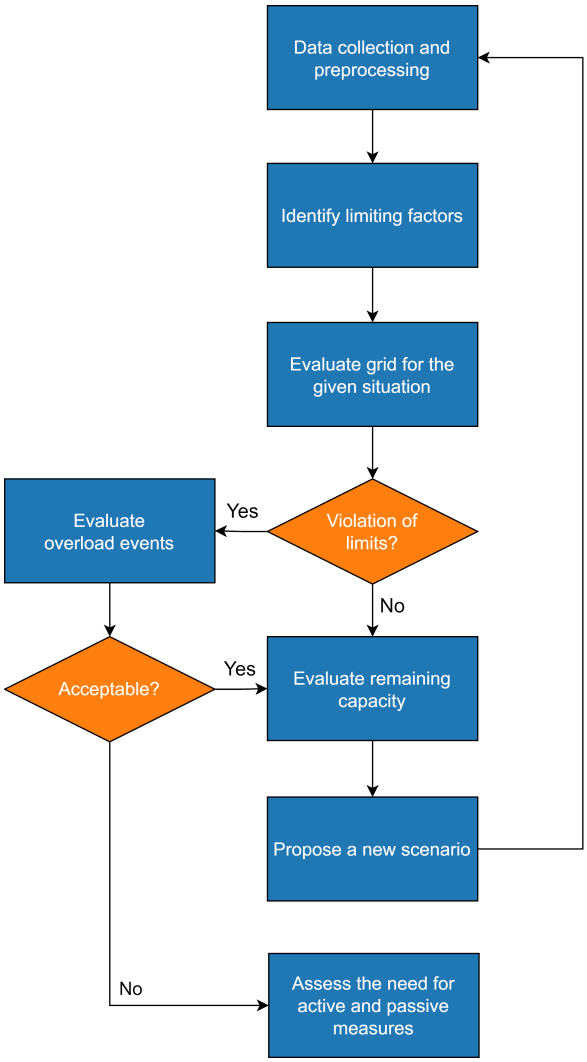

Figure 10: Proposed methodology for evaluation of potential increase in load demand in distribution grids.

3.1 Data collection and preprocessing

Step 1 in the methodology is to collect the relevant data needed for evaluation of the distribution grid. This includes the network topology with the technical data specifications of the components and the load data.

Considering the Python code used in the case study of this project, the preprocessing is also included in the first step. The preprocessing could involve temperature correction of the load time series and correction of daylight saving time measurements with misleading values.

3.1.1 Temperature correction of energy consumption

Temperature correction is performed to remove the fluctuations in the energy consumption due to temperature variation between years. This adjustment makes it possible to compare consumption across different years, and to see load demand trends over time when forecasting future load.

Equation 4 describes a method for temperature correction of metered load values, where the consumption is divided into one temperature dependent part and one temperature independent part [6].

$$P_{i,corr} = P_i + P_i \cdot k \cdot x \cdot (T_n - T_i) \tag{4}$$

where:

- $P_{i,corr}$ is the temperature corrected demand in hour "i" [kWh/h]
- P_i is the measured demand in hour "i" [kWh/h]
- k is the temperature dependent part of the energy use
- x is the temperature sensitivity of the temperature dependent part $[(^\circ C)^{-1}]$
- T_n is the normal daily mean temperature for the specific day $[(^\circ C)]$
- T_i is the average temperature for the last three days $[(^\circ C)]$

Here, the hourly energy consumption is adjusted against the normal temperature T_n, i.e., the historical daily mean temperature for the specific day, for example for the last 30 years. T_i, the 3-days temperature, is the average temperature for the last three days. Because of the time delay of temperature dependency, it is considered to be more correct to use the 3-days temperature as a basis for the correction rather than the daily average [6].

The parameter k represents the temperature dependent part of the energy consumption, and will always be in the interval 0 to 1. The parameter varies between different consumer categories, and will typically be assumed to be lower for industries than for most other groups [54].

3.2 Identify the limits

The next step is to identify the main limiting factors for load increase in the distribution grid for the situation that is evaluated. If the most critical parts of the grid can be determined based on limiting factors, it is possible to reduce the number of scenarios that must be evaluated, and hence reduce the workload of the coming grid evaluation process.

The limiting factors are expressed as power transfer limits, determined by the line ratings of the power lines or the power ratings of the transformers in the grid. As described in Chapter 2.7.1, the line ratings of long power lines is typically determined by stability and voltage limits. For systems with shorter power lines, as the industrial distribution grid of Øra, the power transport limits are often often decided by the thermal rating of the overhead lines, cables or transformers in the grid. To improve the utilization of the actual capacity of the distribution grid, the dynamic line rating can be determined based on real-time operating conditions or with the help of a forecasting model.

In the load data time series used in this project, the demand is given as electric power in kWh/h. Therefore, in order to evaluate if the lines are able to supply the demand of the load points, it would be useful to convert the line ratings from ampacity to power rating. The ampacity, given from the DSO in Ampere, represents the maximum operating line current. The phase voltage of the lines are also known. Then, the power rating of the power lines can be calculated from the following equation:

$$P_{cap} = \sqrt{3} \cdot V_{ph} \cdot I_{max} \tag{5}$$

where:

- P_{cap} is the static line rating of power line [kW]
- V_{ph} is the phase voltage of power line [kV]
- I_{max} is the maximum operating current of power line (ampacity) [A]

For the transformers in the distribution grid, the power limit is defined by the name-plate rating.

As stated in Chapter 2.7.1 and 2.7.2, the rating of a power line or a transformer is normally decided based on "worst-case" conditions. Therefore, occasional short-time overloading could be acceptable to provide better utilization of the actual power rating. This should be evaluated more extensively for each single case.

3.3 Grid evaluation

Further, the situation of the distribution grid is evaluated based on the network data and the historical load data. In the first iteration, the grid will be evaluated in normal operation. while later in the process, different contingency and electrification scenarios can be analyzed. In this chapter, an approach to determine the remaining capacity of the components of the distribution grid is proposed.

The results of the analysis will disclose whether the limiting factors, e.g., the thermal rating of a power line or transformer, are violated or not for the given situation. Given that the one or several of the limiting factors are violated, the severity of the overload events should be evaluated more extensively by the DSO. If the violations are unacceptable, for instance due to reduced lifetime of components or reduced reliability in the grid, the DSO should consider the need for grid measures to meet the load demand. This could imply both passive measures such as grid reinforcement and active measures such as flexibility measures. On the other side, given that limiting factors are not violated or that the violations are seen as acceptable, the next step will be to propose and evaluate future scenarios, e.g., outages of grid components, connection of new loads or increased demand from existing load points.

3.3.1 Time series plot

For a situation where the limiting factors are represented by ratings of the power lines or other components in the network, the load that is seen from the component can easily be compared the limiting power rating. The load can be represented by historical load time series or predicted by a forecasting model. The aggregated load's peak value and profile can be predicted based on the load modelling concepts described in Chapter 2.2. As described in Chapter 3.2, the limitation can be expressed as a constant rating or a dynamic rating, which varies over time, reflecting the actual rating of the component.

An example where a modified load time series of a load point in the industrial distribution grid of Øra is plotted against a selected rating of 100 kW over a three-year period is shown in Figure 11.

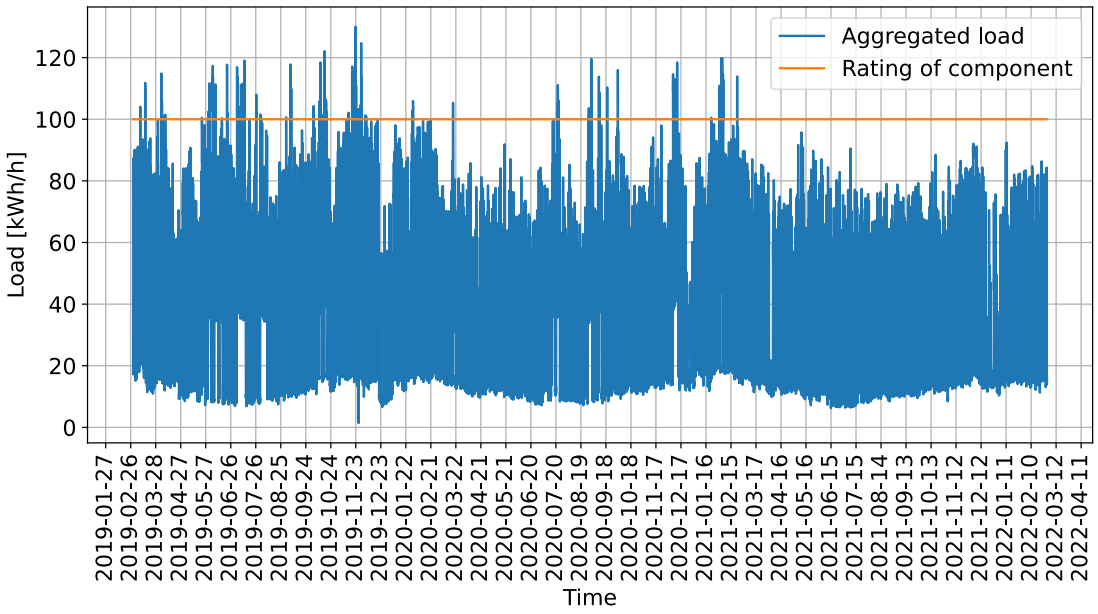

Figure 11: The modified aggregated load time series supplied by a component in a distribution grid and the selected power rating of the component.

As seen from the figure, in this hypothetical example, the rating of the component is exceeded for several hours during the time period. The highest peak exceeds the rating by 30%. Violation of the limiting factors could often be an indication of a need for grid reinforcements or improved flexibility in the grid. However, as described earlier, in some cases, this can be acceptable for the DSO, depending on the duration of the overload, weather conditions and other circumstances. Therefore, for such cases, the potential overload events should be investigated in more detail.

3.3.2 Remaining capacity

As a continuation of the example from Figure 11, the remaining capacity (capacity margin) is the difference between the rating of the component and the load time series over time. The remaining capacity describes the available capacity in the analyzed component, and hence, the room for additional electrification and load increase in the grid. The relationship between the capacity of the components, the load supplied by the component and the resulting remaining capacity is illustrated in Figure 12.

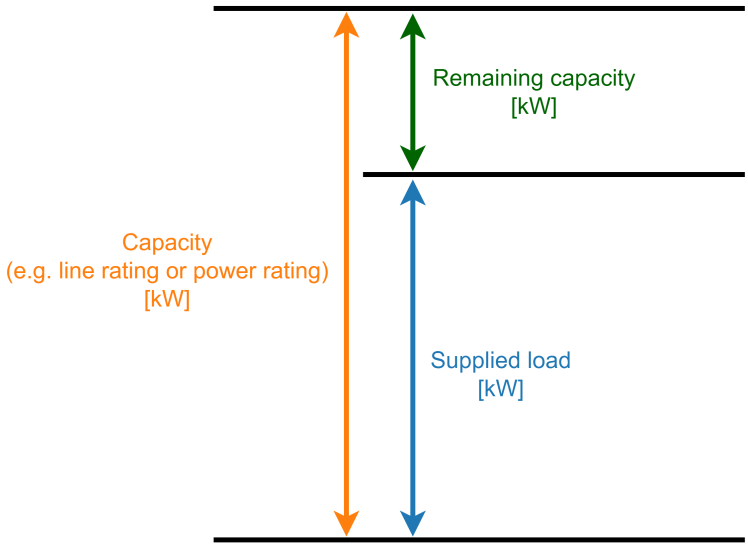

Figure 12: Remaining capacity of grid components.

The remaining capacity of a component in the distribution grid can be calculated as following:

$$\Delta P(t) = P_{lim}(t) - P(t) \tag{6}$$

where:

- $\Delta P(t)$ is the remaining capacity [kW]
- $P_{lim}(t)$ is the rating of the component [kW]
- $P(t)$ is the aggregated load supplied by the component [kW]

The remaining capacity for the example introduced in Chapter 3.3.2 is plotted in Figure 13 for the three-year period. As seen from the figure and Equation 6, the remaining capacity value is defined as positive when the rating of the component is greater than the aggregated load supplied by the grid component. Conversely, an overload event will result in a negative remaining capacity.

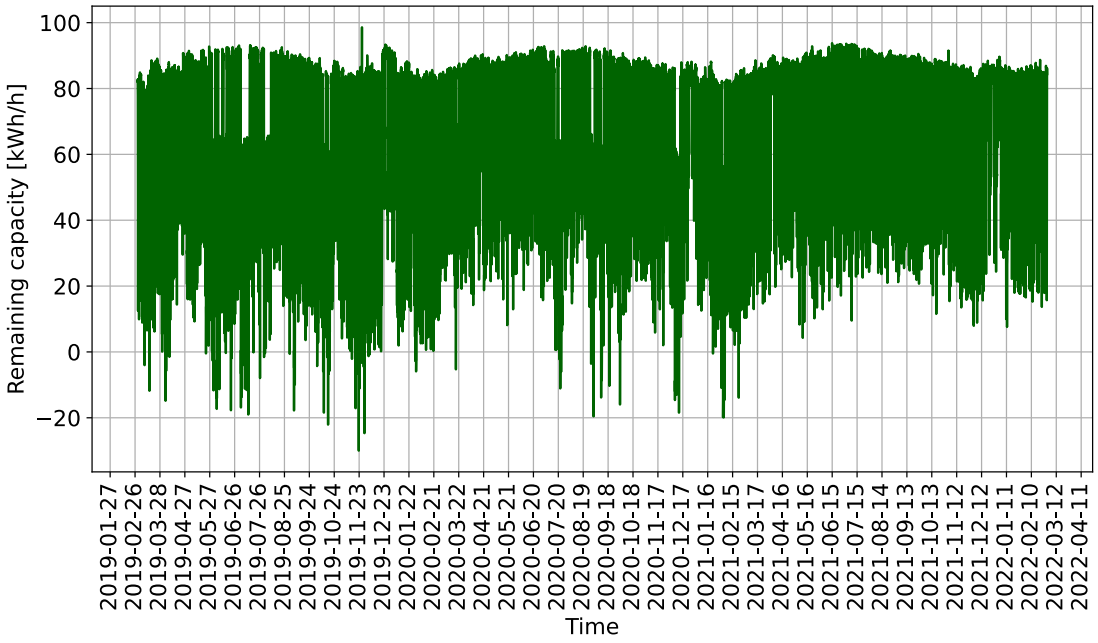

Figure 13: The remaining capacity of a component in a distribution grid during a three-year period.

For the example in Figure 3.3.2, it can be seen that the overload events occur both during summer and during winter. For a component that is placed outdoor, the actual thermal capacity often depends on the outdoor temperature. Thus, the summer peaks could have a greater impact on the component's efficiency and lifetime.

3.3.3 Cumulative distribution

To complement the information, about the point in time an overload event occurs and how the remaining capacity varies over time, provided by the load time series plot in Figure 11 and the remaining capacity plot in Figure 13, the remaining capacity can be presented as a cumulative distribution function. Similar to the measurements in the load duration curve in Chapter 2.2.2, the remaining capacity values are sorted. However, here, the values are sorted in ascending order and the remaining capacity is used as x-axis parameter. The cumulative distribution function describes the probability that the (random) remaining capacity is smaller than or equal to x, $S(x) = P(X \geq x)$.

The corresponding cumulative distribution function to the example remaining capacity plot, in Figure 13, is shown in Figure 14.

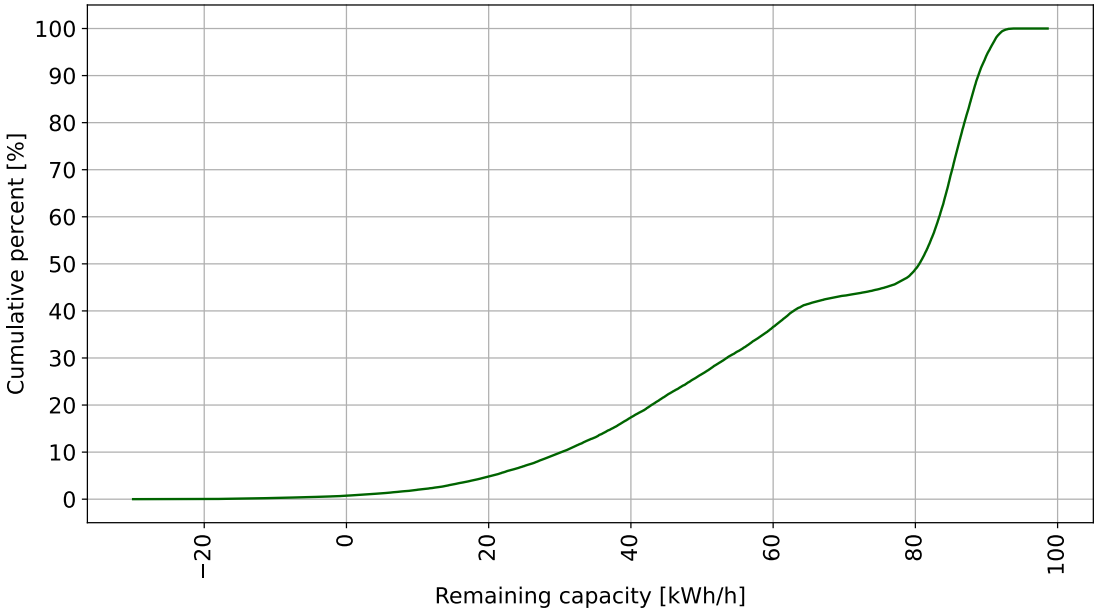

Figure 14: The cumulative distribution function for the remaining capacity of a component in a distribution grid during a three-year period.

The cumulative distribution function is suitable to illustrate how much of the time the excess capacity is below a given value, and hence, the room for increasing the load of the consumers in the grid. For instance, for the example in Figure 14, the excess capacity will be below 30% of the component rating for around 10% of the time period. In Chapter 2.5, the N-0.9 criterion, proposed by Aabø Powerconsulting, was described. Given that the example in Figure 14 shows the cumulative distribution for an outage scenario, and the DSO accepts N-0.9 security for this situation, the consumption can be increased by 30% of the component rating without violating the criterion.

3.3.4 Overload events

Given that the limiting factors are violated for the given situation, the overload events should be analyzed as a part of the grid evaluation step.

In this project, overloading means that the aggregated load supplied by a grid component is greater than the power transfer limit determined in the second step of the methodological approach. In the case study in Chapter 5, the ampacity of the power lines and the nameplate rating of the transformers are used to determine the power transfer limits. As described in Chapter 2.7.1 and 2.7.2, the static ratings of lines and transformers are often based on conservative estimates of the loading capability. Hence, in order to improve the utilization of the existing grid components, overloading during shorter periods of time could be acceptable in some cases.

To investigate the frequency and magnitude of the overload events, the cumulative distribution function can be utilized further. A zoom-in of the overloading part of the cumulative distribution function in Figure 14 is shown in Figure 15. Figure 15a show the cumulative distribution of all the overload events, while Figure 15b shows the distribution for the 20 overload events with the greatest overloading in terms of magnitude.

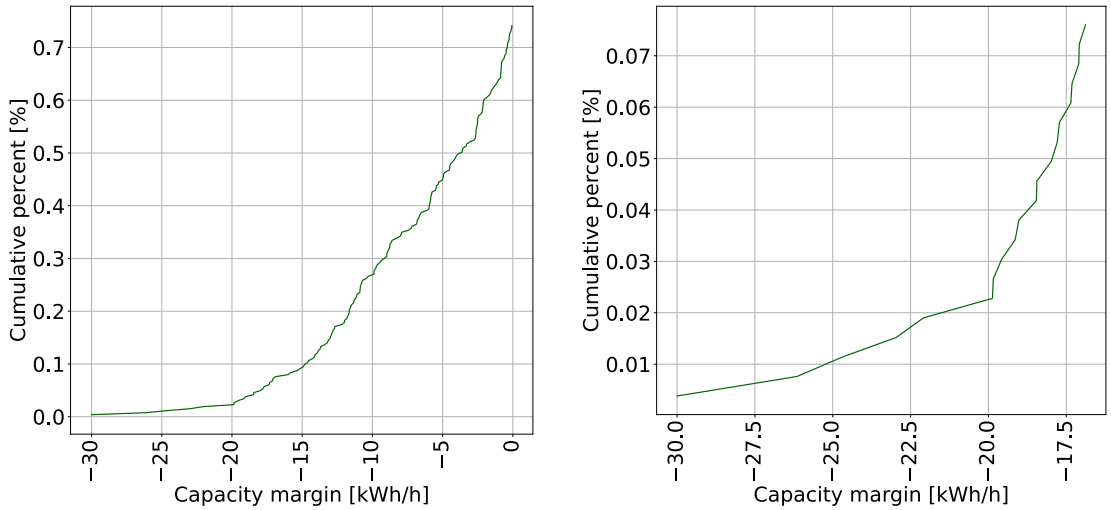

(a) Remaining capacity for all overload events.

(b) Remaining capacity for the 20 overload events with the greatest negative value.

Figure 15: A zoom-in of the overload events of the cumulative distribution function for the remaining capacity of a component in a distribution grid during a three-year period.

From the zoom-in of the cumulative distribution, as shown in Figure 15, the frequency of overload events with magnitude above a certain value can be found. For example, from Figure 15, it can be seen that the rating of the component was exceeded by 15% or more about 0.1% of the three-year period. For about 0.01% of the time, the rating was exceeded by more than 25%. This is seen from Figure 15b. It can be seen that most of the overload event has a relatively small absolute value.

3.4 Future scenarios

As described in Chapter 3.3, if the grid evaluation step concludes with no violation of the limiting factors or that the violations are acceptable, the next step is to point out future scenarios where the distribution grid potentially is put under pressure. For this project, there will be two main types of future scenarios that will be investigated; scenarios with outages of grid components and scenarios with increased load demand. Such a scenario-based approach is suitable to capture uncertainties in the long-term grid development [28].

An outage of a power line or a transformer could possible have fatal consequences for the power supply in a distribution grid. Therefore, a contingency analysis should be included in grid planning and evaluation processes. As described in Chapter 2.6, for complex distribution grids, there will be an extensive number of possible outage scenarios. Thus, the workload can be reduced by pointing out the parts of the distribution grid where an outage will be most critical. For less complex grid, this process could reduce the number of outage scenarios to analyze to only some few. The selection of the most critical parts will be based on both the technical data of the component, e.g., the power rating, and the aggregated load seen by the component.

To evaluate the room for connection of new load points or electrification of processes at the existing load points, the consequences of increased load demand in the distribution system should be investigated. Also here, it could be advantageous to evaluate the "worst-case" scenario in terms to capture numerous different scenarios with various degrees of severity, To reduce the costs of the coming electrification, the DSO should strive to improve the utilization of the existing power grid. Therefore, a relevant scenario for many distribution grid cases would be to evaluate the consequences of increasing the load demand such that the capacity in existing grid components to the full.

4 Data set

4.1 Norgesnett and Øra Industripark

The load and network data used in this project was provided by Norgesnett, which is a Norwegian DSO with about 100 000 customers. In addition to Fredrikstad, Norgesnett operates the distribution grid in Røyken (Asker), Enerbakk and Ski (Nordre Follo), Hvaler and Nesodden in eastern Norway and Askøy in western Norway [55].

Øra industrial park is a port and industrial area outside the old town of Fredrikstad in the south-eastern part of Norway. The area is bordered on Glomma, Norway's longest river, and has, since the early 1900s, been an important centre for industries and development [56]. Today, the area is the home of an assortment of industry actors, including food industry, district heating and LNG storage and distribution. Additionally, Øra houses recycling plants for for example batteries, vehicle parts and waste.

4.2 Network data

As earlier mentioned, the network used in the analysis part is based on a part of the industrial distribution network of Øra industrial park.

The considered part of the network consist of two radials. In this thesis, the radials are labeled as Radial A and Radial B. The radials are connected through an breaker, so that they can work as reserves for each other, in case of a outage or failure of a network component, e.g., a cable or a transformer.

The nodes and loads in each of the radials are anonymized, and renumbered based on voltage level. To illustrate the numbering system, an example radial, Radial R, is drawn in Figure 16.

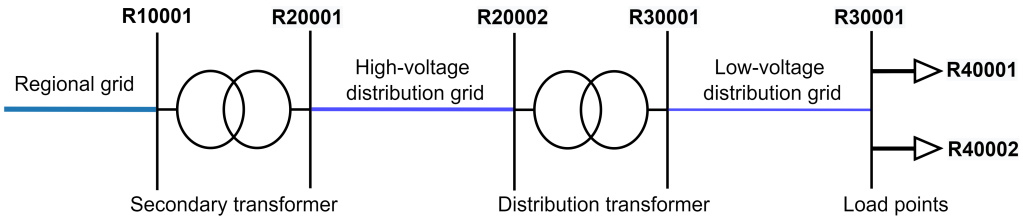

Figure 16: An example radial to illustrate the structure and numbering system for the distribution grid of Øra.

In the example radial in Figure 16, the letter R of the labels indicates that these nodes are a part of Radial R. Furthermore, the nodes are numbered based on voltage level so that all the nodes starting with the same number represents the same voltage segment of the grid. Node R10001, is connected to the regional grid and represents the high-voltage side of the secondary transformer. The secondary transformer, placed between R10001 and R20001, works as the interface between the regional grid and the high-voltage segment of the distribution grid. For the Øra grid, the high-voltage side has a base voltage of 47 kV, before the voltage is transformed down to 11 kV at the low-voltage side. Hence, all the nodes in the radials labeled with "2" as the first number, will have the same base voltage of 11 kV. Further, the power is transmitted through high-voltage cables, in this example network represented by the branch between R20001 and R20002, to the distribution transformers. The distribution transformers transform the base voltage level from 11 kV to the utilization level of 230 V or 400 V, and separates the high-voltage distribution system from the low-voltage distribution system. The nodes in the low-voltage distribution system are labeled with "3" as the first number. Since the low-voltage distribution system is not the main

focus of the coming case study, the low-voltage side of the distribution transformer is considered as only one node. The load points, or end-users, in the network is represented by arrows.

A simplified, anonymized model of Radial A is presented in Figure 17. The secondary transformer, located between the nodes A10001 and A20001, is a part of the Øra secondary substation. Since this is a network with radial structure, the secondary transformer and the main branch sees the aggregated load from all the loads in the radial.

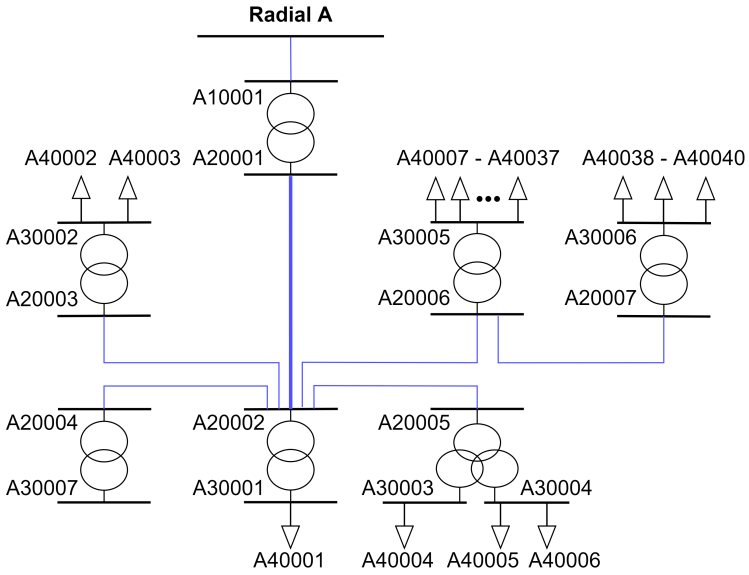

Figure 17: A simplified model of Radial A.

As can be seen in Figure 17, Radial A consists of 40 load points, represented by arrows. Most of the loads, from Load A40007 up to Load A400037, are connected to the distribution transformer placed between Node A20006 and Node A30005. It should also be noticed that the distribution transformer placed between Node A20004 and Node A30007, is not connected to any loads. The distribution transformer to the right in the figure, with A20007 as high-voltage side, is the only that is not directly connected to the node A20002.

A simplified, anonymized model of Radial B is presented in Figure 17. The transformer between B10001 and B20001, as well as the thickened blue line between Node B20001 and Node B20002, sees the aggregated load from all loads in the grid. The numbering system is the same as for Radial A.

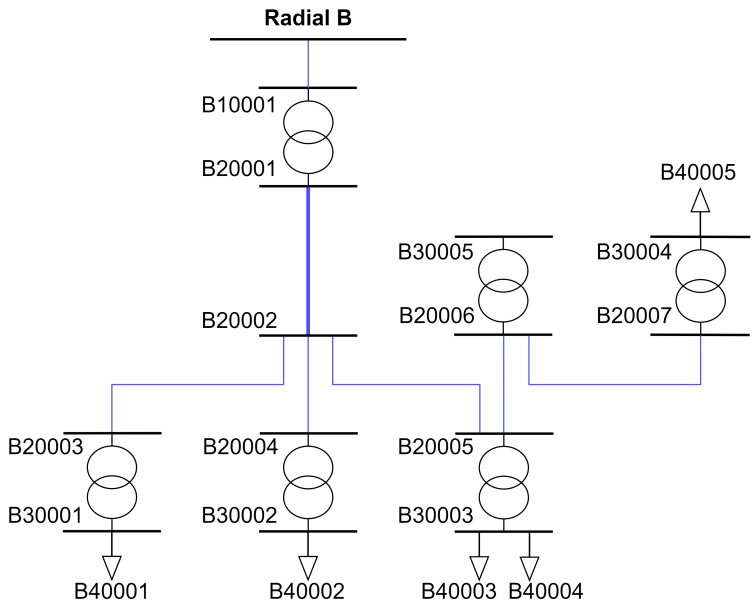

Figure 18: A simplified model of Radial B.

As shown i Figure 18, Radial B consists of 5 load points. The distribution transformer placed between B20005 and B30003 is the only that supplies more than one load. Currently, the transformer with low-voltage side represented by Node B30005 is not connected to any consumption.

The two radials are connected through a breaker, further referred to as the "reserve branch". Figure 19 presents the simplified model of Radial A, Radial B and the connection between them. The red line represents the reserve branch between Radial A and Radial B.

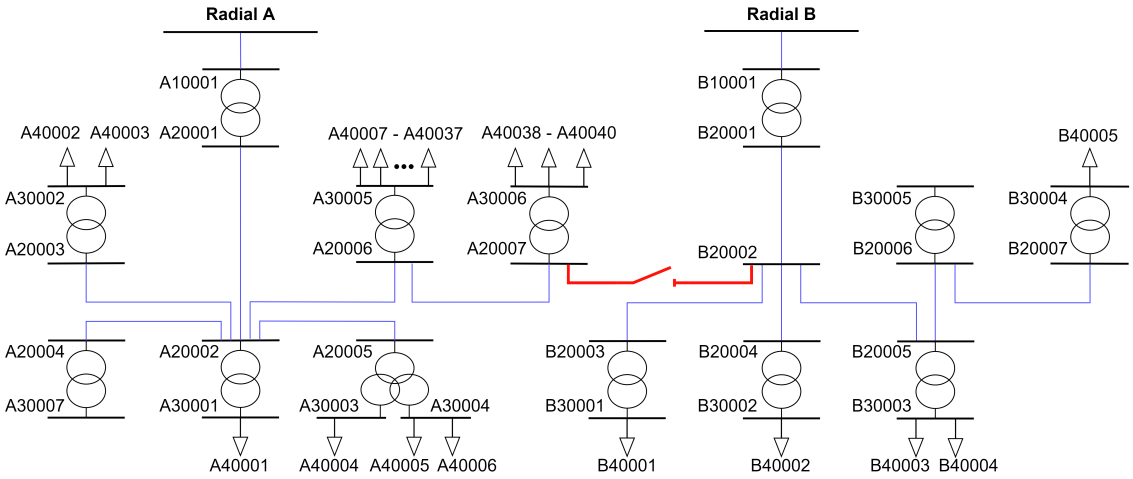

Figure 19: A simplified model of Radial A and Radial B.

According to the description of distribution system structures in Chapter 2.1.1, this grid can be characterized as meshed with a traversing connection structure. Under normal operation, the breaker is open, and Radial A and Radial B are operated as two individual radial distribution grid. However, when a fault occurs in one radial, the breaker can be closed to make it possible to supply the affected consumers from the other radial. The number of consumers that can be supplied depends on the fault location. The outage scenarios will be analyzed in detail in Chapter 5.2.

Further in the report, the term child-loads is used. This term refers to all the loads that contribute

to the aggregated load for the node. Thus, to be considered as child-load of a node, the load is not required to be directly connected to the load. Since the system is assumed to be lossless, the contribution of the load B40001 will be the same in Node B30001 as in Node B10001. To exemplify, in Radial B, Node B30003 has the loads B40003 and B40004 as child-loads. The nodes B10001, B20001, B20002 have all the consumer loads in the system as child-load.

4.3 Load data

The data set contains measured hourly load data for two radials in the distribution network of Øra for a period of 3 years, from 01.03.2019 to 28.02.2022. This equals a duration of 1095 days.

The temperature corrected aggregated load time series for Radial A is shown in Figure 20. The load data is given in kWh/h.

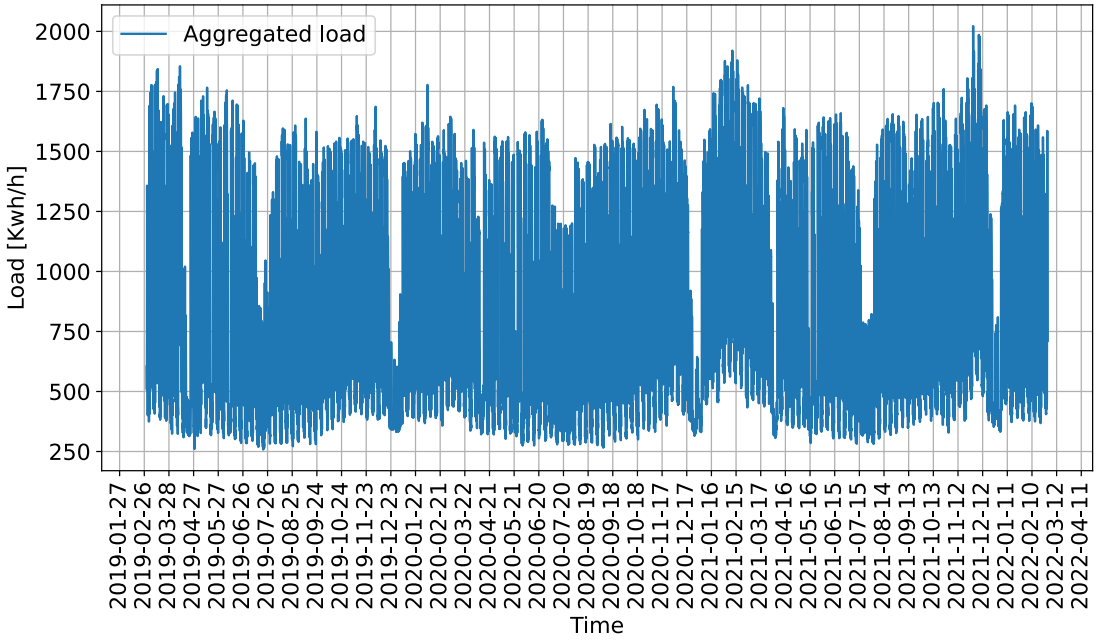

Figure 20: The temperature corrected aggregated load time series for Radial A.

It should be noted that not all the loads have measurements for the entire period. For Radial A, the data set contains load data only from 01.10.2019 for the load A40003 and from 08.05.2020 for A40037. Thus, the data set for Radial 1 has 214 days with 38 loads connected, 220 days with 39 loads connected and 661 days with all 40 loads connected. However, the added loads for this radial are relatively small compared to the aggregated load of the radial, and it is hard to spot any change in the load time series in Figure 20. To quantify the effect, before the addition of A40003, the temperature corrected average load of the radial is calculated to 785.2 kWh/h. With the addition of A40003, the average is increased with 1.03% to 808.9 kWh/h between 01.10.2019 and 08.05.2020. After A40037 is connected, the average is additionally increased with 0.26%, compared to the period with 39 loads connected, to 810.99 kWh/h. The peak load for Radial A during the three years after temperature correction is measured to 2022.1 kWh/h at 30.11.2021 at 10:00.

The characteristics of the Radial 1 network in terms of load aggregation and the behavior in peak load situations was investigated in detail in the specialization project. One of the main results was a strong correlation between A40001, the largest load in the system, and the aggregation of all the loads in the Radial. In average, A40001 was responsible for 48.9 % of the radial's temperature corrected consumption during the three-years period.

The temperature corrected aggregated load time series for Radial B is shown in Figure 21. The

load data is given in kWh/h.

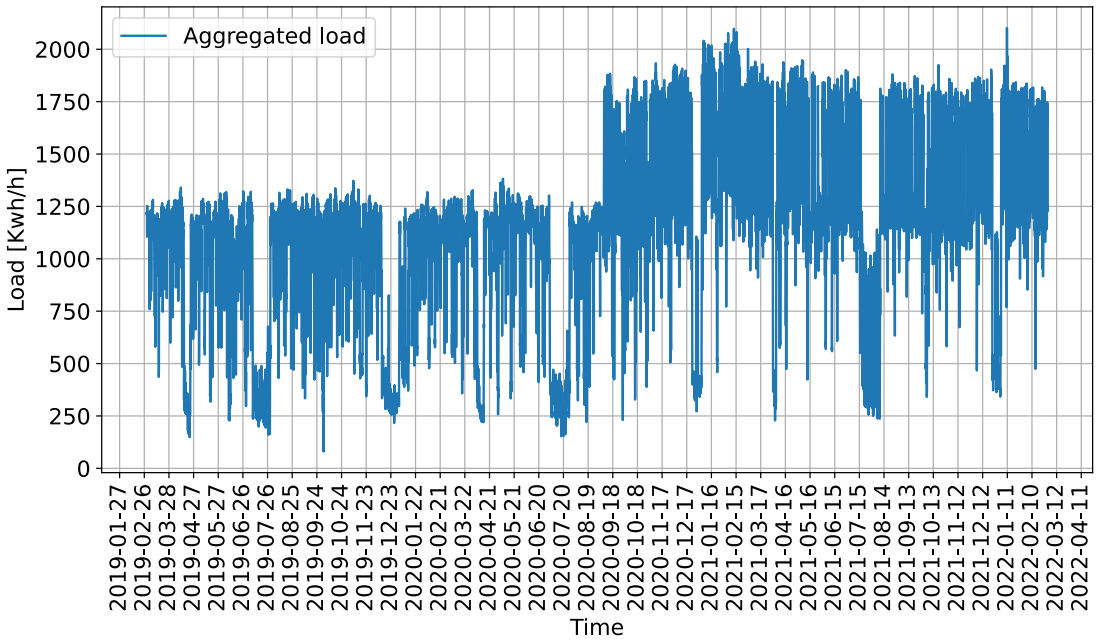

Figure 21: The temperature corrected aggregated load time series for Radial B.

For Radial B, the hourly data for the loads B40001 and B40002 starts at 07.09.2020. Therefore, the data set consists of 556 days with only three connected loads, and 539 days with all five loads. The effect of the added loads is clearly shown by the load lift around the date of addition in the aggregated load time series for Radial 2 in Figure 21. Before the addition of the extra loads, the temperature corrected average load of the radial is calculated to 969.8 kWh/h, while after the addition, the average is calculated to 1307.1 kWh/h. This equals a increase of 34.78% between the two periods. The peak load for Radial B during the three years after temperature correction is measured to 2101.2 kWh/h at 10.02.2021 at 14:00.

Given an outage situation, it is possible that the power source of one of either Radial A or Radial B will need to supply all the load points in the network. In this case, the power source and the main branch of the radial will see the aggregated load from all the loads in the network. After the addition of B40001 and B40002 at 07.09.2020, this includes all the 40 loads in Radial A and all the 5 loads in Radial B. The temperature corrected aggregated load time series for the whole network is shown in Figure 22.

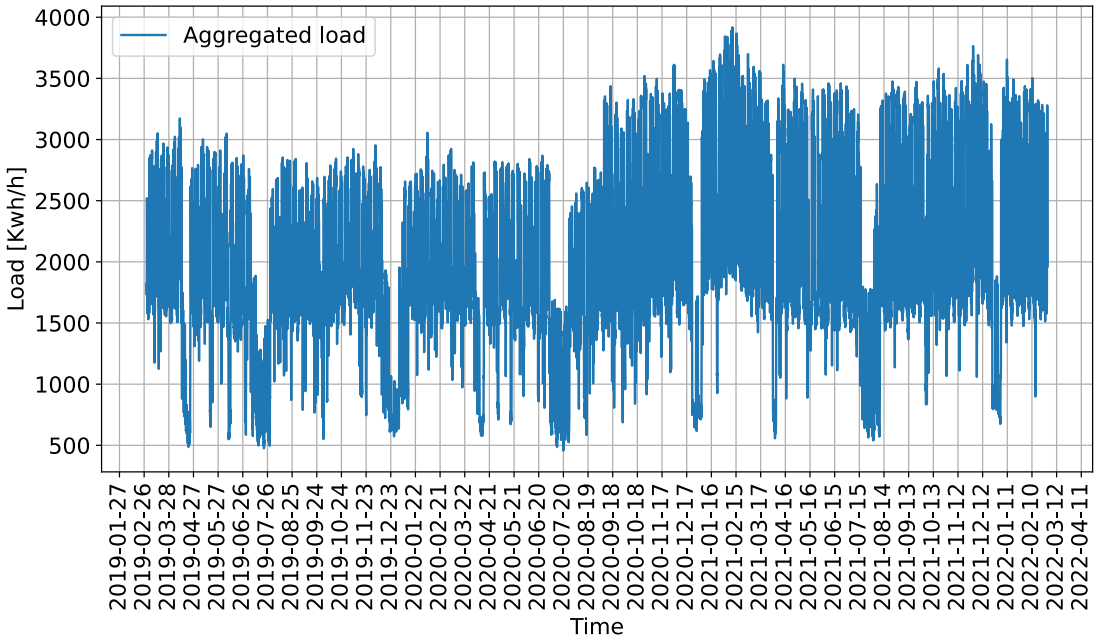

Figure 22: The temperature corrected aggregated load time series for all the loads in the network.

The peak load for the whole network during the three years after temperature correction is measured to 3917.9 kWh/h at 10.02.2021 at 14:00. It should be noted that this is the same hour as the peak load for Radial B occurred.

The aggregated load time series in Figure 20, Figure 21 and Figure 22 illustrate that the consumption drops to lower values for some longer periods of time in the same periods each year. Further investigation reveals that these periods correspond to Easter holiday, summer vacation and Christmas. Since this is a distribution grid with mostly industrial consumers, it is natural that the load is reduced during vacations and on national holidays.

4.3.1 Covid-19 impact

The outbreak of the Covid-19 pandemic at the beginning of 2020 was unprecedented and caused new challenges for different parts of the society. Countries all over the world have undertaken restrictive measures in order to tackle the pandemic and minimize the spread of the virus. The situation with partial or full lockdown had significant impact in numerous industries, including production, agriculture, transport and recycling [57] [58]. The resulting impact on total demand and energy use patterns of the consumers, due to the drastic changes, put pressure on the energy sector [59].

In Norway, the first restrictive measures were introduced in March 2020. Therefore, the given time series includes approximately one year of load data before the beginning of the pandemic and two years of load data affected by more or less intrusive measures. To get an indication of the Covid-19 impact on this industrial distribution network, the average demand before the pandemic can be compared to the demand after the introduction of the measures. To avoid the load increase due to introduction of new load points during the time series, the demand of the loads A40003, A40037, B40001 and B40002 is not included in the calculations.

The results show that the temperature corrected average demand is increased from 799.2 kWh/h to 804.2 kWh/h for Radial A and from 978.6 kWh/h to 1024.1 kWh/h for Radial 2. Thus, the results contradict the obvious assumption that the lockdown and remote working would cause a drop in the consumption. On the other hand, the total increase of energy consumption is in accordance with the ongoing electrification. It should be noted that the examination is based on historical data

from a relatively short time period, and there is a high degree of uncertainty around the results. It seems difficult to isolate the Covid impact from this impact of the electrification process. Hence, it is not clear to what extent the Covid-19 lockdown had an influence on the consumption of the industrial customers in this part of Øra.

4.3.2 Temperature correction

To remove fluctuations due to temperature variation between years, the time series presented in Figure 20 and Figure 21 are temperature corrected according to the method presented in Chapter 3.1.1 and the results from the specialization project. In the specialization project, the outdoor temperature's effect on the energy consumption of the loads in Radial 1 was investigated. The temperature dependent part of the consumption was estimated to 9.1% for workweek days and 15.6% for weekend days. Based on a weighted average of these results, the temperature dependent part of the consumption, represented by the parameter k, is set to 11.0%. It should be pointed out, that this is a relatively low temperature dependency compared to other consumer groups, and the specialization project concluded that other factors, like holiday seasons or weekends, was found to be more determining for the energy consumption. Based on Tønne's Ph.D. thesis [6], the temperature sensitivity x for the temperature dependent part of the consumption is set to 5%.

4.3.3 Daylight saving time correction

In Norway, daylight saving time is practiced so that darkness falls at a later clock time during the summer half term. The clock is set forward by one hour on the last Sunday in March, and back by one hour on the last Sunday in October. As a consequence, one day in the spring has only 23 hours, while one day in the fall has 25 hours. In the time series, this gives one missing hour in March with zero consumption, and one hour in October with "double" consumption, i.e., the sum of the consumption from two subsequent hours. To adjust for these extreme values, a new function was implemented to the preprocessing step. To correct for the missing hour, the average of the measured consumption in the hour before and the hour after the missing hour is used. For the hour in the fall with "double value", the average of the two underlying values are used.

4.4 Meteorological data

For temperature correction of the energy consumption, daily temperature data for the area is needed. In Norway, meteorological data from different climate measuring stations is published by the Norwegian Meteorological Institute monitor and can be downloaded from https://seklima.met.no/. Strømtangen Fyr in Fredrikstad is found to be the station closest to Øra industrial park. Therefore, daily temperatures and normal temperatures for Strømtangen Fyr is used to decide the outdoor temperature used in the temperature correction procedure. The data set used contains daily mean temperature data from 01.01.2000.

It should be pointed out that the downloaded data set was missing temperature data for three of the days within the period; 08.09.2021, 09.09.2021 and 03.11.2021. In these cases the average temperature of the day before and the day after the period with no temperature data was calculated and used.

5 Results and discussion

In this chapter, the results obtained by applying the proposed methodological approach for evaluation of remaining grid capacity, from Chapter 3, on the industrial distribution grid of Øra, will be presented and discussed. The main focus of the analysis will be on the parts of the network where the reserve branch can be utilized in case of a fault or outage.

5.1 Normal operation

According to Norgesnett, the network capacity, and especially the capacities of the cables in the high-voltage distribution grid, is the limiting factor in the coming electrification process for this distribution grid. In this part, the current situation of the two radials in the distribution grid of Øra will be presented and discussed, based on the available grid data and load data from the three-year period. The main focus will be on the remaining capacity of the cables and transformers in peak load situations. Since this part is based on normal operation, without use of the reserve branch, the radials are analyzed individually.

5.1.1 Radial A

A simplified model of the high-voltage distribution grid, including the distribution substations, of Radial A is shown in Figure 23. The branches and the distribution transformers, represented by squares, are labeled based on the connected nodes. For each transformer, the number of child-loads is shown in the parenthesis.

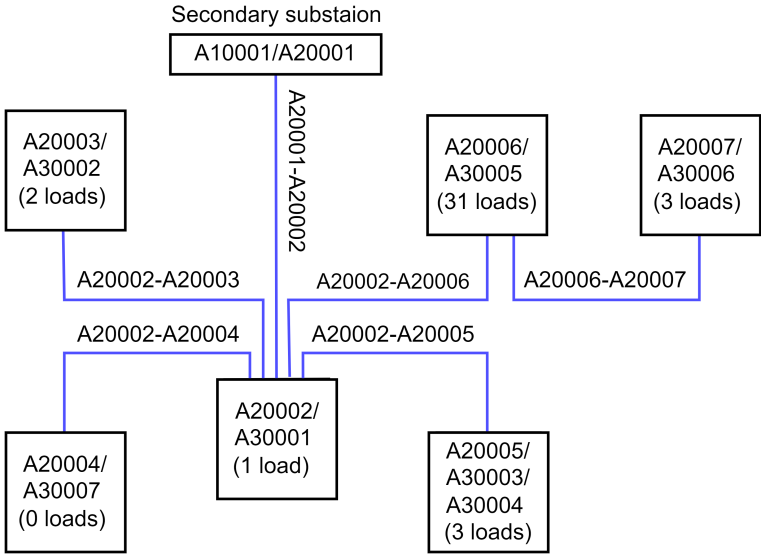

Figure 23: A simplified model of the high-voltage distribution grid of Radial A.

Figure 24 shows the peak load seen from each cable in Radial A during the three-year period. The red line illustrates the corresponding line ratings. For one of the cables, A20002-A20003, the line rating was unknown. Therefore, the lowest of the known rating values was used. Since the historical demand covered by this branch is very low, this will probably not affect the overall results.

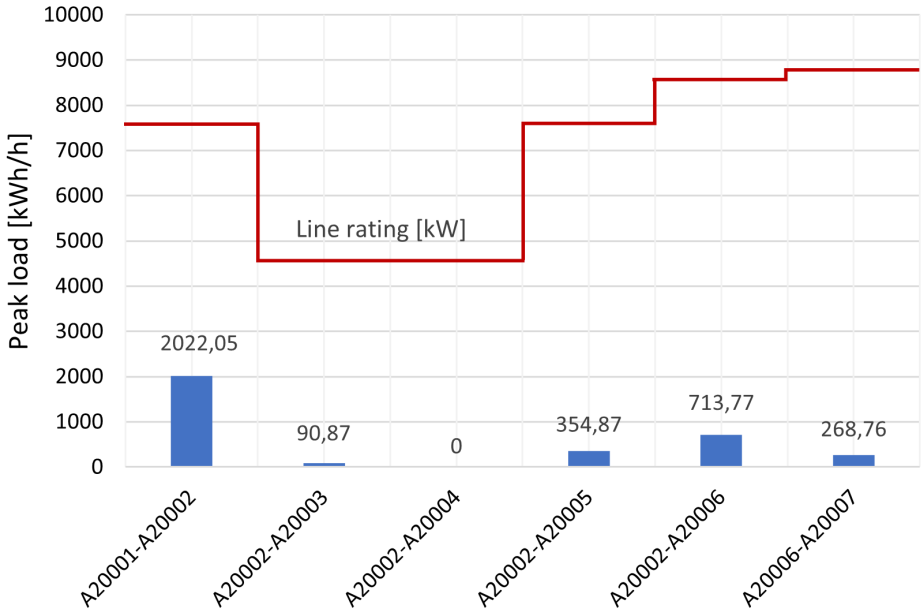

Figure 24: The aggregated peak load for each branch in the 11 kV grid of Radial A during the three-year period and the corresponding line ratings.

As seen from the figure, all the branches have an abundance of remaining capacity during the whole period. The remaining capacity for each branch in aggregated peak load situation is shown in Table 2.

Table 2: Line rating, aggregated peak load and corresponding remaining capacity for the branches in Radial A.

Branch	**Line rating [kW]**	**Peak load [kWh/h]**	**Remaining capacity [kWh/h]**
A20001 - A20002	7621.0	2022.1	5598.9
A20002 - A20003	4572.6	90.9	4481.7
A20002 - A20004	4572.6	0.0	4572.6
A20002 - A20005	7621.0	354.9	7266.1
A20002 - A20006	8668.9	713.8	7955.1
A20006 - A20007	8859.4	268.8	8590.6

As shown in Figure 24 and Table 2, the main branch, which is connecting the secondary substation to the rest of the radial, carries the highest load of the branches in Radial A, both in absolute value and relative to the line rating. However, the margin between the aggregated load and the line rating is never lower than 5598.9 kWh/h. All the branches had a remaining capacity greater than 4.4 MW throughout the whole three-year period. Hence, the cables in Radial A has no problems to supply the required load under normal operation, based on the historical load data.

In addition to the branch capacities, the power rating of the transformers in the grid could also be a limiting factor in the coming electrification process. The bar chart in Figure 25 shows the temperature-corrected aggregated peak loads during the three years seen from the distribution transformers in Radial A. The red line illustrates the corresponding power rating of each transformer.

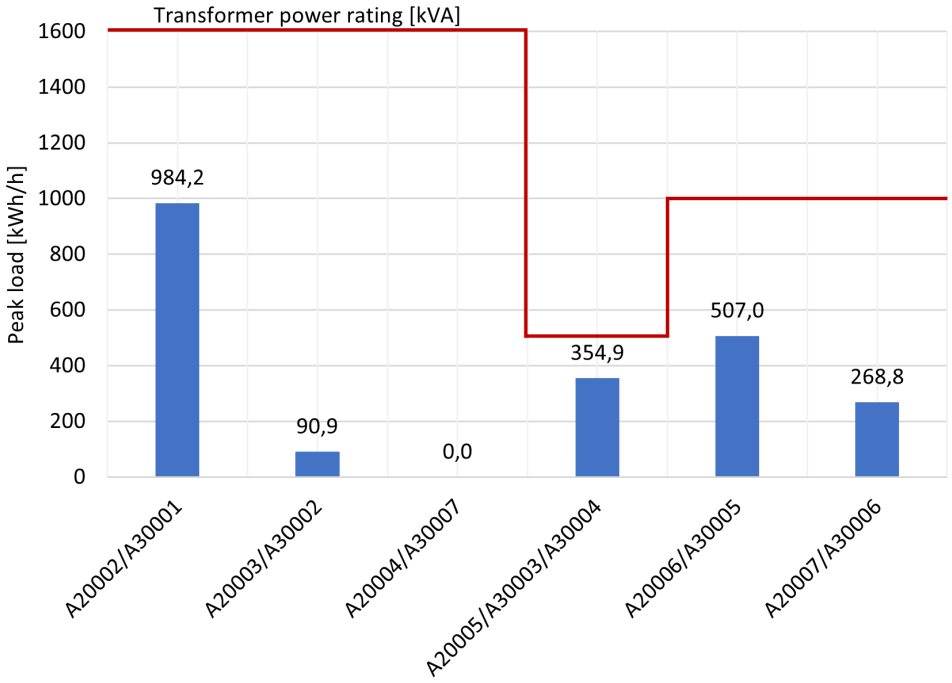

Figure 25: The aggregated peak load seen from each distribution transformer in Radial A during the three-year period and the corresponding transformer power ratings.

It can be seen from Figure that, in general, the distribution transformers of Radial A have sufficient capacity to cover today's energy demand. The remaining capacity for each transformer under peak load is calculated, and presented in Table 3.

Table 3: Power rating, aggregated peak load and corresponding remaining capacity for the distribution transformers in Radial A.

Transformer	**Power rating [kVA]**	**Peak load [kWh/h]**	**Remaining capacity [kWh/h]**
A20002 / A300001	1600	984.2	615.8
A20003 / A30002	1600	90.9	1509.1
A20004 / A30007	1600	0.0	1600.0
A20005 / A30003 / A30004	500	354.9	145.1
A20006 / A30005	1000	713.8	286.2
A20007 - A30006	1000	268.8	731.2

The table shows that all the distribution transformers have sufficient capacity to cover the historical load demand from the load points. Especially the transformers A20003/A30002 and A20004/A30007 have plenty of remaining capacity throughout the whole period, and provide an opportunity to increase the consumption in Radial A without requiring costly transformer investments. Since there is no load points connected to A20004/A30007, the peak load is measured to 0 kWh/h.

For the three-winding transformer A20005/A30003/A30004, the aggregated peak load and power rating are presented only for the primary winding, connected to the high-voltage node A20005. It can be seen that this winding has the narrowest margin in Radial A, both in absolute value and relative to the rating. Here, The ratings of the secondary winding connected to A30003 and the tertiary winding connected to A30004 are 300 and 200 kVA, respectively. As seen from the grid model for Radial A in Figure 17, the secondary winding is connected to one load point (A40004) and the tertiary winding is connected to two load points (A40005 and A40006), and investigation of the load data shows that the tertiary winding node A30004 in general sees the highest aggregated load. Based on the combination of the lowest power rating and the highest load, the temperature-

corrected load time series is plotted against the power rating of the tertiary winding in Figure 26, to check if the rating is exceeded.

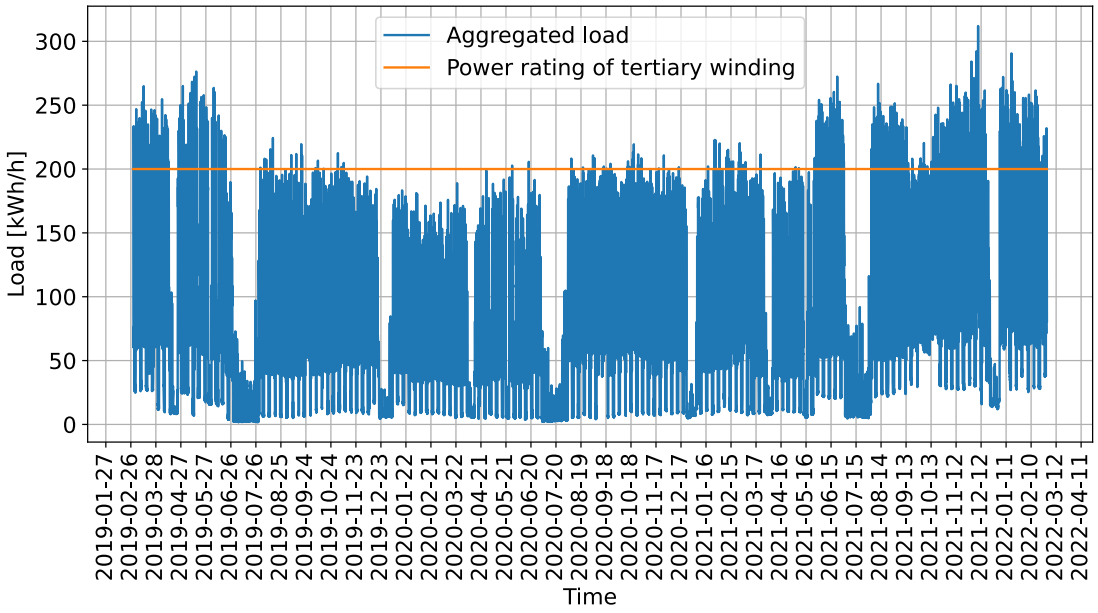

Figure 26: The aggregated load time series of the load points connected to the tertiary winding node A30004 and the corresponding power rating.

As can be seen from Figure 26, the power rating of the tertiary winding is exceeded for a considerable amount of hours, especially at the beginning and the end of the three-year period. Possibly, this could affect the lifetime of the transformer. The cumulative distribution of the capacity margin is drawn in Figure 27a. A negative value for the remaining capacity represents that the power rating is exceeded. A zoomed in plot of the overload events is shown in Figure 27b, and the 20 overload events with the largest margin are shown in Figure 27c.

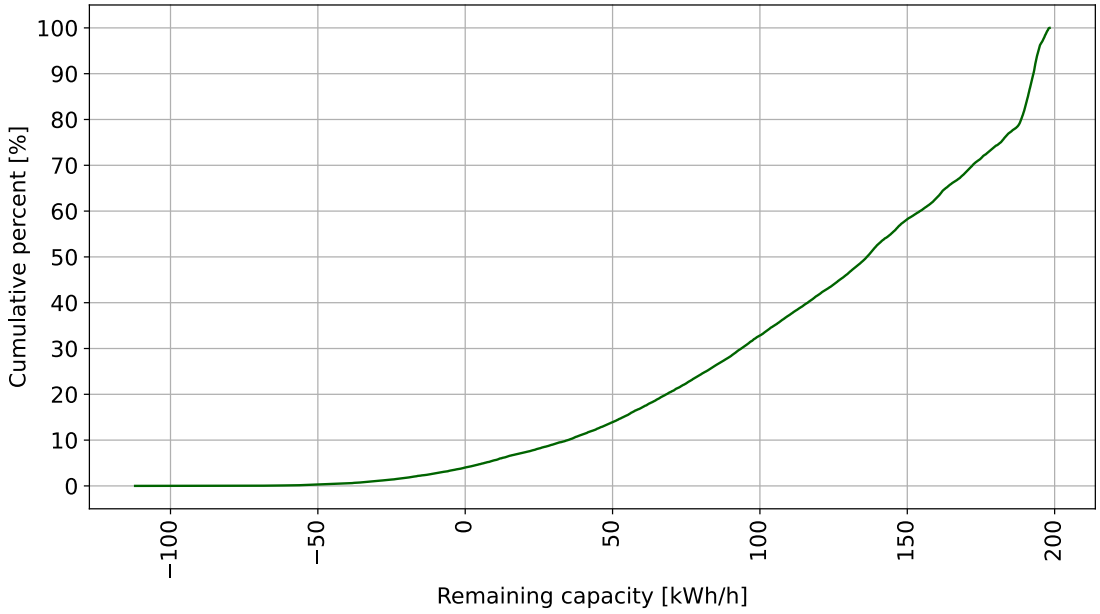

(a) All hours.

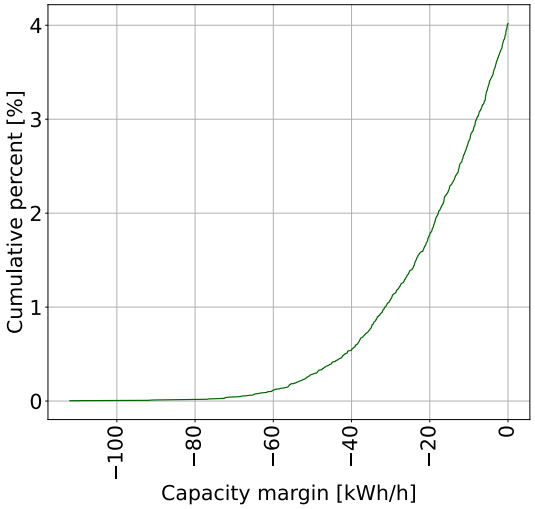

(b) Zoom-in of all overload events.

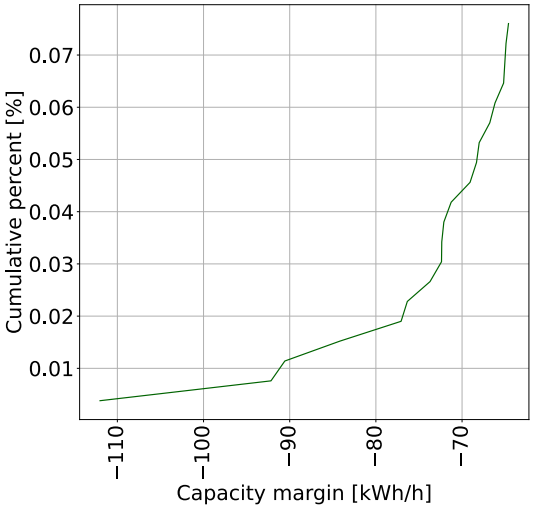

(c) Zoom-in of the 20 overload events with the greatest amplitude.

Figure 27: The cumulative distribution of the remaining capacity for the tertiary winding node A30004.

The curve in Figure 27a has a slow growth to the left in the figure. This indicates that the rating is exceeded for relatively few hours during the three-year period, but in the hours where the capacity is exceeded, the load is often considerably higher than the power rating. This interpretation is confirmed by the load time series in Figure 26.

As shown in Figure 27b, the power rating of the distribution transformer is exceeded for 4.0% of the time period. This equals 1057 hours. Figure 27c, which includes the margin for the 20 highest load measurements, shows that the power rating is exceeded by more than 40%, i.e., more than 80 kWh/h, in only some few hours during the three-year period. The peak load is measured to 312.0 kWh/h, i.e., the power rating is at most exceeded by 56%.

In summary, under normal operation, the network of Radial A has in general few problems with supplying the 40 load points. The analysis showed that all the branches in the radial had an abundance of remaining capacity during all the hourly measurements in the three-year period. Additionally, most of the transformers had sufficient margin between the power rating and the peak demand that were covered during the period. The only component with exceeded capacity is the tertiary winding of the distribution transformer A20005/A30003/A30004. Here, the need for upgrades should be evaluated more extensively in relation to expected future demand from the connected load points.

5.1.2 Radial B

A simplified model of the high-voltage distribution grid, including the distribution transformers, of Radial A is shown in Figure 28. The squares represents the distribution transformers, and the number of child-loads are written in the parenthesis.

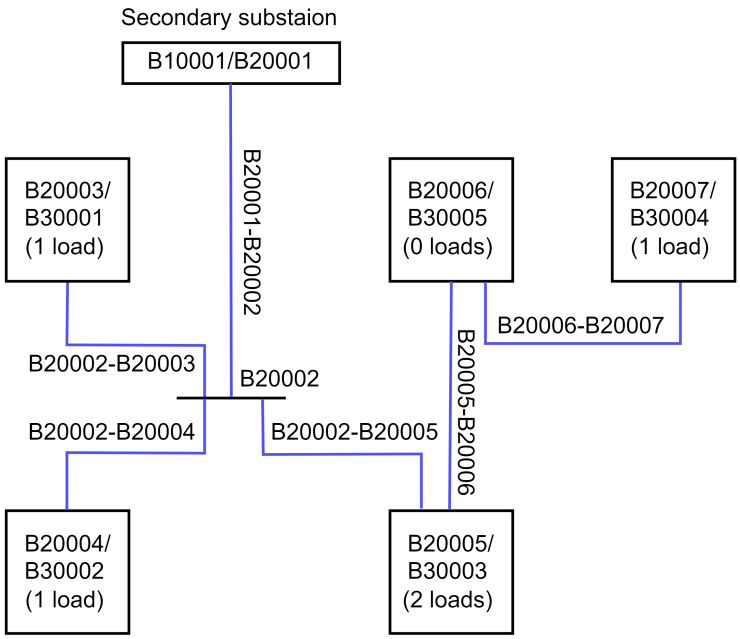

Figure 28: A simplified model of the high-voltage distribution grid of Radial B.

The temperature corrected aggregated peak loads seen from each of the cables in the radial during the three-year period are shown in Figure 29. The line ratings are represented by the red line.

The transformers B20003/B30001 and B20003/B30002 are located in the same distribution substation as the node B20002, and their line ratings are unknown. It is assumed that the connections in the substation are not the limiting factor for the power flow in the network. Thus, the line ratings of the branches B20002-B20003 and B20002-B20004 are set equal to the highest line rating in the radial.

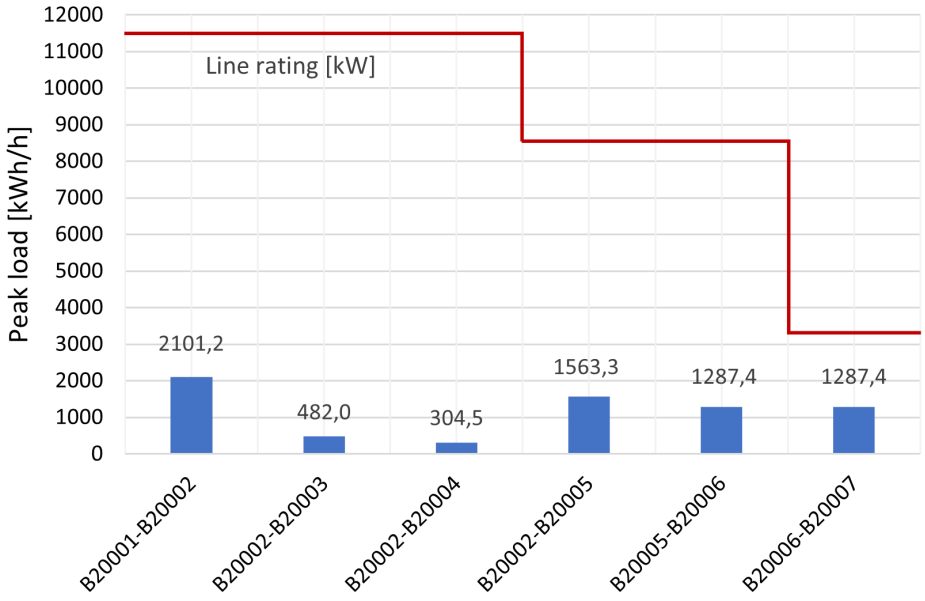

Figure 29: The aggregated peak load for each branch in the 11 kV grid of Radial B during the three-year period and the corresponding line ratings.

From Figure 29, it can be seen that all the branches in Radial B had an abundance of remaining capacity in the whole three-year period. The calculated remaining capacity in the peak load situations are presented in Table 4.

Table 4: Line rating, aggregated peak load and corresponding capacity margin for the branches in Radial B.

Branch	**Line rating [kW]**	**Peak load [kWh/h]**	**Capacity margin [kWh/h]**
B20001 - B20002	11431.5	2101.2	9330.3
B20002 - B20003	11431.5	482.0	10949.5
B20002 - B20004	11431.5	304.5	11126.5
B20002 - B20005	8668.9	1563.3	7105.6
B20005 - B20006	8668.9	1287.4	7381.5
B20006 - B20007	3238.9	1287.4	1951.5

As seen from Figure 29 and the corresponding capacity margins presented in Table 4, in general, the line ratings of the branches are sufficient to cover the load demand from the end users i Radial B under normal operation. 5 of the 6 branches in the radial had a capacity margin greater than 7.1 MWh/h throughout the whole three-year period. The branch B20006-B20007 has distinctly the lowest rating in the radial, and the capacity margin would have been the lowest regardless of the demand of the connected end user.

Figure 25 shows the aggregated peak load during the three-year seen from the distribution transformers in Radial A. and the corresponding power ratings of the transformers represented by the red line.

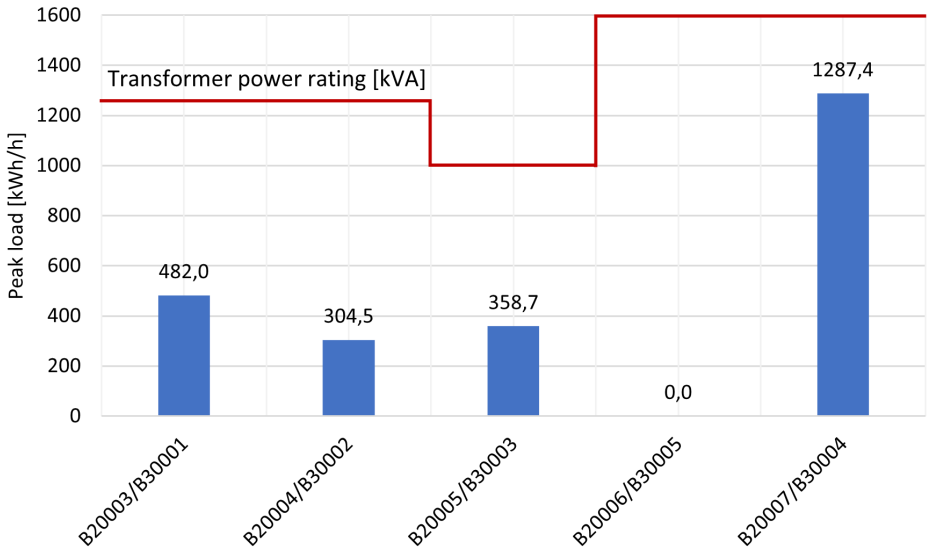

Figure 30: The aggregated peak load seen from each distribution transformer in Radial B and the corresponding transformer power ratings.

As seen from Figure 30, the power rating is not exceeded for any of the distribution transformers in Radial B during the three-year period. The capacity margins for the transformers under peak load are calculated, and presented in Table 5.

Table 5: Power rating, aggregated peak load and corresponding capacity margin for the distribution transformers in Radial B.

Transformer	**Power rating [kVA]**	**Peak load [kWh/h]**	**Capacity margin [kWh/h]**
B20003 / B30001	1250	482.0	768.0
B20004 / B30002	1250	304.5	945.5
B20005 / B30003	1000	358.7	641.3
B20006 / B30005	1600	0	1600.0
B20007 / B30004	1600	1287.4	312.6

The transformer B20006/B30005 is not connected to any load point, and hence, this is the transformer with the most remaining capacity for future load increase. Additionally, the transformers placed to the left in the figure, , B20003/B30001, B20004/B30002 and B20005/B30003, all have relatively generous room for an increase in the demand from the connected load points. The distribution transformer labeled as B20007/B30004 sees the highest peak load and has the narrowest margin between the peak load and the transformer rating for Radial B.

In summary, under normal operation, all the branches and distribution transformers in Radial B have sufficient power rating to cover the load demand for all the hours during the three-year period. The results shows that the dimensioning of the network provides a good opportunity to connect new end users to the radial and increase the load for the existing end users.

5.2 Outage situation

In this part, the parts of the grid where potential outages are most critical will be pointed out, and the consequences of failures in these parts will be evaluated in more detail.

5.2.1 Possible outage situations

Although the given distribution network is categorized as a meshed grid, for most of the connections and substations in the simplified model of the grid, the reserve branch will not be able to take over the supply. An example is illustrated in Figure 31, where a failure has occurred on the branch B20002-B20006. This results in the downstream loads points, highlighted in the red dotted box, being isolated from the power source of Radial B. Since there is not possible to supply the load points from Radial A neither, the end users in this part of the grid will not be supplied until the failure is repaired.

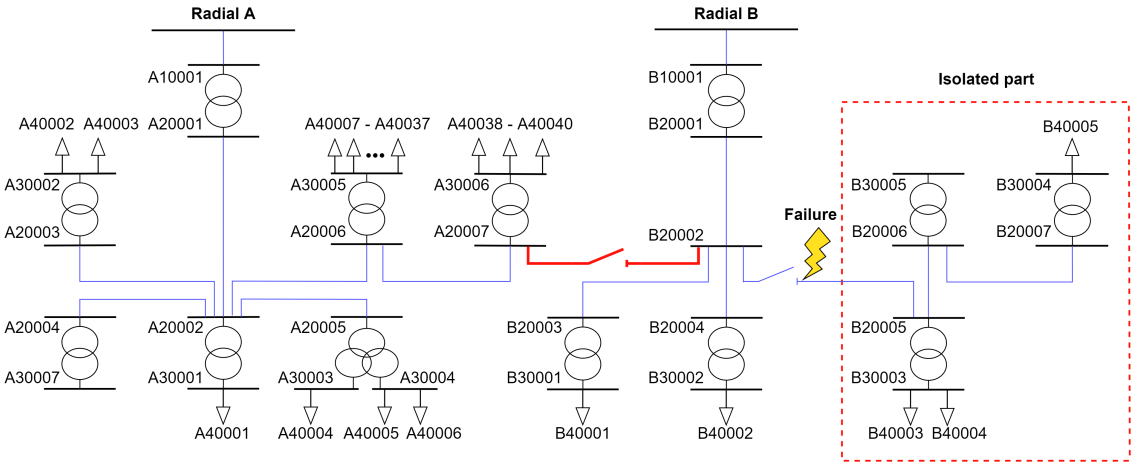

Figure 31: A simplified model of the distribution grid with a failure where the reserve branch can not be used to supply the affected load points.

The situation in Figure 31 where the failure causes isolation of load points will apply for fault situations located in most parts of the grid. This includes the low-voltage segment and all the distribution substations of the distribution system. A failure will also result in isolated parts if the failure is located in the high-voltage branches downstream of the faulted radial's main node, i.e., downstream of A20002 or B20002, seen from both the secondary substation transformers in the system. To specify, this applies for all the 11 kV branches, except the main branch of each radial and the branches A20002-A20006 and A20006-A20006 that is upstream of A20002 seen from Radial B. In this simplified model, these parts of the grid, where a failure leads to isolated load points, will not fulfill the N-1 criterion.

For this contingency analysis, the outages where the reserve branch between Radial A and Radial B can be used as reserve, is the main focus. Therefore, in the following, these situations, where the N-1 criterion is fulfilled with the help of the reserve branch, is investigated more extensively.

An example of a fault situation where the reserve branch is utilized is shown in Figure 32. Here, the failure, located on the branch A20002-A20006, isolates the load points A40007-A40040 from the power source of Radial A. After the breaker of the reserve branch is closed, the loads can instead be supplied from Radial B via the reserve branch. In this example, the reserve branch provides improved flexibility and will probably reduce the duration of the interruption, seen from the perspective of the affected load points.

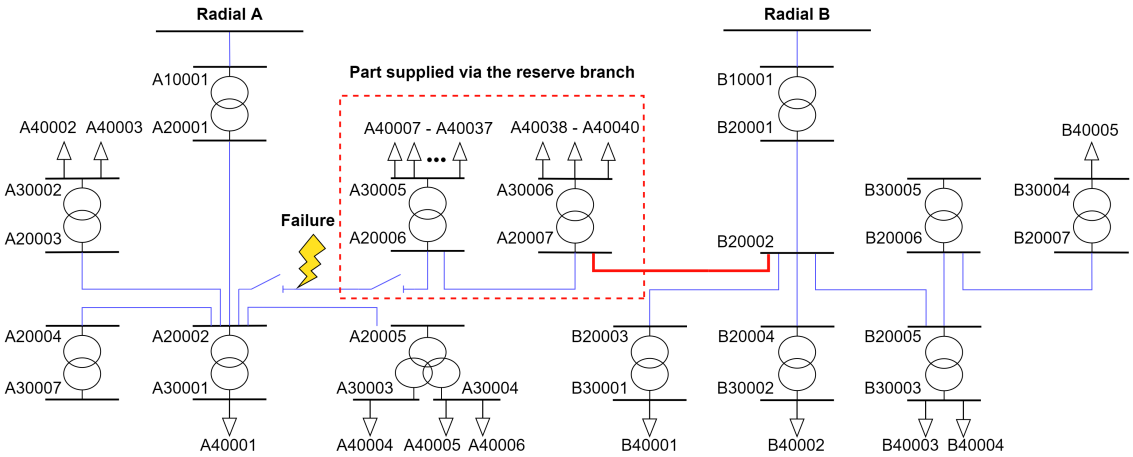

Figure 32: A simplified model of the distribution grid where the isolated part is supplied via the reserve branch.

All the relevant branches where the reserve branch can be used in case of an outage are highlighted with thickened blue lines in the simplified network in Figure 33.

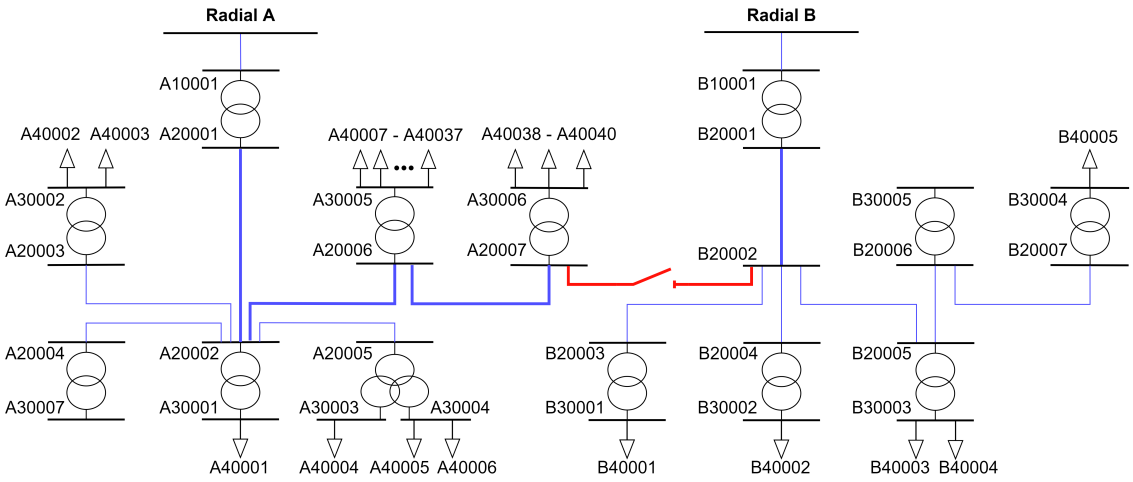

Figure 33: A simplified model of Radial A and Radial B, where the branches that can be replaced by the reserve branch are highlighted with thickened blue lines.

As illustrated in Figure 33, there are four branches in the 11 kV distribution grid where the reserve branch can take over the supply in case of an outage. The four branches can be labeled based on the connected nodes; A10001-A20001, A20002-A20006, A20006-A20007 and B20001-B20002. As mentioned earlier, the main branch coming out from the secondary substation for each radial, A10001-A20001 and B20001-B20002, will under normal operation see the aggregated load from all the end users in Radial A and Radial B, respectively. The aggregated load time series for the radials were shown in Figure 20 and 21 in Chapter 4.3. The two other branches in Radial A highlighted in 33, only see the end users located downstream from the branches under normal operation, i.e., A20002-A20006 sees the aggregated load from 31 end users (A40007-A40040), while A20006-A20007 only sees the load from the three child-loads (A400038, A400039 and A40040). The aggregated load that is seen from the fault location, is the load the reserve branch will need to cover.

For the relevant branches, the severity of an outage can be categorized based on the aggregated load from the end users the reserve branch will have to supply. This aggregated load equals the extra load that must be covered by the secondary substation transformer of the non-faulted radial.

For a failure in the main branch of one of the two radials, A20001-A20002 or B20001-B20002, the secondary substation transformer in the faulted radial will not be able to supply any load points. Subsequently, the reserve branch must cover the aggregated load from all the end users in the faulted radial, while the remaining secondary substation transformer must supply all the load points in both Radial A and Radial B. Therefore, an outage of this type will be the most critical for the given system.

For an outage in one of two remaining relevant branches in Radial A, A20002-A20006 and A20006-A20007, the secondary substation transformer of Radial A will still be able to supply some of the end users in the radial. Hence, the aggregated load seen from the reserve branch and the Radial B secondary substation transformer will decrease compared to the main branch outage scenario. The number of load points from Radial A that must be covered given an outage in A20002-A20006 or A20006-A20007 is 34 and 3, respectively. Comparing with the main branch outage scenario, where the branches will see 40 and 37 load points, respectively, it is obvious that these outages put a smaller burden on the branches. As described in Chapter 4.3, based on the specialization project results, the largest load in Radial A, A40001, was responsible for close to half the radial's consumption during the three-year period. As a result, there is a remarkable difference in the load demand between the scenario where all load points in Radial 1 must be supplied via the reserve branch and the scenarios where only some of the load points must be covered.

In summary, there are four relevant branches in the network where the reserve branch can be utilized to supply the isolated load points in case of an outage; A20001-A20002, B20001-B20002, A20002-A20006 and A20006-A20007. Given an outage in the main branch in one of the radials, i.e., A20001-A20002 or B20001-B20002, all the load points in the faulted radial must be supplied from the secondary substation transformer of the non-faulted radial, via the reserve branch. For an outage in one of the two remaining relevant branches in Radial A, only the aggregated load of the isolated load points is covered via the reserve branch. As a result, the supplied load demand will be notably higher for an outage in one of the two main branches.

5.2.2 Limiting factors in outage situation

According to Norgesnett, the network capacity, is the limiting factor in the coming electrification process. The main focus of this contingency analysis is the high-voltage part of the distribution network and the outage situations where the reserve branch is utilized. Therefore, the load seen from the distribution substations will not change compared to normal operation. Hence, the capacity margins of the transformers are the same as for normal operation for all the relevant outage scenarios.

As the load demand seen from the distribution transformers are not affected by outages of the relevant branches, the line ratings of the cables will be considered as the limiting factor in the contingency analysis. In the following, the line ratings of the relevant branches are presented and briefly discussed.

As illustrated and described in Chapter 5.2.1, there are four relevant branches in the distribution network that are particularly interesting to study in relation to possible outage situations where the reserve branch can be utilized. The line ratings of the relevant branches and the reserve branch are shown in Table 6. The line ratings are calculated according to Equation 5 and based on values for maximum operating current given by Norgesnett. As described in Chapter 2.7.1, the line rating of short power lines is typically determined by thermal limits.

Table 6: Ampacity, voltage level and resulting line rating for the relevant branches and the reserve branch.

Branch	**Ampacity [A]**	**Voltage [kV]**	**Line rating [kW]**
A20001-A20002	400	11	7621.0
A20002-A20006	455	11	8668.9
A20006-A20007	465	11	8859.4
B20001-B20002	600	11	11421.5
A20007-B20002 (Reserve)	465	11	8859.4

It should already be noted that the calculated power transfer capacities, presented in Table 6, are relatively high compared to today's load demand in the network. As presented in Chapter 4.3, the temperature corrected peak load for Radial A and Radial B individually was both found to be around 2 MWh/h, while the aggregated peak load for all the loads was close to 3.8 MWh/h. Thus, the total load demand in the network is remarkable lower than the calculated capacities of the relevant branches. Subsequently, as presented for normal operation in Chapter 5.1, the line ratings of the cables will not limit the power distribution in outage situation with today's load demand.

Although the DSO probably does not experience capacity problems with the current load demand, it is useful to analyze how the system handles failures and how the remaining capacity in the network varies over time in relation to future electrification issues. As described in Chapter 2.6, in large and complex power systems, it is an extensive number of contingencies that must be considered, and it is often hard to cover all combinations in the planning stage. However, for this distribution grid, the limited complexity of the network makes it possible to study the consequences of the outage scenarios more exhaustively.

5.3 Outage scenarios

Based on the outage situations discussed in Chapter 5.2.1 and the power transfer limits presented in Chapter 5.2.2, the outage scenarios of the analysis can be decided.

As described in Chapter 5.2.1, an outage of a power line in the high-voltage distribution grid, i.e., the 11 kV part of the network, will in most cases lead to isolation of load points. There are four branches in the system where the reserve branch can be utilized to cover the demand from the isolated parts. The four relevant branches, in cooperation with the reserve branch, compose the connection between the secondary transformers of the two radials. Therefore, for an outage situation where the reserve branch is used, there are only the power flowing in these branches that will change compared to the normal operation situation covered in Chapter 5.1.

An outage of the main branch of Radial A or Radial B was found to be most severe in term of the extra load that must be supplied via the reserve branch. Therefore, these two outage scenarios are investigated in more detail. Table 7 gives an overview of the two scenarios and the child-loads each of the affected branches must supply in the outage scenarios.

Table 7: Outage branch and child-loads for each of the affected branches in Outage Scenario 1 and 2.

Outage scenario		1	2
Outage branch		A20001-A20002	B20001-B20002
Child-loads (number of child loads)	**A20001-A20002**	-	A40001-A40040 B40001-B40005 (45)
	A20002-A20006	A40001-A40006 (6)	A40007-A40040 B40001-B40005 (39)
	A20006-A20007	A40001-A40037 (37)	A40038-A40040 B40001-B40005 (8)
	B20001-B20002	A40001-A40040 B40001-B40005 (45)	-
	A20007-B20002	A40001-A40040 (40)	B40001-B40005 (5)

5.3.1 Outage scenario 1

In Scenario 1, an outage occurs on the main branch (A20001-A20002) or secondary transformer (A10001/A20001) of Radial A. As a result, all the 40 load points of Radial A must be supplied from the secondary transformer of Radial B, via the Radial B main branch (B20001-B20002), the reserve branch (A20007-B20002) and the two remaining relevant branches of Radial A (A20006-A20007 and A20002-A20006). In addition, the secondary transformer and the main branch must continue to supply the five load points of Radial B.

Scenario 1 is illustrated in the simplified distribution grid model in Figure 34.

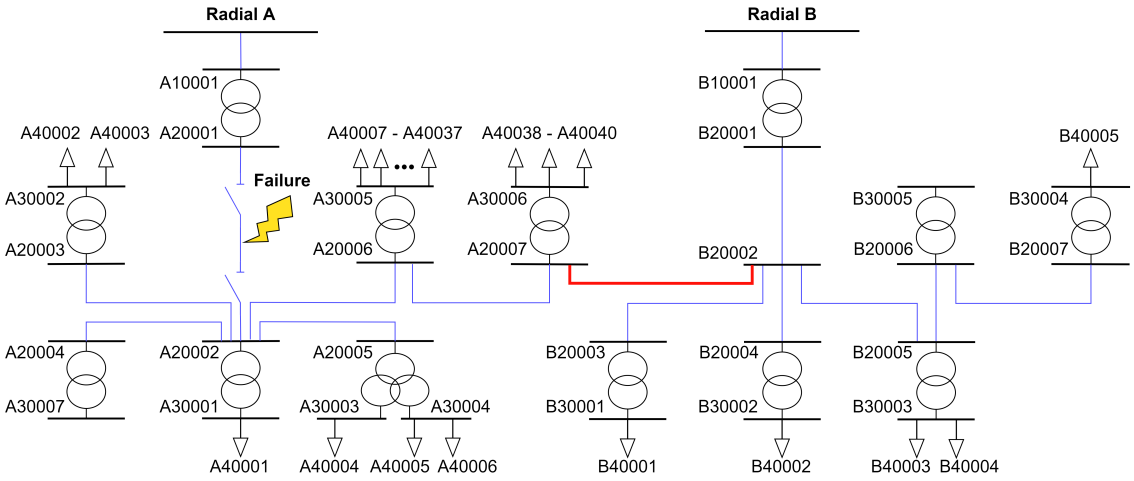

Figure 34: A simplified model of Scenario 1 where a failure occurs on the main branch of Radial A, and all the load points int he network must be supplied from the secondary substation transformer of Radial B.

In this situation, the main branch of Radial B is the power line that must carry the greatest load

in the system. The total demand is the same as the aggregated load of the entire system shown in Figure 22, with a peak load of 3917.9 kWh/h. However, as presented in Chapter 5.2.2, this branch has a line rating of 11.4 MW, which is the highest of all the branches in the system. The other relevant branches cover lower load demands, but also have lower line rating. Therefore, in order to identify the limiting line rating for load increase in this situation, the remaining capacity throughout the time period for each of the branches is drawn in Figure 35.

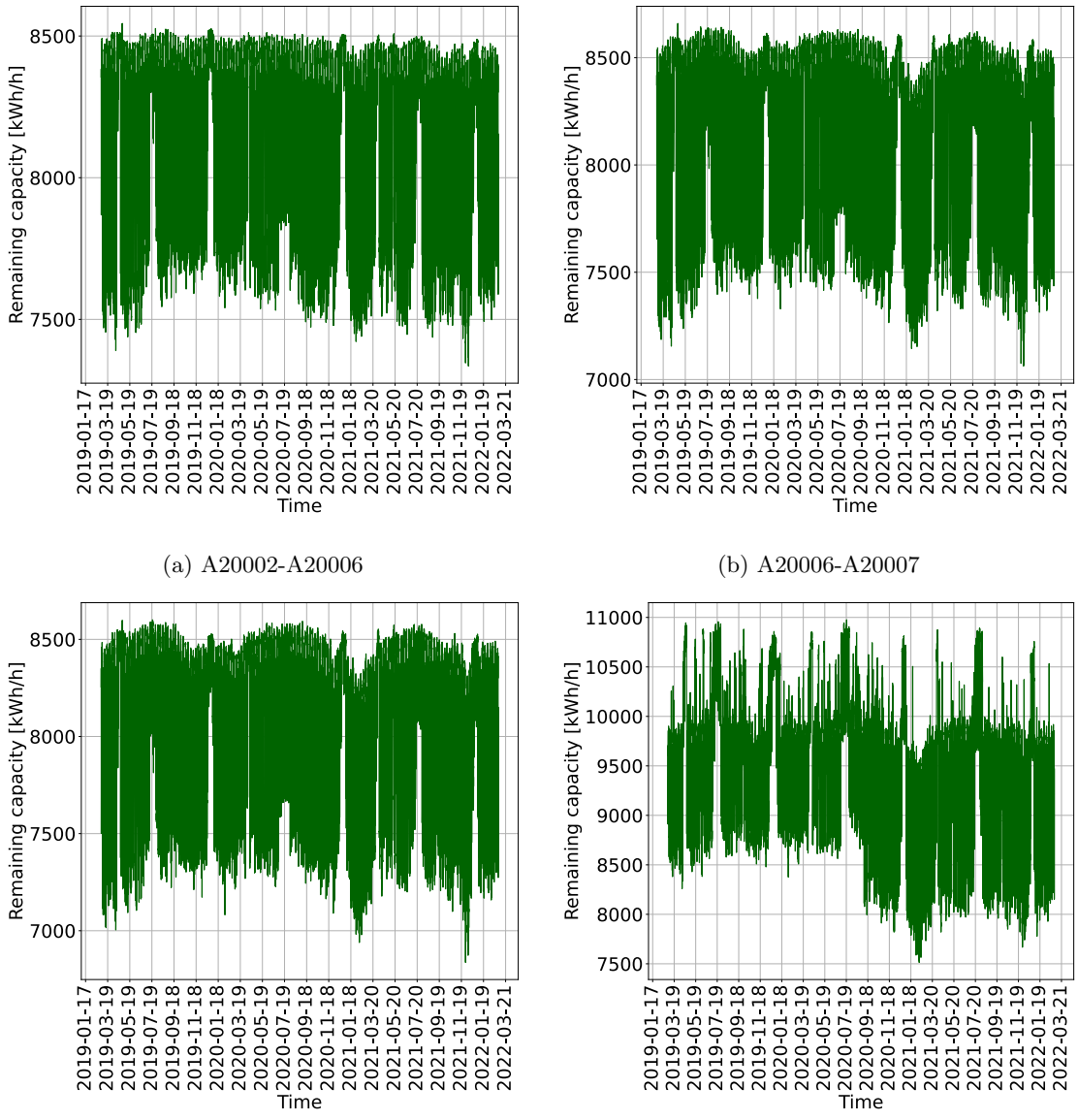

(a) A20002-A20006

(b) A20006-A20007

(c) A20007-B20002 (reserve branch)

(d) B20001-B20002

Figure 35: The remaining capacity of the relevant branches in Scenario 1 during the three-year period.

Figure 35 confirms that all the relevant branches have sufficient capacity to cover the load demand in Scenario 1. For three of the branches, A20002-A20006, A20006-A20007 and B20001-B20002, the remaining capacity is greater than 7 MWh/h for the entire three-year period.

The reserve branch, A20007-B20002, supplies all the load points in Radial A and has the smallest margin of the branches, with a minimal remaining capacity of 6836.9 kWh/h. This margin occurs in the peak load hour of Radial A. Since the reserve branch supplies a higher or the same number of load points in Radial A compared to the branches A20002-A20006, A20006-A20007 and B20001-

B20002, the line rating of the reserve branch will be the limiting factor for load increase in Radial A for Scenario 1.

The cumulative distribution of the remaining capacity for the reserve branch during the three-year period is drawn in Figure 36a. Figure 36b shows a zoom-in of the 25 hours with the lowest remaining capacity.

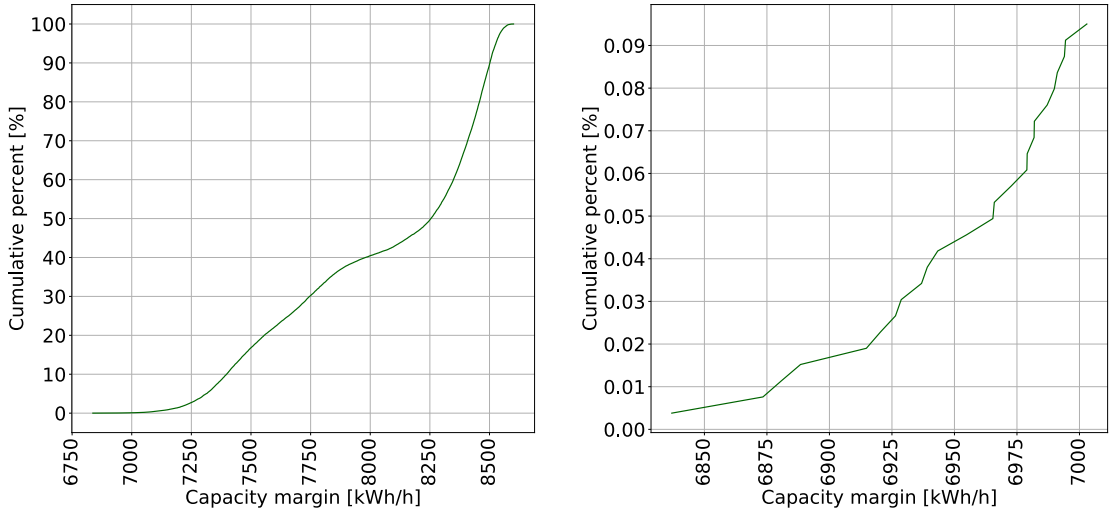

(a) All hours

(b) The 25 hours with the lowest remaining capacity

Figure 36: The cumulative distribution function for the remaining capacity of B20001-B20002 in Scenario 1 during the three-year period.

The cumulative distribution function of the reserve branch has a slow growth for the lowest remaining capacity values. This indicates that the highest peaks only occurs for some few hours during the three-year period. From the zoom-in in Figure 36a, it can be seen that the remaining capacity is smaller than 7 MWh/h for only 24 hours during the period. This equals approximately 0.09% of the hours.

The remaining capacity plots in Figure 35 shows that B20001-B20002, the main branch of Radial B, has the highest margin during peak load. The remaining capacity of the branch is never lower than 7.5 MWh/h during the three-year period. However, this is the only one of the relevant branches that supplies the load points of Radial B in Scenario 1. Hence, for a load increase in Radial B, the remaining capacity of B20001-B20002 will decrease, while the remaining capacity of A20002-A20006, A20006-A20007 and A20007-B20002 will be unchanged. Therefore, the line rating of the main branch B20001-B20002 will be the limiting factor for increased demand from the existing end-users or connection of new load points in Radial B in Scenario 1.

The cumulative distribution of the remaining capacity for the main branch of Radial B is shown i Figure 37.

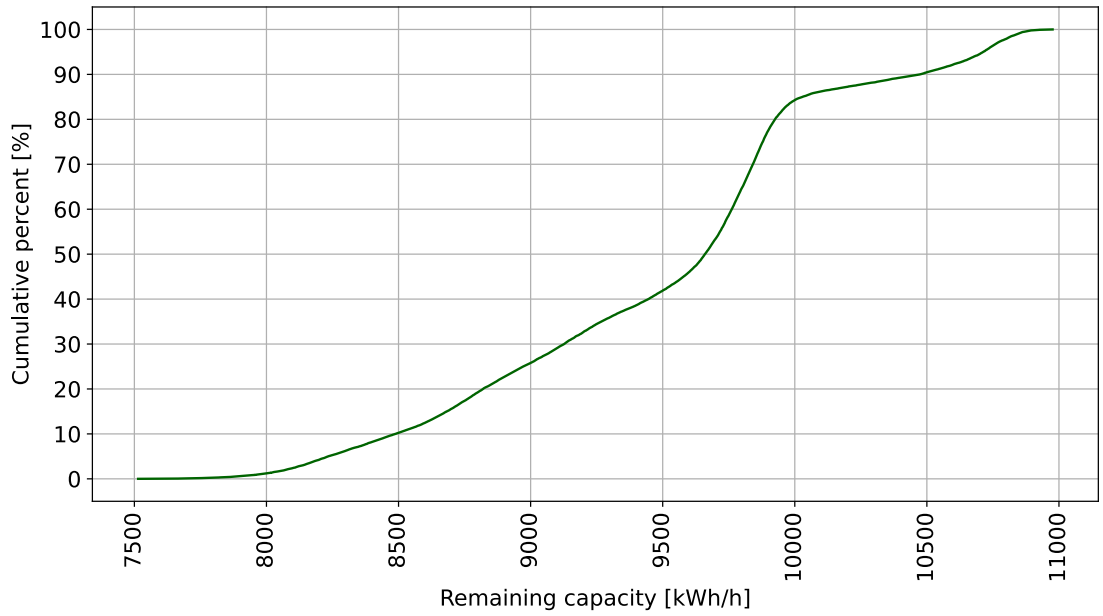

Figure 37: The cumulative distribution function for the remaining capacity of the Radial B main branch B20001-B20002 in Scenario 1 during the three-year period.

The cumulative distribution function illustrates the room for load increase in Radial B for Scenario 1. The smallest remaining capacity, which occurs in the peak load hour for the aggregated load of all the end users in the network, is calculated to 7514.1 MWh/h. It can be seen that for around 90% of the time period, the remaining capacity of the branch is greater than 8.5 MWh/h

In summary, the line ratings of the branches in the network are sufficient to still supply all the load points in case of an outage of the main branch of Radial A (A20001-A20002). Based on the historical load data from the three-year period, the reserve branch (A20007-B20002) has the smallest remaining capacity, with a minimum of 6.8 MWh/h. The line rating of this branch will be the limiting factor for a load increase in Radial A. For a load increase in Radial B, the line rating of the main branch of Radial B (B20001-B20002) will be the limiting factor.

5.3.2 Outage scenario 2

The second of the two most critical outage scenarios, Scenario 2, is a failure on the power source or the main branch (B20001-B20002) of Radial B. In this situation, the secondary substation transformer of Radial A will need to supply the five load points of Radial B, in addition to the 40 load points in Radial A that are already supplied by the transformer. Hence, the total load that must be supplied is the aggregated load of all the load points in the two radials. This is the same load as was supplied from the Radial B secondary substation transformer in Scenario 1.

Scenario 2 is illustrated in the simplified distribution grid model in Figure 38.

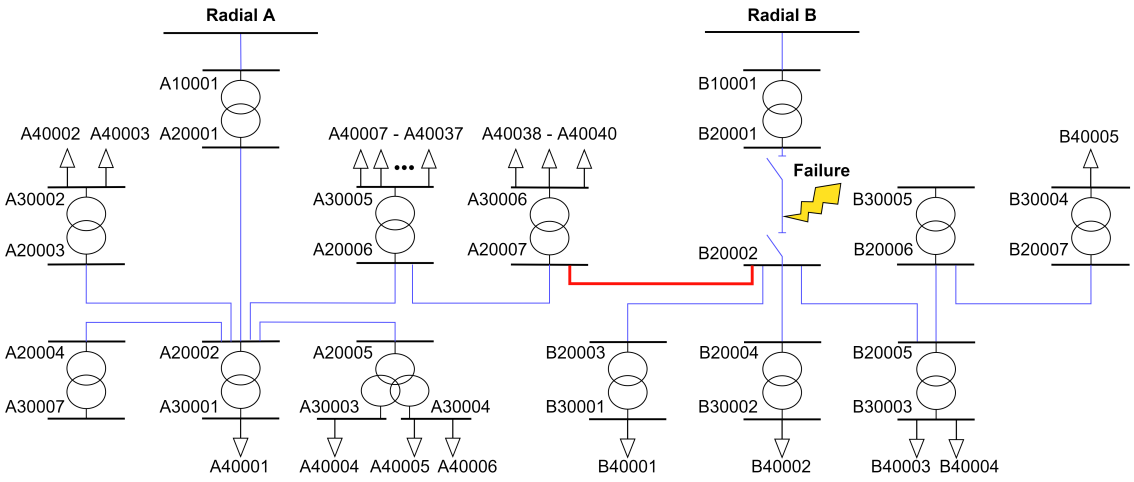

Figure 38: A simplified model of Scenario 2 where a failure occurs on the main branch of Radial B, and all the load points in the network must be supplied from the secondary substation transformer of Radial A.

As seen from Figure 38, the load points of Radial B is supplied via the high-voltage branches A20001-A20002, A20002-A20006 and A20006-A20007, as well as the reserve branch (A20007-B20002). The line ratings of the branches were presented in Table 6 in Chapter 5.2.2. Based on the combination of the highest supplied load demand and the lowest line rating, the main branch (A20001-A20002) will be the limiting factor in this scenario, both for a load increase in Radial A and load increase in Radial B.

As presented in Chapter 5.2.2, the main branch has a line rating of 7621.0 kW, and is under normal operation already covering the aggregated load of the Radial A load points. In Scenario 2, the branch must supply all the 45 end users in the network. As stated earlier, the temperature corrected peak load of the system is 3917.9 kWh/h. Thus, base on the historical load data, the line rating of A20001-A20002 is sufficient to cover the load demand in Scenario 2.

The remaining capacity of the Radial A main branch A20001-A20002 for Scenario 2 during the three-year period is shown in Figure 39.

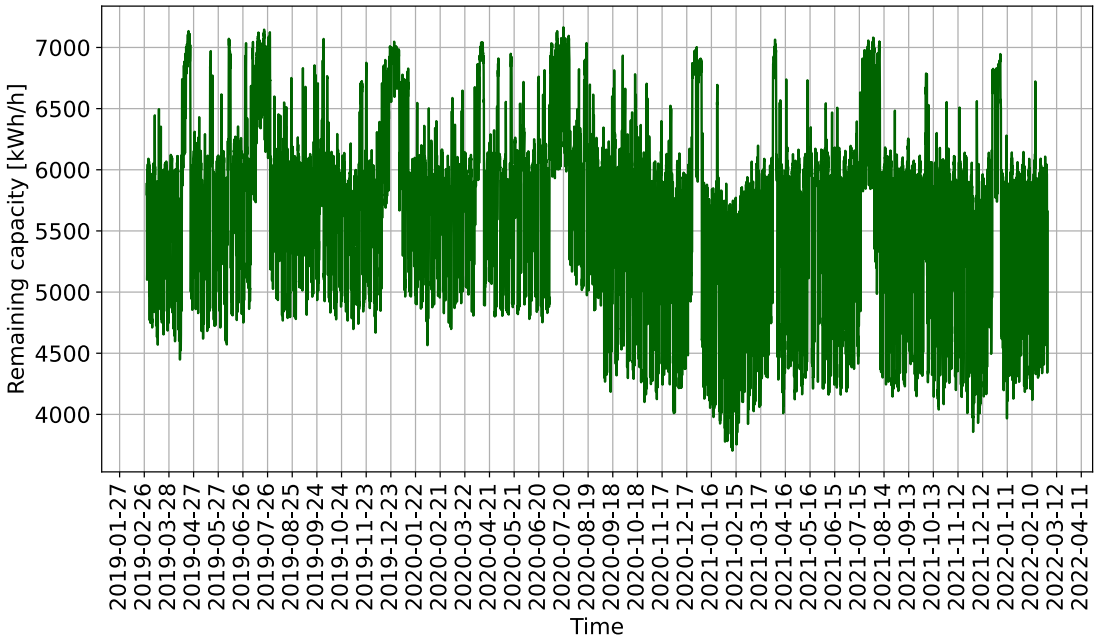

Figure 39: The excess capacity of the Radial A main branch A20001-A20002 during the three-year period in Scenario 2.

Figure 39 illustrates the variation in the remaining capacity over time. Since the remaining capacity is positive for the entire three-year period, Figure 39 confirms that the line rating of the branch is high enough to handle the additional demand from the end users of Radial B. Therefore, the N-1 reliability criterion is fulfilled for this scenario. However, the remaining capacity is clearly decreased after of the connection of the two extra end users (B40001 and B40002) in Radial B at 08.09.2020. This is as expected, due to an increase of the aggregated load of Radial B.

The cumulative distribution of the remaining capacity of the Radial A main branch during the three-year period is shown in Figure 40a. Figure 40b shows a zoom-in of the 100 hours with the lowest remaining capacity.

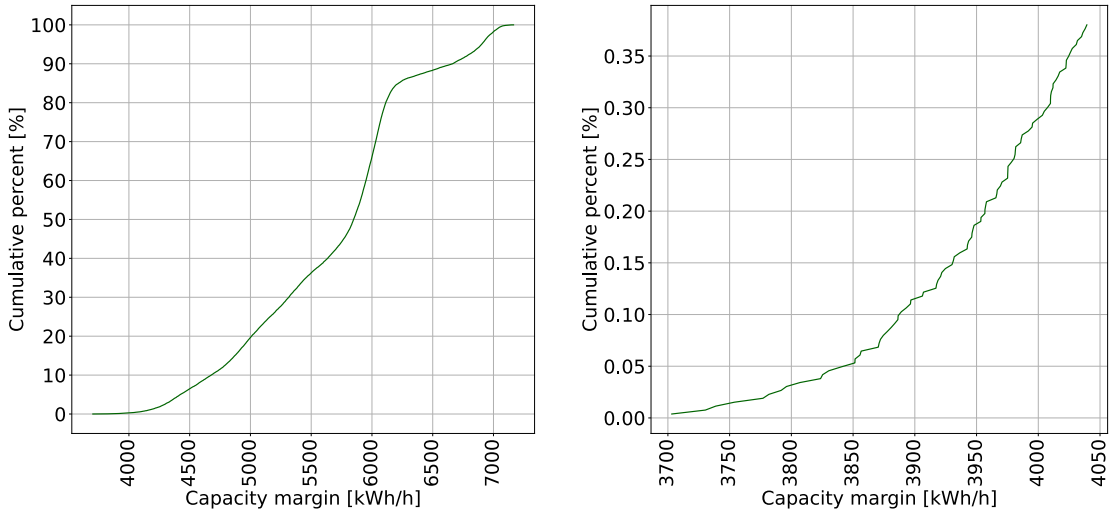

(a) All hours

(b) The 100 hours with the lowest remaining capacity

Figure 40: The cumulative distribution function for the remaining capacity of A20001-A20002 in Scenario 2 during the three-year period.

It can be seen that for about 80% of the three-year period, the remaining capacity of the main branch of Radial A in Scenario 2 was greater than 5 MWh/h. Despite the increase of the demand from the extra end users in Radial B, the remaining capacity is never less than 3703.1 kWh/h. As a result, based on the historical load data, a load point with constant demand of 3700 MW could be added to the system, without violating the N-1 criterion related to outage of the branch B20001-B20002 for this three-year period.

In summary, the line ratings of the branches in the network are sufficient to still supply all the load points in case of an outage of the main branch of Radial B (A20001-A20002). In this scenario, the line rating of the Radial A main branch A20001-A20002 will be the limiting factor, both for a load increase in Radial A and a load increase in Radial B. The smallest remaining capacity of the branch during the three-year period was calculated to 3.7 MWh/h.

5.4 Future scenario

As presented and discussed in Chapter 5.1, based on the consumption from the last three years, the thermal capacity of this part of the Øra grid is not a problem today. However, electrification of industrial processes and new power-intensive industries will possibly put pressure on the existing grid and challenge the DSO in the coming years. Therefore, a scenario with increased load demand in the industrial area is investigated in this part, both for normal operation and for the most critical outage situations.

In Chapter 5.1, the power ratings of the distribution transformers was compared to the historical load demand of the connected load points. The results showed that there was an abundance of remaining capacity in most of the transformers during all the three years. Thus, in the coming electrification process, a measure to limit the costs of grid investments is to improve the utilization of the existing grid infrastructure. Therefore, in this part, the consequences of increased load demand from the existing distribution transformers on the remaining capacity in other parts of the grid is investigated.

To simulate an improved utilization of the capacity of the distribution transformers, the aggregated load time series supplied by each distribution substations is scaled such that the peak load equals the power rating of the transformer. With this approach, today's load profiles of the individual end users are retained.

As an example of the load scaling, the aggregated load for the distribution substation A20003/A30002 is shown in Figure 41. The load seen from the transformer before the scaling is illustrated with the blue curve, while the load after the scaling is represented by the red curve. The load is limited by the orange line, the power rating of the transformer,

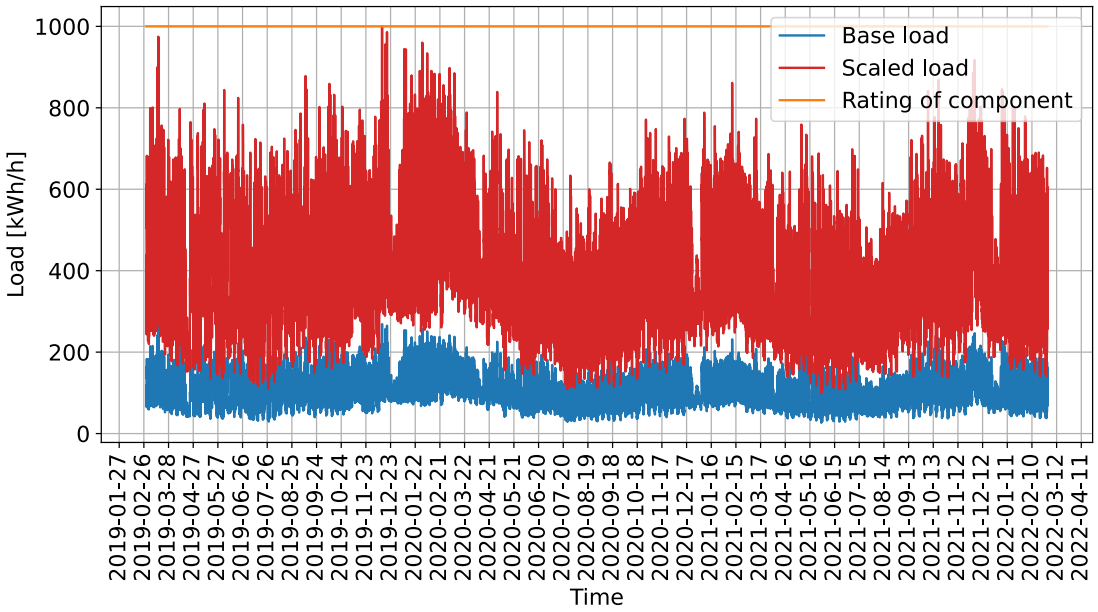

Figure 41: Comparison of aggregated load time series for distribution transformer A20007/A30006 before and after scaling.

The power rating of the transformer in Figure 41 is constant equal to 1000 kVA, and the load is the aggregation of the demand from the load points A40038, A40039 and A40040. As illustrated, the peak load will still occur in the same hour, but the demand in this hour is increased from 268.8 kW to 1000 kW. Thus, all the load points supplied by the transformer under normal operation are increased with a scaling factor equal to the ratio of the transformer power rating to the base peak load, calculated to 3.72 for this example.

The power rating and aggregated peak load for all the distribution transformers in the network are presented in Table 8. Based on these values, the scaling factors are calculated and presented to the right in the table.

Table 8: Power rating of the distribution transformers and the aggregated peak load of the connected load points for the distribution transformers.

Distribution transformer	**Power rating**	**Base peak load**	**Scaling factor**
A20002/A30001	1600	984.2	1.626
A20003/A30002	1600	90.9	17.602
A20004/A30007	1600	-	-
A20005/A30003/A30004	500/300/200	354.9	1.409
A20006/A30005	1000	507.0	1.972
A20007/A30006	1000	268.8	3.720
B20003/B30001	1250	482.0	2.593
B20004/B30002	1250	304.5	4.105
B20005/B30003	1000	358.7	2.788
B20006/B30005	1600	-	-
B20007/B30004	1600	1287.4	1.243

For the distribution substations with no connected loads, a new load point is introduced. This

applies for one substation in each radial, A20004/A30007 and B20006/B20005. The new load points will have a load profile equal to the aggregated load of the radial and peak load equal to the distribution transformer's power rating. Since the new loads will have their individual peaks at the same time as the aggregated loads, the coincidence factors will be slightly increased. A possible problem with this approach is that the load profiles of the new load points will enhance the existing peaks. However, at the same time, this will move the future scenario towards a "worst-case" scenario.

After the modification, Radial A has 41 end users and Radial B has 6 end users. The two new load points are labeled A40041 and B40006. Figure 42 shows the simplified model of the network after the connection of the two extra end users. The new end users are connected to the low-voltage sides of the distribution transformers A20004/A30007 and B20006/B30005.

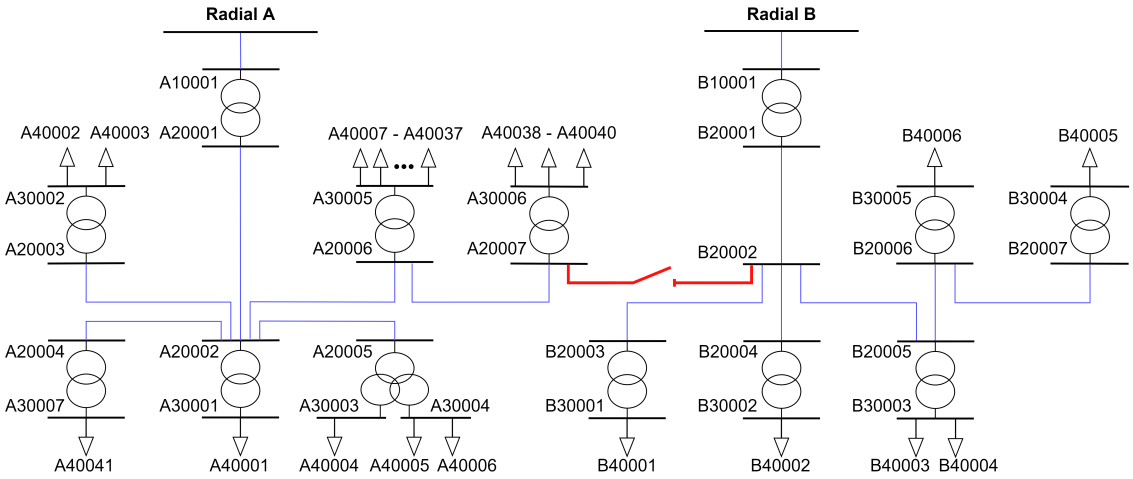

Figure 42: A simplified model of Radial A and Radial B.

The effect of the load scaling and addition of the two new loads on the load aggregation of the system, represented by the coincidence factor, is shown in Figure 43. Here, the coincidence factor of the entire system, i.e., the coincidence factor based on all the load points in the two radials, is calculated for each of the three years. For each year, the factor is calculated for three situations; the base case with the temperature-corrected initial load data, after the load scaling according to Table 8 and after both the load scaling and addition of the two new loads.

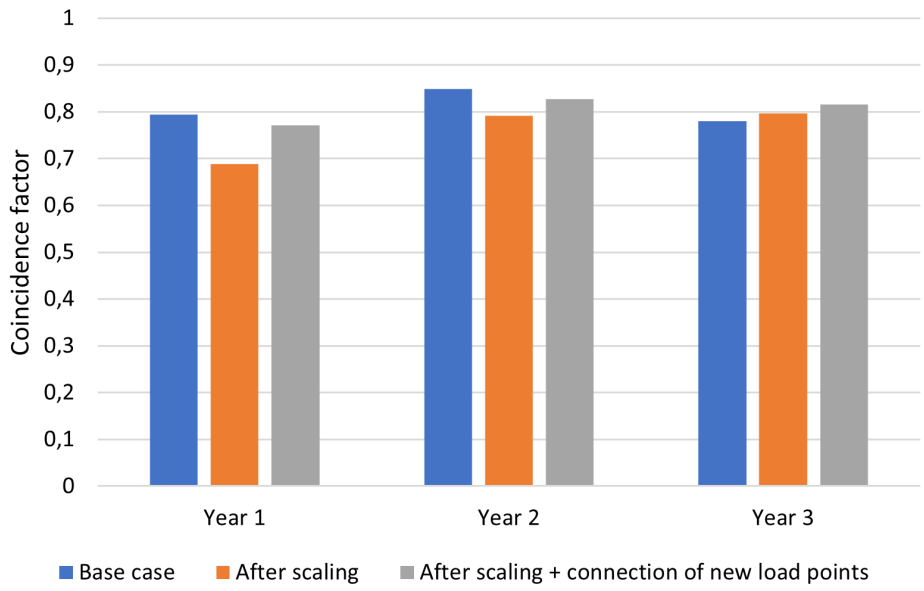

Figure 43: Coincidence factors of the distribution grid for the three years for the base case, after load increase and after both load increase and addition of two new loads.

As shown in the bar chart, after the load modifications, the coincidence factor is slightly decreased for the first two years and slightly increased for the last year compared to the base case. In overall, it seems like the aggregation between the load points in the network is well retained through the modification of the load data.

5.4.1 Normal operation

First, the situation after the load modification for Radial A under normal operation is investigated.

Figure 44 shows the peak load seen from each cable in Radial A during the three-year period after the modification of the load demand in the radial. The red line illustrates the corresponding line ratings. As in Chapter 5.1, for the branch A20002-A20003 with unknown line rating, the lowest of the known rating values was used.

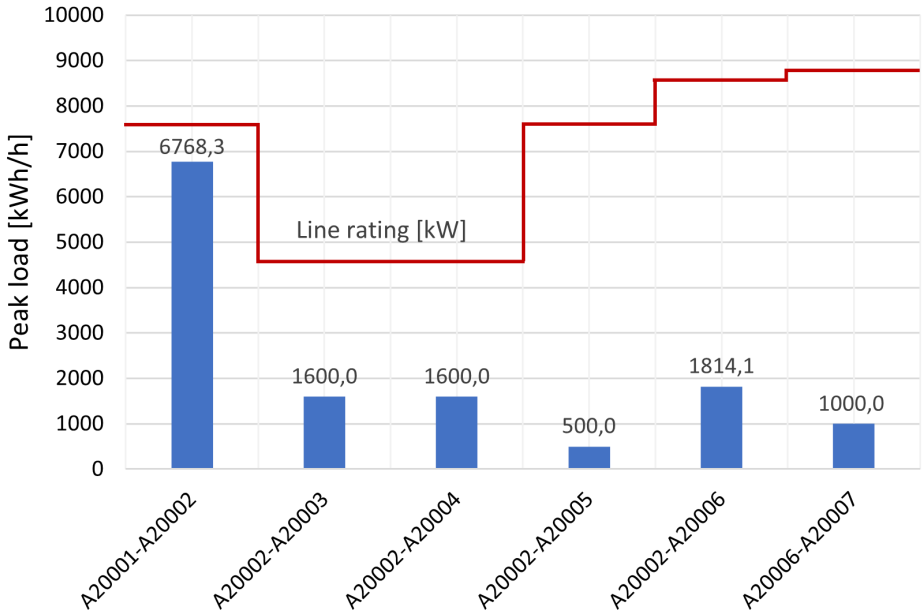

Figure 44: The aggregated peak load for each branch in the 11 kV grid of Radial A during the three-year period after the load modification and the corresponding line ratings.

As a result of the increased load demand, the burden on the branches in the network is increased. The remaining capacity for each branch in peak load situation is shown in Table 9.

Table 9: Line rating, aggregated peak load and corresponding remaining capacity for the branches in Radial A after the load modification.

Branch	**Line rating [kW]**	**Peak load [kWh/h]**	**Remaining capacity [kWh/h]**
A20001 - A20002	7621.0	6768.3	852.7
A20002 - A20003	4572.6	1600.0	2972.6
A20002 - A20004	4572.6	1600.0	2972.6
A20002 - A20005	7621.0	500.0	7121.0
A20002 - A20006	8668.9	1814.1	6854.8
A20006 - A20007	8859.4	1000.0	7859.4

Figure 44 and Table 9 show that the branches in the radial still have an abundance of remaining capacity during the three-year period. However, the margin of the main branch A20001-A20002 is decreased from 5598.9 kWh/h in the base case in Chapter 5.1 to 852.7 kWh/h after the load modification. This indicates that the main branch is the limiting factor for a load increase in Radial A.

The cumulative distribution of the remaining capacity of the branch is drawn in Figure 45a. Figure 45b shows a zoom-in of the 100 hours with the lowest remaining capacity.

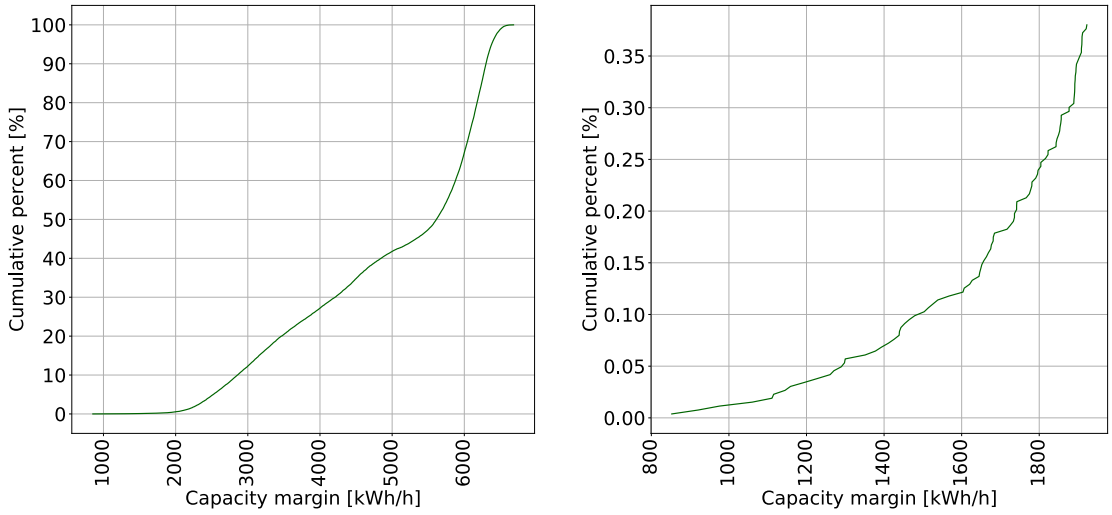

(a) All hours

(b) The 100 hours with the lowest remaining capacity

Figure 45: The cumulative distribution of the remaining capacity for the main branch of Radial A under normal operation after the load modification.

The cumulative distribution function clearly has a slow growth for the hours with the lowest remaining capacity, placed to the left in Figure 45a. The zoom-in of the 100 hours with the lowest remaining capacity in Figure 45b shows a difference of more than 1 MWh/h between the lowest value and the 100th lowest value. This indicates that the aggregated load of Radial A has several hours with distinctly higher demand. One of the reasons for this could be the connection of the new load point, A40041, with the peak demands in the same hours as the aggregated load of the rest of the load points.

During the three-year period, the lowest remaining capacity of the branches in the radial is calculated to 852.7 kWh/h. This shows that the current grid of Radial A, with basis in the historical load data, is able to handle this situation with increased load demand and improved utilization of the power ratings of the existing distribution substations under normal operation.

In the following, the situation after the load modification for Radial B under normal operation is investigated.

The temperature corrected aggregated peak loads supplied by each of the cables in the radial during the three-year period after the load modification are shown in Figure 46. The line ratings are represented by the red line. As in Chapter 5.1, it is assumed that the unknown ratings of the branches B20002-B20003 and B20002-B20004 are not the limiting factor for the power flow in the network. Thus, the line ratings are set equal to the highest of the known line ratings in the radial.

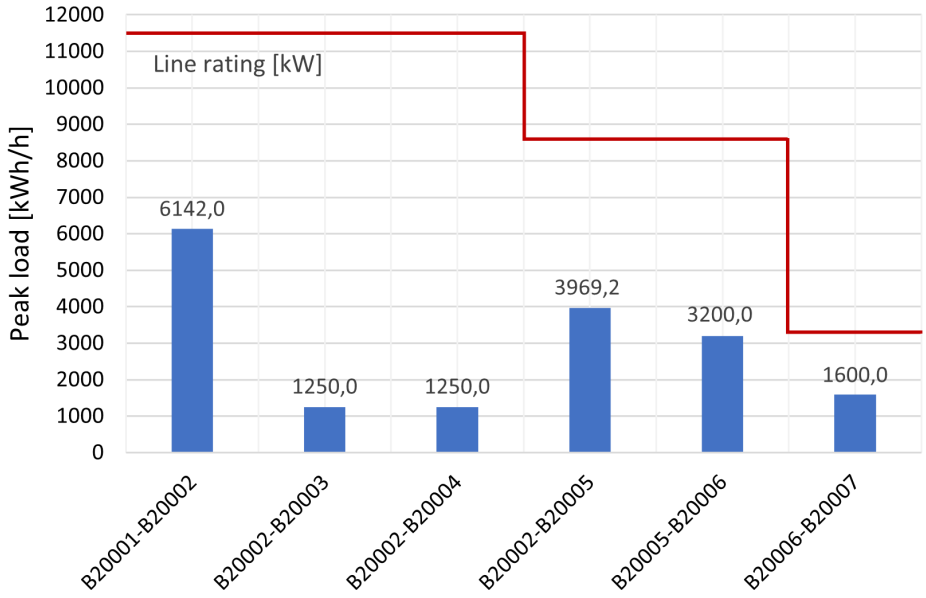

Figure 46: The aggregated peak load for each branch in the 11 kV grid of Radial B during the three-year period after the load modification and the corresponding line ratings.

From Figure 46, it can be seen that all the branches in Radial B still has an abundance of remaining capacity during the entire three-year period. The calculated remaining capacity in the peak load situations are presented in Table 10.

Table 10: Line rating, aggregated peak load and corresponding capacity margin for the branches in Radial B.

Branch	**Line rating [kW]**	**Peak load [kWh/h]**	**Capacity margin [kWh/h]**
B20001 - B20002	11431.5	6142.0	5289.5
B20002 - B20003	11431.5	1250.0	10181.5
B20002 - B20004	11431.5	1250.0	10181.5
B20002 - B20005	8668.9	3969.2	4699.7
B20005 - B20006	8668.9	3200.0	5468.9
B20006 - B20007	3238.9	1600.0	1638.9

Figure 46 and Table 10 show that the branches in the radial still have an abundance of remaining capacity during the three-year period. The margin of the main branch B20001-B20002 is decreased from 9330.3 kWh/h in the base case in Chapter 5.1 to 5298.5 kWh/h after the load modification. The heavy change indicates that this branch will be the limiting factor for a load increase in Radial B.

As a result of the high line rating of the branch, the remaining capacity is, in general, greater for the Radial B main branch than the Radial A main branch under normal operation. However, it could be valuable to investigate the remaining capacity of the branch in normal operation. The cumulative distribution of the remaining capacity of the branch is drawn in Figure 47a. Figure 47b shows a zoom-in of the 100 hours with the lowest remaining capacity.

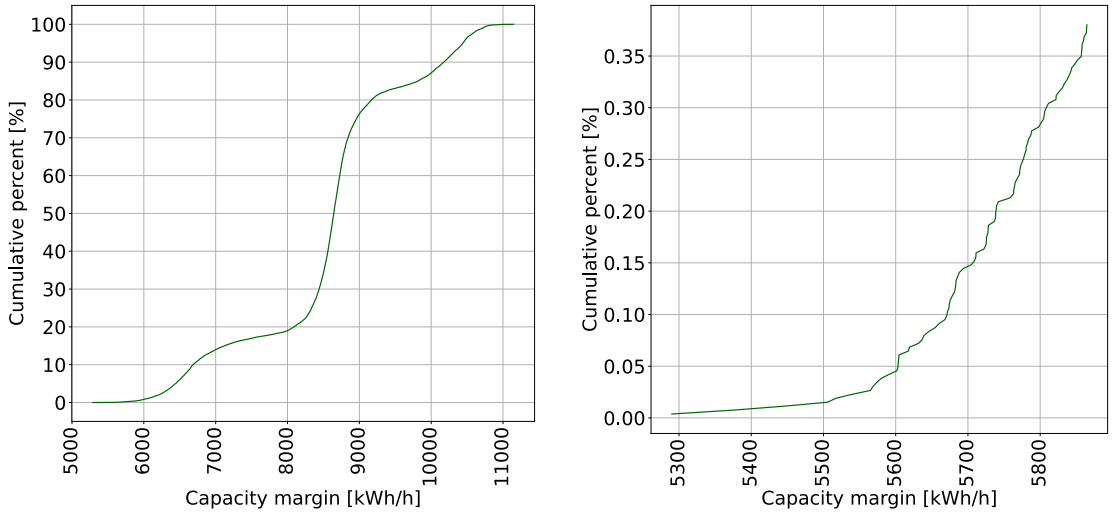

(a) All hours

(b) The 100 hours with the lowest remaining capacity

Figure 47: The cumulative distribution of the remaining capacity for the main branch of Radial B under normal operation after the load modification.

Figure 47 confirms an abundance of remaining capacity for the entire period. The steep slope between 8000 and 9000 kWh/h indicates that the remain ing capacity is in this interval for around 60% of the three-year period. The difference between the lowest and 100th lowest remaining capacity value is not as large as for the main branch of Radial A.

In summary, the line ratings of the main branches of the two radials are sufficient to cover the new load demand after the modification under normal operation. The results indicated that the line ratings of the main branches will be the limiting factors for load increase in the radials. The remaining capacity was, in general, greater for the main branch of Radial B (B20001-B20002) than the main branch of Radial A (A20001-A20002). However, the remaining capacity of both radials are clearly reduced compared to the base case situation from Chapter 5.1.

5.4.2 Outage scenario 3

In the following, the consequences of an outage of the main branch of Radial A is investigated. This situation is similar to Outage Scenario 1 from Chapter 5.2, but here, the load demand is increased according to the description in Chapter 5.4.

The only differences from Scenario 1 in the overview in Table 7 is that all the relevant branches must supply the new load point A40041 and the main branch of Radial B must additionally supply the new load point B40006.

In order to identify the limiting line rating for load increase in this situation, the remaining capacity throughout the time period for each of the branches is drawn in Figure 48.

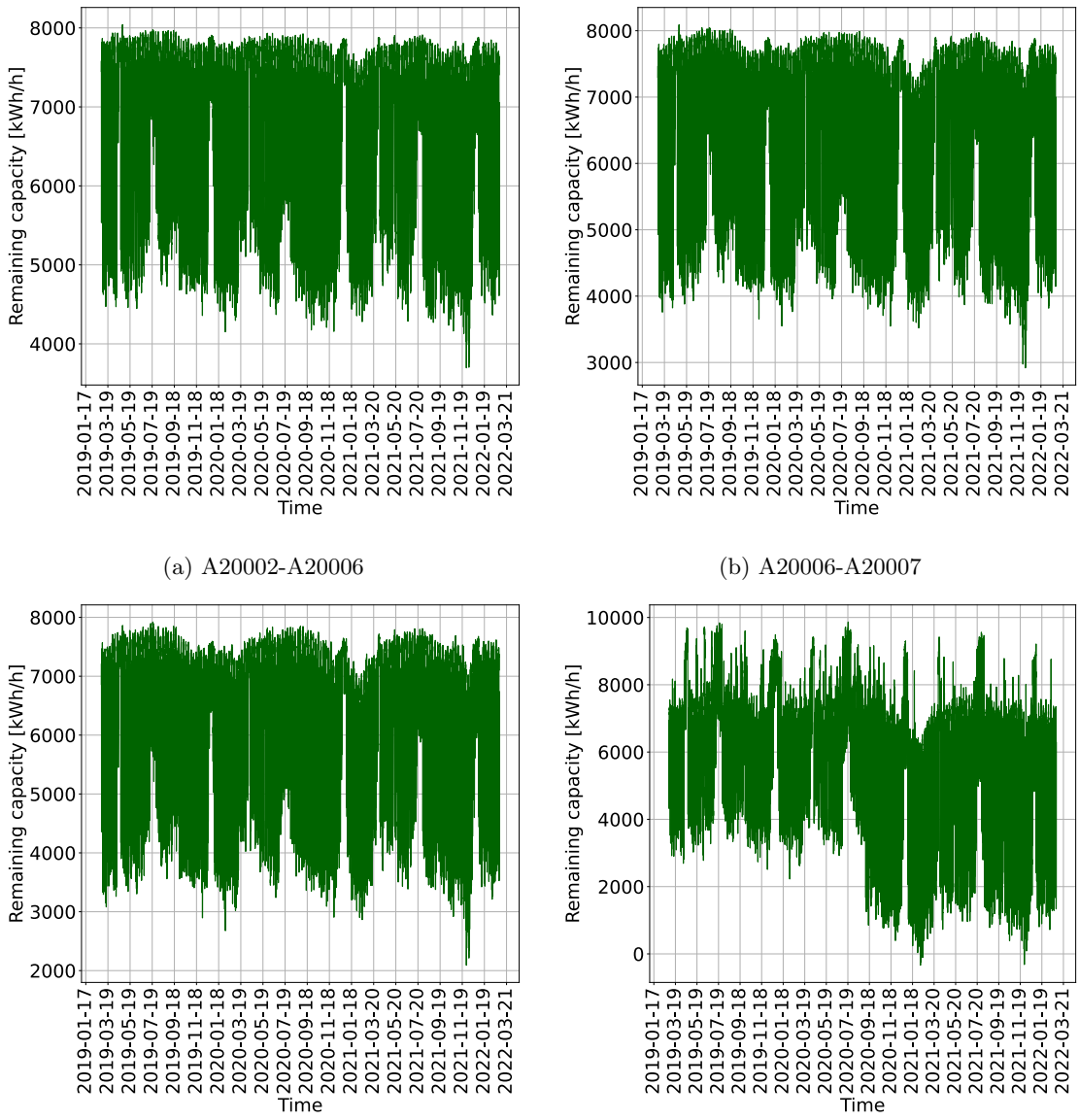

(a) A20002-A20006

(b) A20006-A20007

(c) A20007-B20002 (reserve branch)

(d) B20001-B20002

Figure 48: The remaining capacity of the relevant branches in Scenario 1 during the three-year period after the load modification.

The figure illustrates that the remaining capacity decreases for the branches closer to the secondary substation of Radial B. Since the branches closer to the substation must supply the load demand from more load points, this is expected.

Figure 48d shows that the line rating of the main branch of Radial B is exceeded for several hours during the three-year period. This confirms the indications about this branch as the limiting factor for load increase in this outage scenario. The cumulative distribution function of the remaining capacity of B20001-B20002 is drawn in Figure 49a. Figure 49b shows a zoom-in of the 10 hours with the lowest remaining capacity.

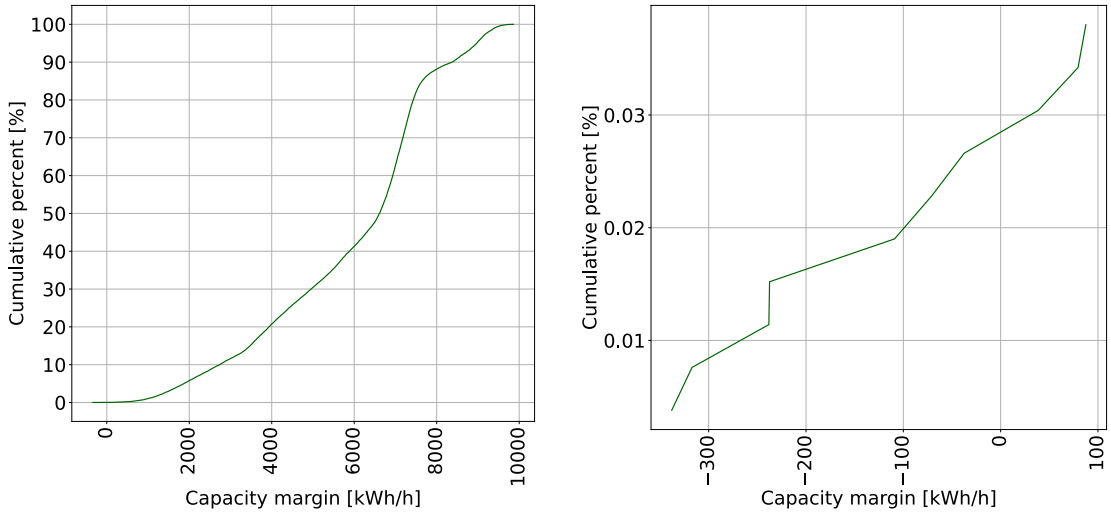

(a) All hours

(b) The 10 hours with the lowest remaining capacity

Figure 49: The cumulative distribution of the remaining capacity for the main branch of Radial B in Scenario 3.

Figure 49b confirms that the line rating of the branch is only exceeded for some few hours during the three-year period. The highest overload is calculated to 338.0 kWh/h, i.e., 3% of the line rating. In most cases, this risk should be accepted by the DSO.

In summary, three out of four relevant branches had positive remaining capacity throughout the entire time period. However, the line rating of the main branch of Radial B, B20001-B20002, was exceeded for 8 hours. In other words, the N-1 criterion is fulfilled for 99.97% of the period.

5.4.3 Outage scenario 4

In the following, the consequences of an outage of the main branch of Radial B is investigated. This situation is similar to Outage Scenario 2 from Chapter 5.2, but here, the load demand is increased according to the description in Chapter 5.4.

The only differences from Scenario 2 in the overview in Table 7 is that all the relevant branches must supply the new load point B40006 and the main branch of Radial A must additionally supply the new load point A40041.

As described in Chapter 5.2, in this situation, all the load points in the system must be supplied by the secondary substation of Radial A, and the line rating of the Radial A main branch will be the limiting factor. The total aggregated load is plotted against the line rating in Figure 50.

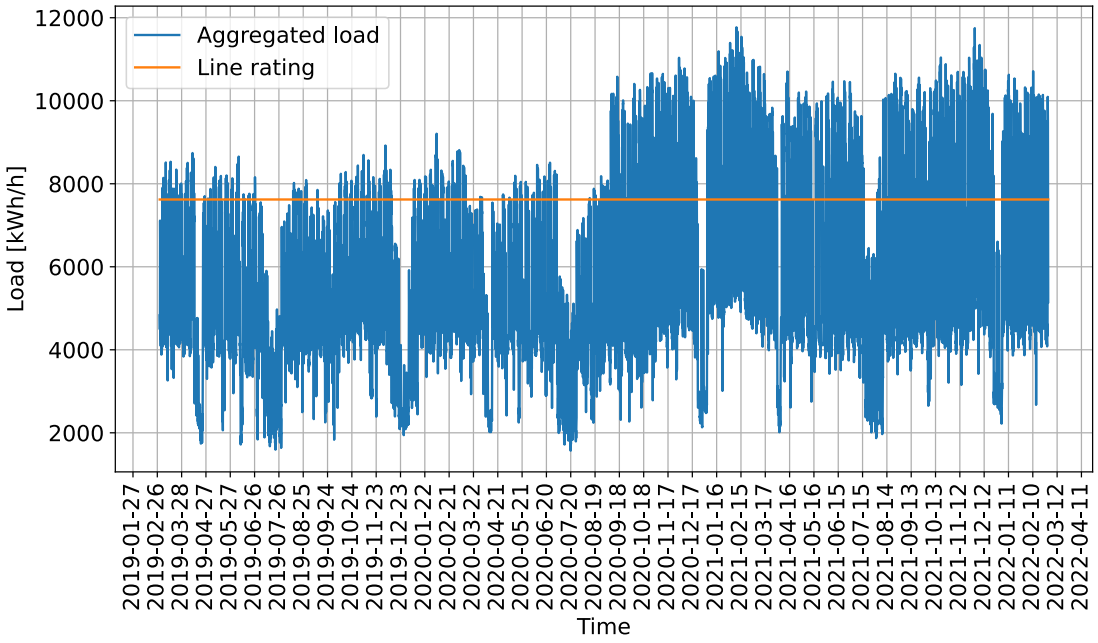

Figure 50: The aggregated load of all Radial A and Radial B load points after the load modification and the line rating of the main branch of Radial A (A20001-A20002).

The figure illustrates that after the load modification, this outage scenario would lead to overload events for a considerable number of hours during the three-year period. Calculations give that the aggregated load time series exceeds the capacity of the branch for 4907 hours, which equals 18.7 % of the time. Especially after the addition of the load points B40001 and B40002, the peaks of the aggregated load are clearly above the capacity line.

The cumulative distribution function of the remaining capacity of A20001-A20002 is drawn in Figure 51a. Figure 51b shows a zoom-in of the 4907 hours with exceeded capacity.

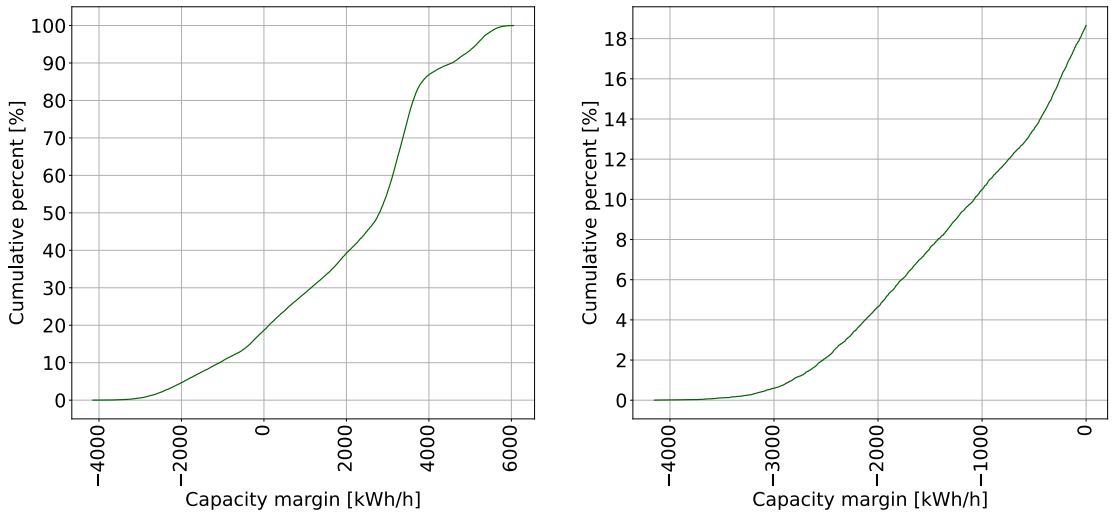

(a) All hours

(b) The hours with negative remaining capacity

Figure 51: The cumulative distribution of the remaining capacity for the main branch of Radial A in Scenario 4.

The line rating is clearly exceeded during large parts of the three-year period. In the peak hour of the aggregated load of all the load points in the system, the line rating is exceeded by 4149 kWh/h. This is a overload of 54.4% of the line rating. This, in combination with that the line rating is exceeded for 18.7% of the hours, would in most cases probably not be accepted by the DSO. In this scenario, the need for measures should be evaluated.

6 Conclusion and future work

6.1 Conclusion

The main objective of this master project is to investigate how smart meter load data can be used to provide better insight into the available capacity of distribution grids and the potential for increase of load demand.

A methodology for evaluation of available capacity in distribution grids is proposed. The methodological approach can be used to provide better insight into the room for connection of new end users and increased load demand. The main focus of the approach is on the remaining capacity of the grid components during normal operation and during outage situations.

The methodological approach is utilized on a part of the distribution grid of the industrial area Øra in Fredrikstad. The available capacity of the grid is evaluated for normal operation and for outage situations. In the coming years, electrification of industrial processes and connection of new power-intensive industries will possibly put pressure on the existing grid and challenge the DSO. Therefore, a scenario with increased load demand in the industrial grid is investigated, both for normal operation and for the most critical outage scenarios. The analysis is based on network data and historical hourly load measurements for two radials, referred to as Radial A and Radial B, of the industrial distribution grid.

The results from the evaluation of the two radials in the industrial distribution grid of Øra can be summarized as following:

- Under normal operation, the ratings of the power lines and transformers in the two radials are, in general, sufficient to cover today's load demand, based on the historical load data from the last three years. Except one of the distribution transformers in Radial A, that had the power rating exceeded for 4% of the hours, all the power lines and transformers in the system had remaining capacity during the entire three-year period.

- Four relevant branches in the high-voltage part of the distribution grid, where the reserve branch can take over the supply in case of an outage, are identified. Further, an outage of one of the main branches, i.e., the branches connecting the distribution grids to the secondary transformer substations, is identified as the most critical outage scenario for this network. However, the contingency analysis shows that the system could handle an outage of any of the relevant branches without violating the power transfer capacities.

- For the future scenario, the historical aggregated load demand supplied by each distribution transformer in the grid is scaled such that the peak demand is equal to the nameplate rating of the transformer. Additionally, new end users are connected to the two distribution substations without end users in today's grid. The results show that, under normal operation, the ratings of the power lines in the two radials are still sufficient to cover the new demand after the load modifications. However, during outage of the main branch of Radial A or the main branch Radial B, the line rating of the remaining main branch is exceeded. An outage of the main branch of Radial B is most critical in terms of the size and number of overload events.

6.2 Future work

Finally, some suggestions for future work are presented.

The investigations performed in this project thesis are based on historical hourly load data from the last three years, of which the load data from two of the years is affected by restrictive measures in relation to the Covid-19 pandemic. As discussed earlier, it is not implicit that the future demand will be similar to the past demand. Therefore, in order to improve the analysis, it could be of

interest to dedicate more attention to the load forecasting. For instance, a forecasting model that takes into account future scenarios and the DSO's plans for the grid regarding new end users and increased demand from existing end users, could provide a more realistic picture of the future situation of the distribution grid.

In the evaluation of the distribution grid of Øra, only the severity and consequences of different outage scenarios is investigated and discussed. It could be useful to see how a more risk based approach taking into account the probability of failures and outages could be used in the distribution grid evaluation. For instance, the fault frequency and repair time of different grid components could be included to improve the analyzation of the reliability of the grid.

Additionally, for future work, it would be of interest to focus on the last step of the methodological approach presented in this project thesis; to assess the need for active and passive measures in the distribution grid. For some grid planning cases, traditional and passive measures such as grid reinforcement is the preferred solution, while for other cases, active measures such as flexibility measure might be a better opportunity. Some times, occasional and short-time overloading could be accepted by the DSO. Hence, it would be valuable to investigate in which situations the different measures are suitable, based on the evaluation of the available capacity in the distribution grid.

The main focus of this master project was evaluation of the relationship between the load supplied by a grid component and the capacity of the component in order to provide better insight into the room for increased load demand. Often the DSOs are requested connections, e.g., from power-intensive industries, that will exceed by far the existing capacity of the grid. Since this is out of the scope of this project, a alternative for future work would be to investigate how the DSO should meet these requests in order to maintain a socio-economic development of the grid.

Bibliography

[1] Klima- og miljødepartementet, 'Klimaendringer og norsk klimapolitikk'. [Online]. Available: https://www.regjeringen.no/no/tema/klima-og-miljo/innsiktsartikler-klima-miljo/klimaendringer-og-norsk-klimapolitikk/id2636812/.

[2] International Energy Agency (IEA), 'Global energy review 2021'. [Online]. Available: https://www.iea.org/reports/global-energy-review-2021.

[3] ——, 'Net zero by 2050'. [Online]. Available: https://www.iea.org/reports/net-zero-by-2050.

[4] Norges vassdrags- og energidirektorat, 'The norwegian power system: Grid connection and licensing', Aug. 2018. [Online]. Available: https://publikasjoner.nve.no/faktaark/2018/faktaark2018_03.pdf.

[5] Olje- og energidepartementet, 'Utvalg skal vurdere utviklingen av strømnettet', Press release. [Online]. Available: https://www.regjeringen.no/no/dokumentarkiv/regjeringen-solberg/aktuelt-regjeringen-solberg/oed/pressemeldinger/2021/03221/id2860399/.

[6] E. Tønne, 'Planning of the future smart and active distribution grids', Norwegian University of Science and Technology, Ph.D. thesis, Dec. 2016. [Online]. Available: https://ntnuopen.ntnu.no/ntnu-xmlui/handle/11250/2484598.

[7] H. Ranjbar, M. Kazemi, N. Amjady, H. Zareipour and S. H. Hosseini, 'Maximizing the utilization of existing grids for renewable energy integration', *Renewable Energy*, vol. 189, pp. 618–629, 2022, ISSN: 0960-1481. DOI: https://doi.org/10.1016/j.renene.2022.03.035.

[8] Energifakta Norge, 'A modern and digital power supply system', [Online]. Available: https://energifaktanorge.no/en/norsk-energibruk/ny-teknologi-i-kraftsystemet/ (visited on 29th May 2022).

[9] FME CINELDI, 'Probabilistic planning methodology', [Online]. Available: https://www.sintef.no/projectweb/cineldi/pilot-projects-in-cineldi/probabilistic-planning-methodology/ (visited on 11th Mar. 2022).

[10] Flexible (loading, storing and) ANalysis of Load and Net-datacorrespondences (FLANLAN). [Online]. Available: https://github.com/SINTEF-Power-system-asset-management/flexible_load_analysis.

[11] Energifakta Norge, 'The electricity grid', [Online]. Available: https://energifaktanorge.no/en/norsk-energiforsyning/kraftnett/ (visited on 17th Mar. 2022).

[12] ——, 'Regulation of grid operations', [Online]. Available: https://energifaktanorge.no/en/regulation-of-the-energy-sector/regulering-av-nettvirksomhet/ (visited on 14th Apr. 2022).

[13] R. Billinton and R. N. Allan, *Reliability evaluation of power systems, 2nd Edition.* Springer Science + Business Media New York, 1996.

[14] A. Lie, 'Systemutforming av distribusjonsnettet', [Online]. Available: https://norgesnett.no/wp-content/uploads/Rutine-Systemutforming-distribusjonsnettet-360.pdf, 2016.

[15] I. Wangensteen, *Power System Economics - the Nordic Electricity Market.* Tapir Academic Press, 2007.

[16] T. Langset and H. H. Nielsen, 'National report 2021', RME rapport Nr. 6/2021, Norges vassdrags- og energidirektorat, 2021. [Online]. Available: https://publikasjoner.nve.no/rme_rapport/2021/rme_rapport2021_06.pdf.

[17] Norges vassdrags- og energidirektorat, 'Economic regulation', [Online]. Available: https://2021.nve.no/norwegian-energy-regulatory-authority/economic-regulation/ (visited on 26th May 2022).

[18] O. Flataker and H. H. Nielsen, 'National report 2020', RME rapport Nr. 5/2020, Norges vassdrags- og energidirektorat, 2020.

[19] Olje- og energidepartementet, 'Lov om produksjon, omforming, overføring, omsetning, fordeling og bruk av energi m.m. (energiloven)', 1990. [Online]. Available: https://lovdata.no/dokument/NL/lov/1990-06-29-50.

[20] Norges vassdrags- og energidirektorat, 'Tilknytningsplikt', [Online]. Available: https://www.nve.no/reguleringsmyndigheten/regulering/nettvirksomhet/nettilknytning/tilknytningsplikt/ (visited on 09th Jun. 2022).

[21] ——, 'Anleggsbidrag', [Online]. Available: https://www.nve.no/reguleringsmyndigheten/regulering/nettvirksomhet/anleggsbidrag/ (visited on 26th May 2022).

[22] D. Edvardsen, F. Førsund, W. Hansen, S. Kittelsen and T. Neurauter, *Productivity and regulatory reform of Norwegian electricity distribution utilities*. Jan. 2006, pp. 97–131.

[23] I. Konstantelos, M. Sun and G. Strbac, *Quantifying demand diversity of households*, Jan. 2014.

[24] SINTEF Energi, 'Planleggingsbok for kraftnett: Fastlegging av belastninger ved analyser av lavspenningsnett', 2014.

[25] J. Dickert and P. Schegner, 'Residential load models for network planning purposes', in *2010 Modern Electric Power Systems*, 2010, pp. 1–6.

[26] L. Pedersen, 'Load modelling of buildings in mixed energy distribution systems', Norwegian University of Science and Technology, Ph.D. thesis, Feb. 2007. [Online]. Available: https://ntnuopen.ntnu.no/ntnu-xmlui/handle/11250/233327.

[27] CIGRÉ Working Group C6.19, *Planning and optimization methods for active distribution systems*, CIGRÉ (International Council on Large Electric Systems), Report 978-2-85873-289-0, Aug. 2014.

[28] I. B. Sperstad, E. Solvang and O. Gjerde, *Framework and methodology for active distribution grid planning in norway*, CINELDI, 2020. DOI: https://doi.org/10.1109/PMAPS47429.2020.9183711.

[29] G. Celli, F. Pilo, G. Pisano, S. Ruggeri and G. G. Soma, 'Risk-oriented planning for flexibility-based distribution system development', *Sustainable Energy, Grids and Networks*, vol. 30, p. 100 594, 2022, ISSN: 2352-4677. DOI: https://doi.org/10.1016/j.segan.2021.100594.

[30] F. Pilo, G. Celli, E. Ghiani and G. G. Soma, 'New electricity distribution network planning approaches for integrating renewable', *Wiley Interdisciplinary Reviews: Energy and Environment*, vol. 2, Mar. 2013. DOI: 10.1002/wene.70.

[31] IEC/IEV, '617-01-01', [Online]. Available: https://www.electropedia.org/iev/iev.nsf/display?openform&ievref=617-01-01 (visited on 20th Apr. 2022).

[32] Kundur, Prabha *et al.*, 'Definition and classification of power system stability ieee/cigre joint task force on stability terms and definitions', *Power Systems, IEEE Transactions on*, vol. 19, pp. 1387–1401, Sep. 2004. DOI: 10.1109/TPWRS.2004.825981.

[33] Eurelectric working group, 'Security of electricity supply, discussion paper, nov. 2004'.

[34] 'Classification and trend analysis of threats origins to the security of power systems', *International Journal of Electrical Power Energy Systems*, vol. 50, pp. 50–64, 2013, ISSN: 0142-0615. DOI: https://doi.org/10.1016/j.ijepes.2013.02.008.

[35] M. Cepin, *Assessment of Power System Reliability, 1st Edition.* Germany: Springer Verlag, 2011.

[36] J. Setréus, 'Identifying critical components for system reliability in power transmission systems', Kungliga Tekniska högskolan, Sep. 2011.

[37] E. Heylen, M. Ovaere, S. Proost, G. Deconinck and D. Van Hertem, 'A multi-dimensional analysis of reliability criteria: From deterministic n1 to a probabilistic approach', *Electric Power Systems Research*, vol. 167, pp. 290–300, 2019, ISSN: 0378-7796. DOI: https://doi.org/10.1016/j.epsr.2018.11.001. [Online]. Available: https://www.sciencedirect.com/science/article/pii/S0378779618303626.

[38] G. Kjølle, S. H. Jakobsen, F. M. Baldursson, S. Galant and L. Haarla, 'State of the art on reliability assessment in power systems including socioeconomic impact', Technical report, GARPUR report D1.1, 2014.

[39] M. Ovaere and S. Proost, 'Optimal electricity transmission reliability: Going beyond the n-1 criterion', *The Energy Journal*, vol. 39, Oct. 2018. DOI: 10.5547/01956574.39.4.mova.

[40] J. Alexandersson, T. I. Vevatne, Y. Aabø and V. Fosse, 'Det norske kraftsystemet i det grønne skiftet: Fra n-1 til n-0,9', 2022.

[41] L. R. Løland, '- noreg har meir enn nok kraftlinjer til ny, grøn industri', 2022. [Online]. Available: https://www.nrk.no/vestland/_-noreg-har-meir-enn-nok-kraftlinjer-til-ny_-gron-industri-1.15855251.

[42] M. Chen, 'Dynamic contingency re-definition in power system security analysis', in *2011 4th International Conference on Electric Utility Deregulation and Restructuring and Power Technologies (DRPT)*, 2011, pp. 63–66. DOI: 10.1109/DRPT.2011.5993863.

[43] M. Paramasivam, S. Dasgupta, V. Ajjarapu and U. Vaidya, 'Contingency analysis and identification of dynamic voltage control areas', *IEEE Transactions on Power Systems*, vol. 30, no. 6, pp. 2974–2983, 2015. DOI: 10.1109/TPWRS.2014.2385031.

[44] S. Karimi, P. Musilek and A. M. Knight, 'Dynamic thermal rating of transmission lines: A review', *Renewable and Sustainable Energy Reviews*, vol. 91, pp. 600–612, 2018, ISSN: 1364-0321. DOI: https://doi.org/10.1016/j.rser.2018.04.001. [Online]. Available: https://www.sciencedirect.com/science/article/pii/S1364032118302119.

[45] Morgan, Vincent T., 'The loss of tensile strength of hard-drawn conductors by annealing in servicec', *IEEE Transactions on Power Apparatus and Systems*, vol. PAS-98, no. 3, pp. 700–709, 1979. DOI: 10.1109/TPAS.1979.319273.

[46] E. Eberg, K. Espeland, S. M. Hellesø and S. Hvidsten, 'Full-scale case study of a road crossing thermal bottleneck in a buried medium-voltage cable installation', *CIRED - Open Access Proceedings Journal*, vol. 2017, pp. 194–197, Oct. 2017. DOI: 10.1049/oap-cired.2017.0820.

[47] Norsk Elektroteknisk Komite (NEK), 'Norske normer for kraftkabler', 1975.

[48] E. Eberg, K. Espeland, S. M. Hellesø, S. Hvidsten and K. T. Solheim, 'Development of a web-based user-friendly cable ampacity calculation tool', 2019. DOI: 10.34890/9645.

[49] The Norwegian Smartgrid Centre, 'Nytt medlem i smartgridsenteret - heimdall power', 2019.

[50] M. Z. Degefa, M. Koivisto, R. J. Millar and M. Lehtonen, 'Dynamic thermal state forecasting of distribution network components: For enhanced active distribution network capacity', in *2014 International Conference on Probabilistic Methods Applied to Power Systems (PMAPS)*, 2014, pp. 1–6. DOI: 10.1109/PMAPS.2014.6960607.

[51] R. Godina, E. M. G. Rodrigues, J. C. O. Matias and J. P. S. Catalão, 'Effect of loads and other key factors on oil-transformer ageing: Sustainability benefits and challenges', *Energies*, vol. 8, no. 10, pp. 12 147–12 186, 2015, ISSN: 1996-1073. DOI: 10.3390/en81012147. [Online]. Available: https://www.mdpi.com/1996-1073/8/10/12147.

[52] T. I. Kopperud, 'Dynamic current rating of power transformers', M.Sc. thesis, Norwegian University of Science and Technology, 2021.

[53] IEC 60076-7:2018, 'In power transformers—part 7: Loading guide for mineral-oil-immersed power transformers', *Renewable Energy*, 2018.

[54] M. Havskjold, A. S. R. Risnes and N. M. Espegren, 'Veileder for lokale energiutredninger', Norges vassdrags- og energidirektorat, 2009. [Online]. Available: https://publikasjoner.nve.no/veileder/2009/veileder2009_02.pdf.

[55] Norgesnett, 'Om norgesnett', [Online]. Available: https://norgesnett.no/om-oss/ (visited on 20th Mar. 2022).

[56] Fredrikstad Innovasjonspark, 'Industrilokaler', [Online]. Available: https://frip.no/industrilager/ (visited on 25th May 2022).

[57] Nicola, Maria et al., 'The socio-economic implications of the coronavirus pandemic (covid-19): A review.', *International journal of surgery (London, England) vol. 78 (2020): 185-193.*, 2020. DOI: 10.1016/j.ijsu.2020.04.018.

[58] C. Zhoua, G. Yanga, S. Maa, Y. Liua and Z. Zhao, 'The impact of the covid-19 pandemic on waste-to-energy and waste-to-material industry in china', *Renewable and Sustainable Energy Reviews*, vol. 139, p. 110 693, Apr. 2021. DOI: 10.1016/j.rser.2020.110693.

[59] Y. Ding, D. Ivanko, G. Cao, H. Brattebø and N. Nord, 'Analysis of electricity use and economic impacts for buildings with electric heating under lockdown conditions: Examples for educational buildings and residential buildings in norway', *Sustainable Cities and Society*, vol. 74, p. 103 253, 2021, ISSN: 2210-6707. DOI: https://doi.org/10.1016/j.scs.2021.103253.

Appendix

A Component data

Table 11: Nameplate rating and voltage levels of all transformers in the distribution system.

Transformer **High-voltage node / Low-voltage node**	**Nameplate rating** **[kVA]**	**Voltage levels** **Primary / Secondary (/ Tertiary)** **[kV]**
A10001 / A20001	15000	47 / 11
A20002 / A30001	1600	11 / 0.400
A20003 / A30002	1600	11 / 0.400
A20004 / A30007	1600	11 / 0.400
A20005 / A30003 / A30004	500 / 300 / 200	11 / 0.400 / 0.230
B10001 / B20001	15000	47 / 11
B20003 / B30001	1250	11 / 0.400
B20004 / B30002	1250	11 / 0.400
B20005 / B30003	1000	11 / 0.400
B20006 / B30005	1600	11 / 0.400
B20007 / B30004	1600	11 / 0.400

Table 12: Ampacity, voltage level and line rating for all the branches in the distribution system.

Branch **From node - To node**	**Ampacity** **[A]**	**Voltage level** **[kV]**	**Line rating** **[kW]**
A20001 - A20002	400	11	7621.0
A20002 - A20003	?	11	?
A20002 - A20004	240	11	4572.6
A20002 - A20005	400	11	7621.0
A20002 - A20006	455 / 465	11	8668.9 / 8859.4
A20006 - A20007	465	11	8859.4
A20007 - B20002	465	11	8859.4
B20001 - B20002	600	11	11431.5
B20002 - B20003	-	11	-
B20002 -B20004	-	11	-
B20002 - B20005	455 / 465	11	8668.9 / 8859.4
B20005 - B20006	455 / 465	11	8668.9 / 8859.4
B20006 - B20007	170	11	3238.9

B Summary of specialization project

In the specialization project, the traditional methods of load modelling in the distribution network was investigated for a part of the industrial grid of Øra in Fredrikstad. The analyzed part of the grid was the same as Radial A in this master project. The traditional methods used, was based on the deterministic methodology of distribution system planning, presented by Tønne in [6]. The sufficiency of these methods for an industrial distribution network, like Øra, was discussed, based on comparison between the results calculated with the traditional methods and the actual metered values. In addition, the characteristics of the network was investigated regarding load aggregation and the underlying behaviour of the different loads in peak load situations.

The results can be summarized as following:

- The aggregated daily load demand of the industrial area was found to be, to some extent, dependent on the outdoor temperature. The temperature dependent part of the consumption was estimated to 9.1% for workweek days and 15.6% for weekend days. Based on a weighted average of these results, the temperature dependent part of the consumption was decided to 11% for the further analysis. Despite this, other factors, like holiday seasons or weekends, was found to be more determining for the daily consumption.

- The calculations of the utilization time for the different nodes in one of the radials in the network showed that, in general, a higher number of child-loads gives higher utilization times, as well as lower variability for the utilization times between different time periods. For the loads, the load profile of the loads with the highest utilization times was found to be more consistent throughout the week, compared to the loads with lower utilization times.

- Calculations of the peak demand for the different nodes in the network, based on the derived expressions for the Velander coefficients, gave a clear mismatch between the calculated and measured peak values for the nodes with more than one child-load. In general the calculated peak load was lower than the measured peak loads. Most likely, this is a result of large differences between the size and profile of the different child-loads, and hence, less load aggregation than assumed in the derivation of the coefficients.

- In general, the coincidence factor calculations showed a trend of higher coincidence factors for the nodes in the system with a lower number of child-loads. This is a result of less load aggregation effect when the number of underlying loads is decreased.

- The responsibility factor was calculated to be highest for the largest load in the system, Load 40001 (A40001). Further investigation illustrated a strong correlation between this load and the aggregation of all the loads in the network. The large size difference between the different loads, especially Load 40001 (A40001) compared to the rest of the loads, had influence on the results and was discussed in several parts of the analysis.

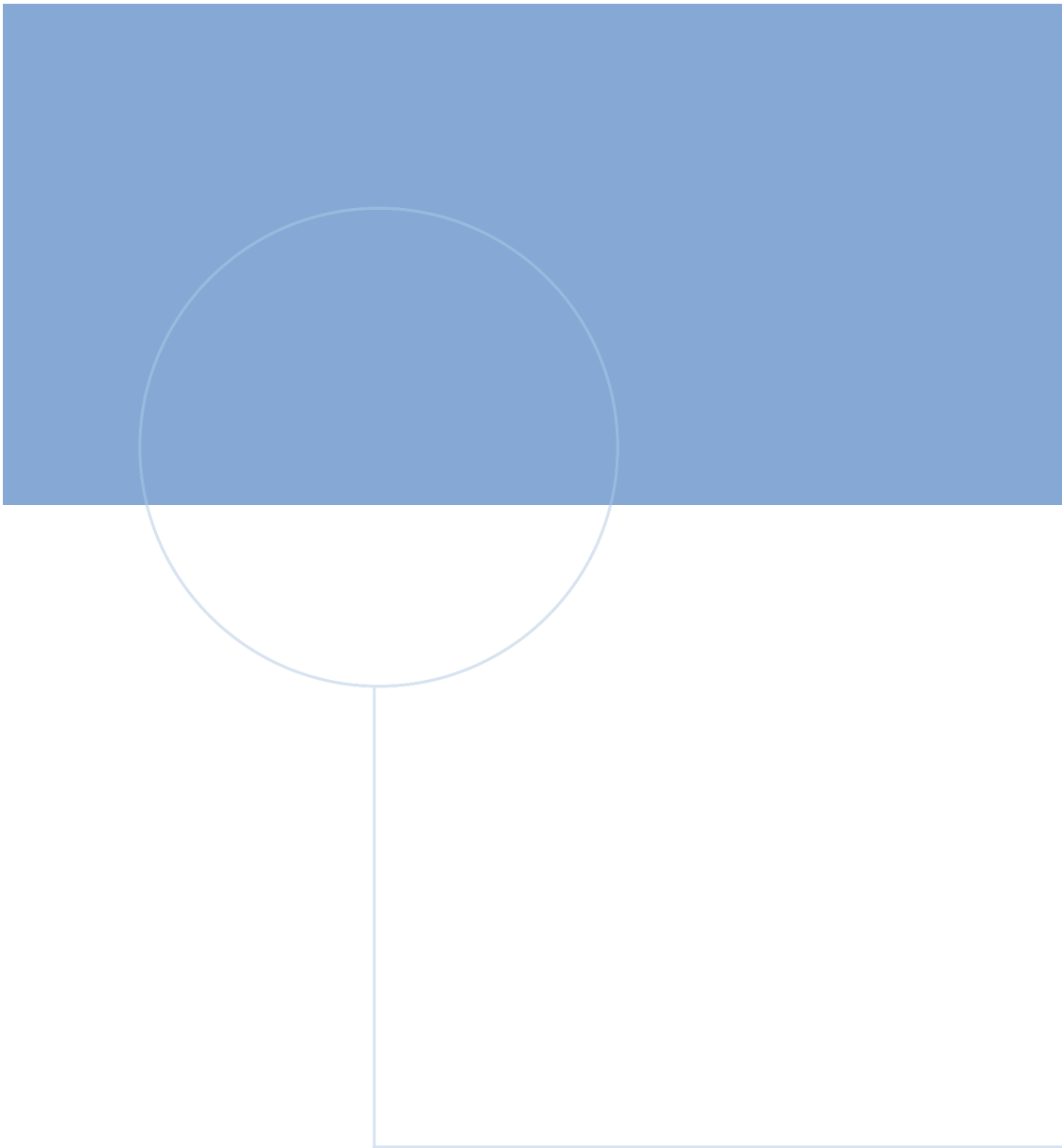

NTNU

Norwegian University of
Science and Technology